

## **Acknowledgements**

First and foremost, I am heartily grateful to my supervisor Professor Jian-Mei Li for offering me the opportunity to work on this PhD project. Her determination to succeed has encouraged me to work hard to produce data in a good quality, and her encouragement and inspiration allowed me to potentiate and progress to my fullest capabilities and capacities on completion of the thesis. I thank her for having confidence in me even when I did not always have it myself. It would be impossible for me to complete this PhD without her invaluable advice, guidance and support.

Secondly, I would like to thank the entire JML research group and in particular, I am very grateful to Sarah Cahill-Smith for her help and guidance in generating animal tissues. My thanks also go to other members in the group, Junjie Du, Mohd Ghazaly and Anna Mai, for their help at the beginning of my PhD.

Thirdly, I would like to show my deep gratitude to my parents, who attributed unconditioned mental and financial support throughout my PhD study. I sincerely appreciate for their understanding and patience, for giving me strength to overcome the most difficult time of my life.

Finally, I would like to thank all the staff members of the University of Reading for the help during my PhD and I would like to acknowledge the University of Reading for a well facilitated and friendly study environment.

## Abstract

The average age of our population continues to grow as a result of increasing longevity. Indeed, according to WHO, by the year 2100, nearly one third of the global population will be 60+ years old. However, the key factors and signalling pathways involved in cellular ageing remain largely unknown. Our hypothesis is that oxidative stress generated by the activation of a Nox2-containing NADPH oxidase plays a key role in ageing-related vascular and neuro-degenerative disorder. Therefore, the overall aim of this PhD research project is to investigate the role of Nox2 activation in ageing-related brain oxidative stress and cerebral endothelial damage using littermates of age-matched wild-type (WT) and Nox2 knockout (KO) mice (C57BL/6J background) at young (3-4 months, similar to human ~20-30 years old) and old age (21-22 months, similar to human ~70-80 years old).

I have found a significant increase in the levels of reactive oxygen species (ROS) production in multiple organs of WT ageing mice in comparison with WT young mice, and this can be significantly inhibited by knockout of Nox2. There was a significant reduction of locomotor function in WT ageing mice but not in Nox2 KO ageing mice. Increased ROS production in the WT ageing brain was accompanied by (1) significant decreases in brain endothelial cells and neurons; (2) significant increases in microglial cells and brain Nox2 expression; and (3) an activation of stress signalling pathways such as ERK1/2. Once again, these ageing-related changes were inhibited significantly by knockout of Nox2. The crucial role of ageing related Nox2 activation in oxidative damage of endothelial function was further investigated *in vitro* using coronary microvascular endothelial cells isolated from WT versus Nox2KO mice stimulated with

high glucose plus insulin, and this was further confirmed using brain tissues of endothelial specific Nox2 overexpression mice at young and old ages. Furthermore, ageing-associated increases in brain ROS production and Nox2 activation was confirmed using human post-mortem brain tissues.

In conclusion, Nox2-derived oxidative stress plays an important role in ageing-associated systemic oxidative stress, cerebral endothelial damage, neurodegeneration and loss of locomotor function. Targeting Nox2 represents a valuable therapeutic strategy to treat these ageing-related diseases.

## Published abstracts and publication

1. Geng L, Cahill-Smith S, Li JM Nox2 Activation and Oxidative Damage of Cerebral Vasculature and Locomotor Function in Ageing Mice *Heart* 2014;**100**: A105-A106
2. Geng L, Cahill-Smith S, Li JM Increased Nox2 expression and activity in ageing-related loss of locomotor function and neuronal damage *Proceedings of the British Pharmacological Society*, 2014
3. Geng L, Li JM A Crucial Role of Nox2-Derived Reactive Oxygen Species in Ageing-Associated Metabolic Disorders and Brain Oxidative Damage *Heart* 2016;**102**: A114
4. Geng L, Li JM Glucose metabolic disorders in aging-associated microglial NADPH oxidase 2 activation and oxidative damage of cerebral microvasculature and neurons *Arteriosclerosis, Thrombosis, and Vascular Biology*. 2017;**37**: A113
5. Fan LM, Geng L, Li JM Knockout of NADPH oxidase 2 improves global metabolism and endothelial function in aging mice *Arteriosclerosis, Thrombosis, and Vascular Biology*. 2017;**37**: A362
6. Fan, L. M., Cahill-Smith, S., Geng, L., Du, J., Brooks, G. and Li, J. M. (2017) 'Aging-associated metabolic disorder induces Nox2 activation and oxidative damage of endothelial function', *Free Radic Biol Med*, 108, pp. 940-951.

## Conference Presentations

1. Poster titled “Nox2 Activation and Oxidative Damage of Cerebral Vasculature and Locomotor Function in Ageing Mice” at the British Society for Cardiovascular Research, Manchester on 2<sup>nd</sup> – 3<sup>rd</sup> June 2014
2. Poster titled “Increased Nox2 expression and activity in ageing-related loss of locomotor function and neuronal damage” at the British Pharmacological Society, London on 16<sup>th</sup> – 18<sup>th</sup> Dec. 2014
3. Poster titled “A crucial role of Nox2-derived reactive oxygen species in ageing-associated metabolic disorders and brain oxidative damage” at the British Society for Cardiovascular Research, Manchester on 6<sup>th</sup> - 7<sup>th</sup> June 2016
4. Poster titled “Metabolic disorders and brain oxidative stress in aging: A crucial role of Nox2-derived reactive oxygen species” at the British Pharmacological Society, London on 13<sup>th</sup>-15<sup>th</sup> Dec. 2016
5. Poster titled “Glucose metabolic disorders in aging-associated microglial Nox2 activation and oxidative damage of cerebral microvasculature and neurons” at the ATVB/PVD 2017 Scientific Sessions, Minneapolis, Minn, U.S. on 4<sup>th</sup> – 6<sup>th</sup> May, 2017
6. Poster titled “Knockout of Nox2 improves global metabolism and endothelial function in aging mice” at the ATVB/PVD 2017 Scientific Sessions, Minneapolis, Minn, U.S. on 4<sup>th</sup> – 6<sup>th</sup> May 2017
7. Poster titled “Metabolic disorder-induced global Nox2 activation and endothelial dysfunction in aging” at the British Society for Cardiovascular Research, Manchester on 5<sup>th</sup> - 6<sup>th</sup> June 2017

## Contents

|  |    |
|--|----|
| Acknowledgements.....  | 1  |
| Abstract.....  | 2  |
| Published abstracts and publication.....                             | 4  |
| Conference Presentations.....  | 5  |
| List of abbreviations.....   | 11 |
| List of figures.....   | 14 |
| Chapter 1  |    |
| General Introduction.....  | 16 |
| 1.1 Ageing and ageing-related diseases.....                          | 16 |
| 1.1.1 Ageing population.....   | 16 |
| 1.1.2 Ageing and theories of ageing.....                             | 17 |
| 1.1.3 Ageing-related diseases.....                                   | 18 |
| 1.2 Reactive oxygen species.....                                     | 19 |
| 1.2.1 Sources of reactive oxygen species.....                        | 19 |
| 1.2.2 NADPH oxidase.....   | 21 |
| 1.2.3 Other sources of ROS.....                                      | 23 |
| 1.3 Nox2.....  | 24 |
| 1.4 ROS in physiology and pathology.....                             | 26 |
| 1.5 Ageing-related oxidative stress and endothelial dysfunction..... | 29 |
| 1.6 Ageing-related oxidative stress and neurodegeneration.....       | 31 |
| 1.6.1 Central nervous system and NADPH oxidase.....                  | 31 |
| 1.6.2 ROS in the CNS.....  | 32 |
| 1.6.3 Microglia and microglial activation.....                       | 33 |
| 1.6.4 Microglial Nox2 activation.....                                | 37 |
| 1.7 Endothelial dysfunction and blood-brain barrier damage.....      | 40 |
| 1.8 Hypothesis and aim.....  | 40 |

## Chapter 2

|   |    |
|---|----|
| Materials and methods .....   | 42 |
| 2.1 Animal and sample information.....  | 42 |
| 2.2 Genotyping.....   | 43 |
| 2.3 Collection of mouse organs and tissues .....  | 45 |
| 2.4 Isolation of coronary microvascular endothelial cell (CMEC).....  | 46 |
| 2.5 Cell culture.....   | 47 |
| 2.5.1 Thawing cells .....   | 47 |
| 2.5.2 Passaging cells .....   | 48 |
| 2.5.3 Cell count and cell Viability .....   | 48 |
| 2.5.4 Freezing cells .....  | 49 |
| 2.6 Beta-amyloid stimulation.....   | 49 |
| 2.7 Tissue homogenisation, protein extraction and quantification .....  | 51 |
| 2.8 Measurement of ROS production by lucigenin chemiluminescence Assay .....  | 52 |
| 2.9 <i>In situ</i> Dihydroethidium (DHE) detection of superoxide production by tissue sections.....                                 | 55 |
| 2.10 DCF (5-(and 6)-chloromethyl-2',7'-dichlorodihydrofluorescein diacetate) detection of intracellular superoxide production ..... | 56 |
| 2.11 SOD-inhibitable cytochrome c reduction assay for the measurement of superoxide production by tissue homogenates .....          | 56 |
| 2.12 Catalase-inhibitable amplex red assay for the measurement of hydrogen oxide production by tissue samples .....                 | 57 |
| 2.13 Immunofluorescence.....  | 59 |
| 2.14 Western blotting.....  | 60 |
| 2.15 Assessment of locomotor activity .....   | 62 |
| 2.16 Statistical analysis.....  | 63 |
| Appendix.....   | 64 |

## Chapter 3

|   |    |
|---|----|
| Knockout of Nox2 attenuates the increased oxidative stress in multiple organs and preserves locomotor function in ageing mice ..... | 69 |
| 3.1 Introduction.....   | 69 |
| 3.1.1 Aims and objectives.....  | 72 |
| 3.2 Results.....  | 73 |
| 3.2.1 The global effect of ageing on multiple organ oxidative stress and the role of Nox2.....                                      | 73 |
| 3.2.2 The effect of ageing and the role of Nox2 on brain ROS production detected by lucigenin chemiluminescence.....                | 78 |
| 3.2.3 The effect of ageing and the role of Nox2 on brain ROS production detected by cytochrome c reduction assay.....               | 81 |
| 3.2.4 The effect of ageing and the role of Nox2 on brain ROS production detected by DHE fluorescence.....                           | 84 |
| 3.2.5 The effect of ageing and the role of Nox2 on brain hydrogen peroxide production detected by Amplex Red assay.....             | 87 |
| 3.2.6 Difference in total activities between WT and Nox2 knockout mice detected by PIR (passive infrared) sensor.....               | 90 |
| 3.2.7 Difference in total activities between WT and Nox2 knockout mice detected by running wheel .....                              | 93 |
| 3.3 Discussion .....  | 96 |

## Chapter 4

|   |     |
|---|-----|
| Knockout of Nox2 reduces cerebral endothelial damage, neuronal death and oxidative signalling in the brain..... | 100 |
| 4.1 Introduction.....   | 100 |
| 4.1.1 Aims and objectives.....  | 103 |
| 4.2 Results.....  | 104 |
| 4.2.1 The effect of ageing on cerebral endothelial cells detected by immunofluorescence.....                    | 104 |
| 4.2.2 The effect of ageing on neuronal cells detected by immunofluorescence.....                                | 107 |
| 4.2.3 The effect of ageing on microglial Nox2 expression detected by immunofluorescence.....                    | 110 |

|  |     |
|--|-----|
| 4.2.4 The effect of ageing on NADPH oxidase subunit expression in the brain detected by Western blot .....   | 113 |
| 4.2.5 The effect of ageing on MAPK and Akt phosphorylation in the brain detected by Western blot .....   | 116 |
| 4.2.6 The effects of PMA and TNF $\alpha$ on microglial cell ROS production measured by lucigenin chemiluminescence and DHE fluorescence.....                          | 119 |
| 4.2.7 The effects of A $\beta$ (1-42) on microglial cell (BV-2) ROS production measured by lucigenin chemiluminescence and DHE fluorescence .....                      | 122 |
| 4.3 Discussion .....   | 125 |
| Chapter 5  |     |
| Overexpression of Nox2 increases brain oxidative stress and endothelial damage, studies using human Nox2 transgenic mice; and the clinical significance .....          | 129 |
| 5.1 Introduction.....  | 129 |
| 5.2 Results.....   | 131 |
| 5.2.1 The effect of ageing and the role of Nox2 on superoxide production from Nox2 transgenic brain detected by lucigenin chemiluminescence and DHE fluorescence ..... | 131 |
| 5.2.2 The effect of ageing and the role of endothelial Nox2 overexpression on cerebral endothelial cells detected by immunofluorescence .....                          | 134 |
| 5.2.3 The effect of high glucose and insulin on endothelial Nox2 activation and endothelial ROS production detected by DCF fluorescence .....                          | 137 |
| 5.2.4 The effect of high glucose and insulin on endothelial Nox2 activation detected by immunofluorescence .....   | 141 |
| 5.2.5 The effect of ageing on human brain superoxide production detected by lucigenin chemiluminescence and DHE fluorescence.....                                      | 144 |
| 5.2.6 The effect of ageing on NADPH oxidase subunit expression and cell apoptosis in human brain detected by Western blot .....  | 147 |
| 5.3 Discussion .....   | 150 |
| Chapter 6  |     |
| General discussion and future work.....  | 153 |
| 6.1 General Discussion .....   | 153 |

|                      |     |
|----------------------|-----|
| 6.2 Future work..... | 157 |
| References.....      | 158 |

## List of abbreviations

|                         |   |
|-------------------------|---|
| A $\beta$               | Beta-amyloid                                    |
| ATP                     | Adenosine triphosphate                          |
| BSA                     | Bovine serum albumin                            |
| BH <sub>4</sub>         | Tetrahydrobiopterin                             |
| CGD                     | Chronic granulomatous disease                   |
| CMEC                    | Coronary microvascular endothelial cells        |
| CM-H <sub>2</sub> DCFDA | Chloromethyl-2, 7-dichlorofluorescein diacetate |
| CNS                     | Central nervous system                          |
| CVD                     | Cardiovascular diseases                         |
| DCF                     | Dichlorofluorescein                             |
| DHE                     | Dihydroethidium                                 |
| DMEM                    | Dulbecco's modified Eagle's medium              |
| DMSO                    | Dimethyl sulphoxide                             |
| DNA                     | Deoxyribonucleic acid                           |
| Dnase                   | Deoxyribonuclease                               |
| DPI                     | Diphenyleneiodonium                             |
| EDTA                    | Ethylenediaminetetraacetic acid                 |
| EGF                     | Epidermal growth factor                         |
| EGTA                    | Ethylene glycol tetraacetic acid                |
| ERK                     | Extracellular signal-regulated kinase           |
| FAD                     | Flavin adenine dinucleotide                     |

|                               |   |
|-------------------------------|---|
| H <sub>2</sub> O <sub>2</sub> | Hydrogen peroxide                           |
| HBSS                          | Hanks' Buffered Salt Solution               |
| HRP                           | Horseradish peroxidase                      |
| iNOS                          | Inducible nitric oxide synthase             |
| JNK                           | c-Jun N-terminal kinase                     |
| L-NAME                        | N-nitro-L-arginine methyl ester             |
| MAPK                          | Mitogen-activated protein kinase            |
| NADPH                         | Nicotinamide adenine dinucleotide phosphate |
| NF-κB                         | Nuclear factor kappa B                      |
| NO                            | Nitric oxide                                |
| NOS                           | Nitric oxide synthase                       |
| NOX                           | NADPH oxidase                               |
| O <sub>2</sub> <sup>-</sup>   | Superoxide                                  |
| OCT                           | Optimum cutting temperature compound        |
| OH <sup>·</sup>               | Hydroxyl radical                            |
| ONOO <sup>·</sup>             | Peroxynitrite                               |
| Oxy                           | Oxypurinol                                  |
| PB1                           | Phox and Bem 1                              |
| PBS                           | Phosphate buffered saline                   |
| PCR                           | Polymerase chain reaction                   |
| PEI                           | Polyethylenimine                            |
| PHOX                          | Phagocytic NADPH oxidase                    |

|       |  |
|-------|--|
| PKC   | Protein kinase C                                 |
| PI3K  | Phosphoinositide 3-kinase                        |
| PMA   | Phorbol myristate acetate                        |
| PVDF  | Polyvinylidene Difluoride                        |
| PX    | Phox homology                                    |
| ROS   | Reactive oxygen species                          |
| SDS   | Sodium dodecyl sulphate                          |
| SH3   | Src Homology 3                                   |
| SOD   | Superoxide dismutase                             |
| TAE   | Tris-acetate EDTA                                |
| TBS   | Tris-buffered saline                             |
| TBST  | Tris-buffered saline-0.1% Tween 20               |
| TEMED | N,N,N',N'-tetramethylethylenediamine             |
| TNF   | Tumor necrosis factor                            |
| TNFR  | Tumor necrosis factor receptor                   |
| TRAF  | Tumor necrosis factor receptor-associated factor |
| VEGF  | Vascular endothelial growth factor               |
| VSMC  | Vascular smooth muscle cell                      |
| WT    | Wild-type  |
| XDH   | Xanthine dehydrogenase                           |
| XO    | Xanthine oxidase                                 |
| XOR   | Xanthine oxidaseductase                          |

## List of figures

|  |    |
|--|----|
| Figure 1.1 Percentage of world population at 60 or over by country   | 16 |
| Figure 1.2 Generation of different reactive species derived from oxygen  | 20 |
| Figure 1.3 the representation of the activation of the Nox2 and NADPH acts as an electron donor to produce superoxide  | 26 |
| Figure 1.4 Microglia activation  | 35 |
| Figure 2.1 The procedures of examining ROS from BV-2 microglial cells stimulated by A $\beta$ (1-42).  | 51 |
| Figure 2.2 Illustration of lucigenin-chemiluminescence technique   | 54 |
| Figure 2.3 Photoshoot of a wheel-running cage (left) for mouse circadian assessment and a digital electronic record of the mouse movement shown on computer screen (right) | 63 |
| Figure 3.1 The effects of ageing on multiple organ weight and ROS production detected by NADPH-dependent lucigenin chemiluminescence                                       | 75 |
| Figure 3.2 The effect of ageing on NADPH derived ROS production detected by lucigenin chemiluminescence in WT and Nox2KO mice brains                                       | 79 |
| Figure 3.3 The effect of ageing on NADPH dependent ROS production detected by cytochrome c reduction assay in WT and Nox2KO mice brains                                    | 82 |
| Figure 3.4 The role of Nox2 in ageing-related oxidative stress on WT and Nox2KO brain sections detected by DHE fluorescence  | 85 |
| Figure 3.5 The hydrogen peroxide production detected by Amplex Red assay in WT and Nox2KO mice   | 88 |
| Figure 3.6 Difference in total activities between WT and Nox2 knockout mice detected by PIR (passive infrared) sensor  | 91 |
| Figure 3.7 Difference in total activities between WT and Nox2 knockout mice detected by running wheel  | 94 |

|   |     |
|---|-----|
| Figure 4.1 The effect of ageing on cerebral endothelial cells detected by immunofluorescence  | 105 |
| Figure 4.2 The effect of ageing on neuronal cells detected by immunofluorescence  | 108 |
| Figure 4.3 The effects of ageing on microglial Nox2 expression detected by immunofluorescence   | 111 |
| Figure 4.4 The effects of ageing on NADPH subunits expression detected by western blot  | 114 |
| Figure 4.5 The effect of ageing on MAPK and Akt phosphorylation in the brain detected by Western blot   | 117 |
| Figure 4.6 The effects of PMA and TNF $\alpha$ on microglial cell (BV-2) ROS production measured by lucigenin chemiluminescence and DHE fluorescence                  | 120 |
| Figure 4.7 The effects of A $\beta$ (1-42) on microglial cell (BV-2) ROS production measured by lucigenin chemiluminescence and DHE fluorescence                      | 123 |
| Figure 5.1 The effect of ageing and the role of Nox2 on superoxide production from Nox2 transgenic brain detected by lucigenin chemiluminescence and DHE fluorescence | 132 |
| Figure 5.2 The effect of ageing and the role of endothelial Nox2 over expression on cerebral endothelial cells detected by immunofluorescence                         | 135 |
| Figure 5.3 The effect of high glucose and insulin on CMEC ROS production detected by DCF fluorescence   | 139 |
| Figure 5.4 The effect of high glucose and insulin on endothelial Nox2 activation in WT versus Nox2KO CMECs detected by immunofluorescence                             | 142 |
| Figure 5.5 The effect of ageing on human brain superoxide production detected by lucigenin chemiluminescence and DHE fluorescence                                     | 145 |
| Figure 5.6 The effect of ageing on NADPH oxidase subunit expression and cell apoptosis in human brain detected by Western blot  | 148 |

# Chapter 1

## General Introduction

### 1.1 Ageing and ageing-related diseases

#### 1.1.1 Ageing population

Ageing is associated with an impaired ability to adapt to environmental changes (Marin and Rodriguez-Martinez, 1999). Due to the fact that we are living longer, the proportion of people aged over 60 years (defined as ‘elderly’) is growing faster than any other age group in almost every country and the United Nations estimate the elderly population worldwide will double or even more by 2050, see figure 1.1 (WPA, 2015). Therefore, there is an increased need for research activity to understand the ageing biology in order to improve the quality of life in the elderly (Martin, 2011, Tsamis et al., 2013).

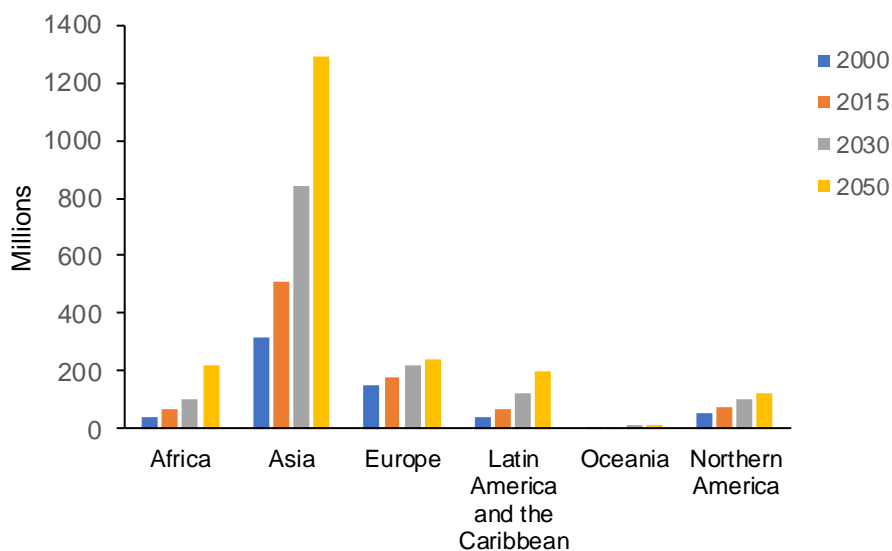


Figure 1.1. The number of people aged 60 or over in different regions (Data from World Population Ageing, United Nations, 2015)

### **1.1.2 Ageing and theories of ageing**

Ageing is described as the process of progression through lifespan and the consequential loss of regulation of interactions at cellular, tissue and organ levels (Mangoni and Jackson, 2004). There are many theories of ageing which can generally be grouped into programmed theories and damage-based theories. The former theories suggest that ageing is preprogrammed and follows a constitutional biological clock (Jin, 2010). One of the popular programmed theories is focused on telomeres, which are DNA sequences located at the end of chromosomes. During every cell division, they become gradually shorter and eventually the cell can no longer proliferate and turns into a senescent cell (Takahashi et al., 2000). The later theories suggest that ageing is mainly caused by the damage accumulated throughout the lifespan, which has attracted a lot of attention during the past few years. Among these theories, the developmental-genetic theory suggests that there are numbers of specific genes playing a major role in ageing, such as TOR (Johnson et al., 2013) and FOXO (Rollo, 2010). However, one of the most prominent and well-established theories of ageing is the damage-based free radical theory of ageing which hypothesises that the damage from free radicals progressively accumulates particularly in post-mitotic tissues resulting in ageing (Desai et al., 2010).

In 1956, Denham Harman was the first person to discover the free radical theory (Harman, 1956). This theory defines that ageing results from the accumulation of free radical-induced oxidative damage to DNA, lipids and protein. Over the past decades, based on this theory, an oxidative stress theory of ageing has been developed, suggesting that not only free radicals but other reactive oxygen species (ROS) can cause oxidative damage that leads to a progressive loss in biological function resulting in

ageing. An abundance of experimental evidence supports the oxidative stress theory of ageing in the vascular and central nervous systems (Rodriguez-Manas et al., 2009, Sasaki et al., 2008, Liochev, 2014, Liochev, 2013). These studies demonstrated the increased ROS with ageing in various organ tissues. Furthermore, the oxidative stress theory of ageing can be linked with other theories. Oxidative stress was found to have close association with telomere shortening in fibroblast from human and sheep (Richter and von Zglinicki, 2007). Reduced oxidative stress has also been found to be associated with increased longevity. Caloric restriction, a widely used method to improve longevity, was found to be associated with reduced oxidative stress (Qiu et al., 2010, Walsh et al., 2014). p66Shc is a gene responsible for regulating the level of ROS, apoptosis induction, and lifespan in mammals (Galimov, 2010). The deletion of the p66Shc gene, which extends the lifespan of mice, was also seen to be associated with reduced oxidative stress (Tomilov et al., 2010). These research findings support that the oxidative stress theory of ageing is widely accepted and is a sound theory which links to other theories and mechanisms of ageing.

### **1.1.3 Ageing-related diseases**

Ageing is one of the major risk factors for the development of cardiovascular disease which is still the number one killer disease around the world (WHO, 2017). Ageing causes significant structural and functional changes in the vascular system that contribute to other organ dysfunction (Oxenham and Sharpe, 2003) and increases the incidence of hypertension, coronary heart disease, heart failure, vascular dementia and stroke. During the ageing process, the thickness of the arterial wall is increased, characterized by fibrosis and collagen deposition. Ageing also leads to changes in endothelial cells (Wei, 1992). It is well known that endothelial cells play a crucial role

in vascular tone regulation. Ageing reduces endothelium-dependent relaxation elicited by vasodilators that release nitric oxide (NO) from the endothelium (Novella et al., 2013).

Importantly, ageing has been found to produce negative effects on cerebral blood vessels (Modrick et al., 2009) and it has been considered as the major risk factor for cerebral diseases and neurodegeneration, such as Alzheimer's disease, stroke and vascular cognitive impairment (Mariani et al., 2005). Vascular dementia, where cognitive impairment attributes to cerebrovascular pathologies, is responsible for at least 20% of cases of dementia. (Gorelick et al., 2011). Neurodegeneration is defined as the progressive loss of structure or function of neurons causing neuronal death and therefore leading to dysfunction of the central nervous system (CNS) (Haass and Selkoe, 2007). There were extensive studies promoting an interest to gain a better understanding of the interaction between brain vascular pathology and neurodegeneration to amplify their respective pathogenic contribution with ageing (Iadecola, 2013).

## **1.2 Reactive oxygen species**

### **1.2.1 Sources of reactive oxygen species**

Reactive oxygen species (ROS) are highly active small molecules derived from molecular oxygen that can be classified into: oxygen-centred radical (superoxide anion ( $O_2^-$ ), hydroxyl radical ( $OH\cdot$ ), alkoxy radical ( $RO\cdot$ ), and peroxy radical ( $ROO\cdot$ ) and oxygen-centred non-radical (hydrogen peroxide ( $H_2O_2$ ) and singlet oxygen ( $O_2$ )) (Lee et al., 2003). Then enzymatic sources of ROS include uncoupled nitric oxide synthase (NOS), xanthine oxidoreductase, mitochondrial respiratory enzymes and most importantly NADPH oxidases (Lambeth, 2004). ROS are produced as intermediates in



### 1.2.2 NADPH oxidase

Nicotinamide adenine dinucleotide phosphate (NADPH) oxidase (Nox) was first identified in phagocytes, acting as an essential non-specific host defence mechanism responsible for the reactive oxygen burst against microbial organisms (Freeman and Crapo, 1982). NADPH oxidase plays a crucial role in host defence. It was well documented that patients with chronic granulomatous diseases (CGD), a rare genetic disease, had defects in subunits of NADPH oxidase (Kuhns et al., 2010). NADPH oxidase can be activated via a few physiological and pathological stimuli including the following: 1) cytokines such as tumour necrosis factor alpha (TNF $\alpha$ ), interleukin 1 (IL-1) and transforming growth factor beta (TGF $\beta$ ); 2) metabolic factors such as non-esterified fatty acid (NEFA), oxidised low-density lipoprotein; 3) growth factors including insulin, thrombin and vascular endothelial growth factor (VEGF); 4) G protein-coupled receptor agonists including angiotensin II and endothelin-1; 5) oscillatory shear stress; 6) hypoxia-reoxygenation and ischaemia-reperfusion (Li and Shah, 2004, Panday et al., 2015). The NADPH oxidase-derived ROS are essential in cell signalling and regulation. Furthermore, induction of ROS production leads to their role as a second messenger to regulate multiple cellular processes, including inflammatory gene expression and control of the cell cycle (Li and Shah, 2003). Cells have defence against overproduction of ROS including antioxidants such as vitamin C, vitamin E, uric acid and antioxidant enzymes such as catalase and superoxide dismutase (SOD). However, when the ROS production increases to a level that outweighs the antioxidant capability, the excessive ROS can cause oxidative stress.

NADPH oxidase is a multi-component enzyme consisting of a membrane-bound catalytic core called flavocytochrome *b*<sub>558</sub>, and a group of cytosolic regulatory subunits.

Flavocytochrome *b*<sub>558</sub> consists of p22<sup>phox</sup> ( $\alpha$  subunit) and gp91<sup>phox</sup> ( $\beta$  subunit) (Rae et al., 1998). The gp91<sup>phox</sup> subunit is encoded by the gene CYBB located on the short arm of the X chromosome (Patino et al., 1999) and is a large glycoprotein of 570 amino acids with 91 kDa in its glycosylated form and 65 kDa in pre-glycosylation form (Meischl and Roos, 1998). It contains 6 transmembrane helices with 2 bound haems in the N-terminal half and in the C-terminal region the FAD and NADPH binding residue (Takeya and Sumimoto, 2003). Both COOH and NH<sub>2</sub> termini are situated in the cytoplasm (Vignais, 2002).

The original gp91<sup>phox</sup> has been renamed to Nox2, and other homologues of gp91<sup>phox</sup> have been identified, such as Nox1, Nox3, Nox4, Nox5 and Duox1 and 2. Nox1, 3 and 4 share a similar structure with Nox2. Nox1 is highly expressed in colon and it is also found in vascular smooth muscle cells, prostate, uterus, endothelial cells, neurons, microglia and astrocytes (Banfi et al., 2000, Lassegue and Griendling, 2010, Sorce and Krause, 2009). Nox2 is widely expressed in phagocytes, endothelial cell, fibroblasts microglia, neurons and astrocytes (Lassegue and Griendling, 2010, Sorce and Krause, 2009, Takac et al., 2012). Nox3 expresses in inner ear and foetal kidney (Banfi et al., 2004). Nox4 can be found in kidney, endothelial cells, vascular smooth muscle cells and in the brain (Lassegue and Griendling, 2010, Sorce and Krause, 2009, Takac et al., 2012). Nox5 is highly expressed in spleen, testis and foetal tissues (Sorce and Krause, 2009, Takac et al., 2012). Duox1 and 2 is expressed in thyroid, testis, pancreases and foetal tissues (Bedard and Krause, 2007, De Deken et al., 2000). In research investigating both the vascular and central nervous systems in the brain, the highly expressed and most researched Nox isoforms are Nox1, Nox2 and Nox4. Nox2 expression was found to be increased with ageing in the brain and vessels (Dugan et al., 2009, Roos et al., 2013). Nox2-derived oxidative stress therefore may play an important

role in the development of ageing-related diseases such as vascular disease and neurodegeneration.

### **1.2.3 Other sources of ROS**

In the cell, oxidative phosphorylation occurs when energy is produced in the form of adenosine triphosphate (ATP) in the mitochondria. This process involves an electron transport chain which consists of the following: complex I (NADH-ubiquinone oxidoreductase), complex II (succinate-ubiquinone oxidoreductase), complex III (ubiquinol-cytochrome C reductase), complex IV (cytochrome c oxidase), coenzyme Q (ubiquinone) and cytochrome c (Balaban et al., 2005, Madamanchi et al., 2005). Along the electron transport chain, electrons can react with molecular oxygen to produce superoxide and other types of ROS. The two major sites producing ROS are believed to be at complex I and complex III (Balaban et al., 2005).

Nitric oxide synthase (NOS) is a heme-containing monooxygenase which produces nitric oxide (NO) during the oxidation of L-arginine to L-citrulline (Porasuphatana et al., 2003). It has three isozymes: nNOS which is constitutive in neuronal tissue; iNOS which is induced by cytokines; eNOS which exists in vascular endothelial cells (Porasuphatana et al., 2003). Each NOS contains binding sites for flavin adenine dinucleotide (FAD), flavin mononucleotide (FMN) and NADPH at the reductase domain and binding sites for haem, the substrate L-arginine and tetrahydrobiopterin (BH<sub>4</sub>) at the oxygenase domain (Sun et al., 2010). NOS can produce superoxide instead of nitric oxide when levels of L-arginine or BH<sub>4</sub> are low (Bevers et al., 2006). This reaction is called NOS uncoupling that is caused by the reduction of molecular oxygen by NADPH and becomes uncoupled from L-arginine oxidation and nitric oxide synthesis (Fukai, 2007).

Xanthine oxidase (XO) and xanthine dehydrogenase (XDH) are the two forms generated from xanthine oxidoreductase (XOR), a molybdoflavin enzyme. In vivo, most XOR exists in the XDH form and can be reversibly or irreversibly converted to XO. The active form of XDH is a homodimer with independent subunits consisting of 2 iron-sulphur centres at the N-terminal, a flavin adenine dinucleotide (FAD) domain in the centre and a molybdopterin (Mo) binding domain at the C-terminal (Enroth et al., 2000). It can catalyse the oxidation of hypoxanthine to xanthine and xanthine to uric acid. During this process, the FAD can be divalently oxidised by O<sub>2</sub> to produce H<sub>2</sub>O<sub>2</sub> or univalently oxidised to produce 2O<sub>2</sub><sup>-</sup> (Galbusera et al., 2006).

ROS can be generated by the endoplasmic reticulum (Zeeshan et al., 2016). Endoplasmic reticulum is involved in various functions, including protein synthesis and folding, transport of Golgi, lysosomal, secretory, and cell-surface proteins. It also plays an important role in lipid metabolism, calcium storage and drug detoxification (Groenendyk and Michalak, 2005) (Koch, 1990) (Cribb et al., 2005). Smooth endoplasmic reticulum presents a chain of electron transport, constituted by two systems devoted to xenobiotic metabolism and introduction of double bonds in fatty acids, which are also able to produce ROS (Di Meo et al., 2016).

### **1.3 Nox2**

The Nox2 human protein (570 amino acid residues) can be seen as a 91-kDa band by sodium dodecyl sulphate (SDS) polyacrylamide gel electrophoresis due to its post-translational glycosylation. Therefore, Nox2 is also known as gp91<sup>phox</sup>. The Nox2 subunit is not constitutively active and requires interaction with its cytosolic subunits

to become activated. It is often associated with p22<sup>phox</sup> to form a stable heterodimer. The activation occurs starting with the phosphorylation of p47<sup>phox</sup> at multiple serine residues (Takeya and Sumimoto, 2003). Following the phosphorylation of p47, the SH3 (Src homology 3) and PX domains become accessible. The p47<sup>phox</sup> translocates to the membrane taking with p67<sup>phox</sup> and p40<sup>phox</sup>. Interactions then occur between the SH3 domain of p47<sup>phox</sup> with proline rich regions at the C-terminal of p22<sup>phox</sup>, between the PX domain of p47<sup>phox</sup> with membrane phospholipids and between the proline rich region of the p47<sup>phox</sup> with the SH3 domain of p67<sup>phox</sup> (Bedard and Krause, 2007). The small G protein Rac is also involved in the translocation of the cytosolic subunits and has been shown to translocate p67<sup>phox</sup> to the membrane (Vignais, 2002). The activated Rac interacts with the membrane via its prenylated tail. On translocation to the membrane p67<sup>phox</sup> binds with gp91<sup>phox</sup>, via its domain, and p47<sup>phox</sup> acts as an adaptor protein which helps to stabilise the interaction (Brandes and Kreuzer, 2005) (Figure 1.3).

Once activated the NADPH oxidase complex can produce superoxide by a series of electron transfer reactions. Electrons are donated by NADPH which becomes oxidised (NADP<sup>+</sup>). Then electrons are transferred to FAD. After, electrons transfer from the reduced FAD to the first haem and then move onto the second haem. The second electron can only be transferred from the partially reduced FADH to the first haem after the first electron has already been transferred to the second haem, as the iron centre in the haem can only accommodate one electron at a time (Bedard and Krause, 2007). From the second haem, the electrons are transferred to molecular oxygen producing 2 molecules of superoxide.

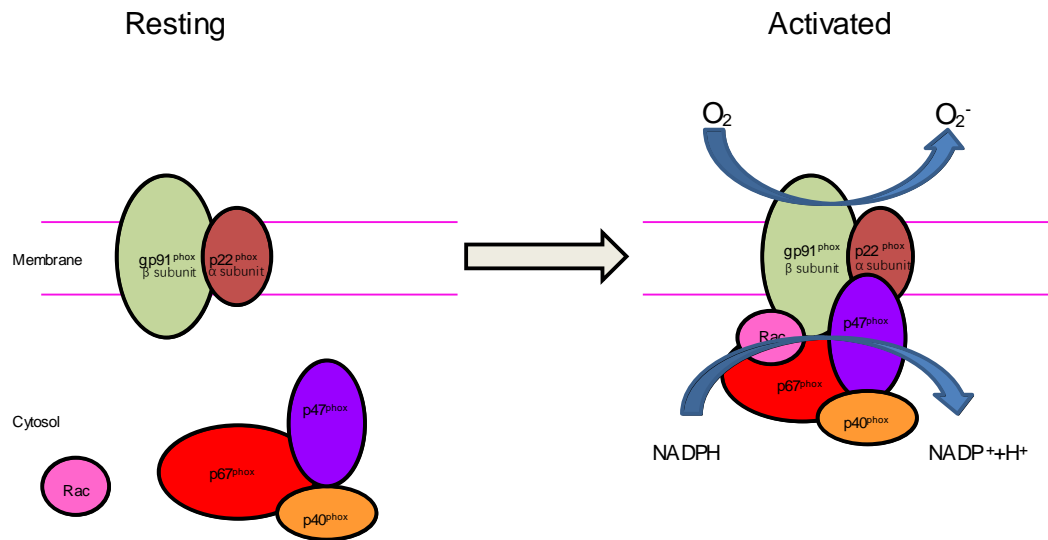


Figure 1.3. A representation of the activation of the Nox2. NADPH acts as an electron donor to produce superoxide.

## 1.4 ROS in physiology and pathology

NADPH oxidase is a fundamental enzyme existing in phagocytes which are an essential part of the immune system responsible for protecting against invading pathogens such as bacteria, cellular debris and any other foreign particles. It is required for the respiratory burst involving conversion of molecular oxygen to superoxide and is responsible for destroying invading pathogens. Phagocytes lacking NADPH oxidase are unable to destroy pathogens in an effective way and therefore it is the cause of CGD. It was reported that nearly 70% of CGD patients have mutations in the CYBB gene encoding for the gp91<sup>phox</sup> subunit (Heyworth et al., 2003). Additionally, other less common forms include mutation in genes encoding for p22<sup>phox</sup>, p40<sup>phox</sup>, p47<sup>phox</sup> and p67<sup>phox</sup> (Heyworth et al., 2003).

Although ROS is essential for mammalian cell biology, excessive ROS production can lead to oxidative stress which damages cellular components including lipids, proteins and nucleic acids, subsequently resulting in the loss of biological function. ROS can induce the production of carbon-centred radicals by attacking the polyunsaturated fatty acid residues of phospholipids. The carbon-centred radicals can then react with oxygen to form peroxy radicals (Marnett, 1999). Damage to DNA by ROS can cause base and nucleotide modifications as well as breaks in the DNA strand (Bennett, 2001). The oxidised form of DNA can lead to incorrect transcription and translation and therefore generate abnormal proteins. Subsequently, protein oxidation occurs at the protein polypeptide backbone and on the side chains of all amino acid residues of proteins by attack from the hydroxyl radical (Stadtman, 2004).

The redox-sensitive signalling pathways can be activated by ROS under the oxidation of cysteine residues on protein such as kinases, phosphatases and transcription factors. The mitogen-activated protein kinases (MAPK) are widely accepted as the most common downstream targets of Nox2-derived ROS, including the extracellular signal-regulated kinase (ERK), p38 MARK and c-Jun N-terminal kinases (JNK) (Fan et al., 2017, Li et al., 2005, Teng et al., 2012) as well as the protein kinase B (Du et al., 2013), nuclear factor kappa B (Li et al., 2009), TNF $\alpha$  receptor associated factor 4 (Li et al., 2005) and cell apoptosis related signalling molecules such as p21 and p53 (Li et al., 2007). Activation of the above redox sensitive pathways can result in both physiological and pathological cellular responses such as endothelial dysfunction, inflammation, migration, apoptosis and senescence. (Li and Shah, 2004, Fan et al., 2017).

ROS can also play a crucial role in the regulation of vascular tone. Hydrogen peroxide, one species of ROS, acts as an endothelium-derived hyperpolarising factor (EDHF)

which contributes to flow-induced dilation of human coronary arterioles (Miura et al., 2003). In addition, nitric oxide is important in the regulation of blood vessel relaxation. It plays a vital role in vasodilation of blood vessels and reduced bioavailability of NO is one of the causes leading to hypertension.

However, to protect excessive ROS production in the organisms, there are a wide variety of either antioxidant enzymes or antioxidant compounds that help to keep ROS at optimal levels. Firstly, uric acid is an oxidant compound that donates an electron to free radicals to neutralise them from becoming a radical itself, however the uric acid free radical is much more stable than oxygen-based radicals and can be converted back to uric acid (Becker, 1993). Secondly, vitamin C, also called ascorbic acid, can donate an electron to free radicals to become the ascorbate radical which is a relatively unreactive free radical and subsequently can be converted to ascorbic acid (Buettner and Jurkiewicz, 1996). Vitamin E, with its most common form called  $\alpha$ -tocopherol, is another powerful antioxidant compound that can donate a labile hydrogen to a lipid or lipid peroxy free radical, and subsequently can be reduced to the  $\alpha$ -tocopherol free radical. The  $\alpha$ -tocopherol free radical can then be converted to  $\alpha$ -tocopherol by ascorbic acid (Valko et al., 2006). Nevertheless, due to the limitation of the intestinal absorption and the concentration of vitamins in normal plasma, vitamins are insufficient to protect an organism against oxidative damage with ageing.

In addition to antioxidant compounds, antioxidant enzymes are also important in maintaining the ROS levels, for instance, superoxide dismutase (SOD). It was identified by McCord and Fridovich as an antioxidant enzyme which catalyses the dismutation of superoxide to oxygen and hydrogen peroxide (McCord and Fridovich, 1969). Catalase which exists in cell peroxisomes can reduce hydrogen peroxide to water (Valko et al.,

2006). Another antioxidant enzyme was found to be glutathione peroxidase (GPx) that reacts with glutathione (GSH) to convert hydrogen peroxide to water (Wassmann et al., 2004). Peroxiredoxins (Prx) are a family of antioxidants which can reduce various types of ROS including hydrogen peroxide and ONOO<sup>-</sup> (Loumaye et al., 2011).

### **1.5 Ageing-related oxidative stress and endothelial dysfunction**

Endothelial dysfunction has been implicated in the development of cardiovascular disorders including hypertension, atherosclerosis and heart failure (Bauersachs and Schafer, 2004, Cai and Harrison, 2000, MacCarthy et al., 2001, Potenza et al., 2009, Victor et al., 2009). Although many factors are capable of inducing endothelial dysfunction, their regulatory mechanisms are still not fully understood. In the past, the endothelium-derived NO has been well studied and the reduced NO bioavailability is considered to be one the major factor leading to endothelial dysfunction. In vasculature, the main biological function of NO is responsible for endothelium-dependent vasorelaxation, as well as inhibition of platelet and leukocyte adhesion (Harrison et al., 2003). The decline in NO bioavailability is therefore considered to be an early step in the pathogenesis of CVD. The reduction of NO bioavailability may be triggered by reduced expression of eNOS, or deficiency of eNOS substrate (L-arginine) and/or cofactor (tetrahydrobiopterin), or increased inactivation of NO by superoxide. Among these factors, NO inactivation by superoxide is recognised as a fundamentally important underlying mechanism in most settings. However, hydrogen peroxide derived from catalysing the dismutation of superoxide by SOD, increases level of eNOS expression through transcriptional and posttranscriptional mechanisms (Drummond et al., 2000).

Endothelial cells regulate and maintain ROS at a required level via a pro-oxidative and anti-oxidative system. However, increased and sustained high levels of ROS production

lead to an imbalance of ROS regulation, which is recognised as oxidative stress. It has become clear that excessive superoxide can directly interact with NO to form ONOO-, which consequently induces degradation of tetrahydrobiopterin and leads to eNOS uncoupling (Landmesser et al., 2003). In most conditions of oxidative stress-related endothelial dysfunction, the increased superoxide generation is not only from the endothelium itself but also contributed to from other cell types in the vessel wall, such as vascular smooth muscle cells and adventitial fibroblasts.

Ageing has been extensively studied as a major risk factor for the progressive increase in endothelial dysfunction which therefore leads to cardiovascular diseases (Herrera et al., 2010, Stampfli et al., 2010). Although the mechanisms behind this are not completely understood, increased superoxide production and decreased bioavailability of nitric oxide were found to be associated. Ageing-related decrease in endothelial function was seen in mice (Francia et al., 2004) and was associated with an increased superoxide production and a declined bioavailability of nitric oxide. The increased oxidative stress was also found to be correlated to endothelial dysfunction with advancing age in humans (Donato et al., 2007). Furthermore, the ageing vessels were found to produce more superoxide, along with increased expression of NADPH oxidase which was improved in the presence of an NADPH oxidase inhibitor and ONOO-scavenger (Rodriguez-Manas et al., 2009). The above findings support the role of NADPH-oxidase derived ROS in ageing-related endothelial dysfunction.

Nox2 and p47<sup>phox</sup> have been found to play a crucial role in NADPH-oxidase derived endothelial damage as the research linking NADPH oxidase and endothelial dysfunction has been carried out in Nox2 knockout and p47<sup>phox</sup> knockout mice. Nox2 knockout mice were generated by insertion of an expression cassette for neomycin

resistance into exon 3 of the Nox2 gene (Cybb) and attaching a flanking herpes thymidine kinase gene (Pollock et al., 1995). They were found to protect against high fat diet induced endothelial dysfunction (Du et al., 2013). p47<sup>phox</sup> knockout mice were created by obtaining a neo cassette interrupting exon 7, at amino acid 221 of the neutrophil cytosolic factor 1 (Ncf1) gene to abolish gene function (Jackson et al., 1995). They were shown to protect against angiotensin II induced endothelial dysfunction (Li et al., 2004). Furthermore, in mice with endothelium specific overexpression of Nox2, angiotensin II induced endothelial dysfunction was accelerated (Murdoch et al., 2011).

## **1.6 Ageing-related oxidative stress and neurodegeneration**

### **1.6.1 Central nervous system and NADPH oxidase**

Ageing is a major risk factor for the development of neurodegenerative diseases, which are characterised by the progressive neuronal death leading to the dysfunction of the central nervous system (CNS). Neurodegenerative diseases, in association to the ageing process, include Alzheimer's diseases, Parkinson's diseases and amyotrophic lateral sclerosis. The CNS consists of similar numbers of neuronal and non-neuronal cells, which were estimated as 86.1 billion neurons and 84.6 billion non-neuronal cells (Azevedo et al., 2009). Non-neuronal cells include microglia, astrocytes, oligodendrocytes and ependymal cells. They can interact with each other allowing the efficient transfer of action potentials throughout the CNS.

The NADPH isoforms existing in the CNS are Nox1, Nox2 and Nox4 (Infanger et al., 2006). Nox2 is expressed in microglia and astrocytes, where it is implicated in the inflammatory response (Infanger et al., 2006). Nox1 is expressed in human fetal brain tissue and microglia (Infanger et al., 2006). Nox4 exists in neurons and capillaries after

ischaemia (Vallet et al., 2005). Nox2, the classical NADPH oxidase, is predominantly located in intracellular phagosomes and in the plasma membrane of microglia (Guilarte et al., 2016). Nox2 also exists in endosomes which are responsible for early receptor mediated signalling (Oakley et al., 2009). It was shown that microglia also express Nox4. Despite that its function and subcellular localisation are not well characterised, it was believed to be implicated in intracellular H<sub>2</sub>O<sub>2</sub> production (Ambasta et al., 2004).

### **1.6.2 ROS in the CNS**

Excessive ROS are often seen in Alzheimer's disease (Markesbery, 1997) and it is thought that cytokines such as TNF $\alpha$  and IL-1 $\beta$  are originally released from activated microglia and subsequently contribute to microglia ROS production (Sawada et al., 2006). Increased ROS production were induced by these cytokines through activation of the NADPH oxidase, along with expression of iNOS and subsequent NO production (Brown and Bal-Price, 2003, Brown and Neher, 2010). In Parkinson's disease, the presence of aggregated  $\alpha$ -synuclein and lewy bodies (characteristic of Parkinson's diseases) promote microglial activation, and subsequent phagocytosis of these aggregates by microglia can induce ROS production (Thomas et al., 2007).

Microglial ROS production is also believed to be involved in AD progression. Beta-amyloid (A $\beta$ ), a characteristic peptide in Alzheimer's disease, activates NADPH oxidase in microglia and induces superoxide production (Brown and Neher, 2010). In addition, A $\beta$  also promotes microglial TNF $\alpha$  which feeds back onto microglial TNF $\alpha$  receptors to enhance microglial activation and ROS production (Meda et al., 1995). It was well documented that activation of microglial NADPH oxidase occurs when exposed to pathological substances such as A $\beta$  (250nM, three days), TNF $\alpha$  (50ng/ml, 24 hours) or other cytokines (Jekabsone et al., 2006) (Neniskyte et al., 2014) (Neniskyte

et al., 2016) (Turchan-Cholewo et al., 2009). Subsequently increased superoxide production promotes the activation of intracellular signalling cascades, such as Protein kinase C (PKC) (Konishi et al., 1997) and NF- $\kappa$ B (Schreck et al., 1991) which mediate the expression of pro-inflammatory genes and therefore exacerbate disease pathology. In this way microglial derived intracellular ROS activate microglia and enhance pro-inflammatory signalling (Block, 2008).

### **1.6.3 Microglia and microglial activation**

Microglia were first discovered and characterised by Rio Hortega, who recognized focal areas of invasion termed fountains of microglia in the corpus callosum and other white matter areas (Farber and Kettenmann, 2005). Among all the immune cells existing in the central nervous system (CNS), microglia represent 12% of the total cell number in the brain and 20% of glial cells (Block and Hong, 2007) and can instigate innate immunity within the brain parenchyma following an immune challenge (Walter and Neumann, 2009). A huge number of further investigations were carried out into the protective and immune roles of microglia. Microglial cells are derived from myeloid precursors and exists in a range of activation states, enabling them to respond appropriately to their environment (Stence et al., 2001).

In the normal environment, microglia have a ramified morphology and are termed “resting microglia”. However, microglial cells are highly dynamic in this state and they can constantly survey their microenvironment through extension and retraction of their processes (Nimmerjahn et al., 2005, Davalos et al., 2005). In this way, microglia monitor a defined area of the CNS and respond rapidly to any changes in their environment without making physical contact with other cells (Farber and Kettenmann, 2005). Resting microglia do not express the full repertoire of immune receptors seen on

activated microglia, however, they do express enzymes implicated in the removal of neurotransmitters from the cerebrospinal fluid, and are involved in maintaining neuronal function and structure (Booth and Thomas, 1991, Rimaniol et al., 2000). Although there are arguments over the role of microglia in the normal brain under physiological conditions, their highly dynamic resting state suggests that their main role is to monitor and protect the CNS from any damage. This has been supported by in vivo imaging of GFP-expressing microglia, which has shown that microglia continuously reorganise their processes, activating signals radiating from damaged neurons (Davalos et al., 2005, Fetler and Amigorena, 2005). Although microglial cells are retained in this ramified state by a range of neuronal interactions, the signals responsible for this continuous remodelling of microglial processes are not well understood (Garden and Moller, 2006). Microglial cells are also actively repressed by electrically active neurons, and the removal of this tonic inhibition following neuronal damage leads to microglial activation (Neumann, 2001). Neurons therefore play an important role in microglial activation state.

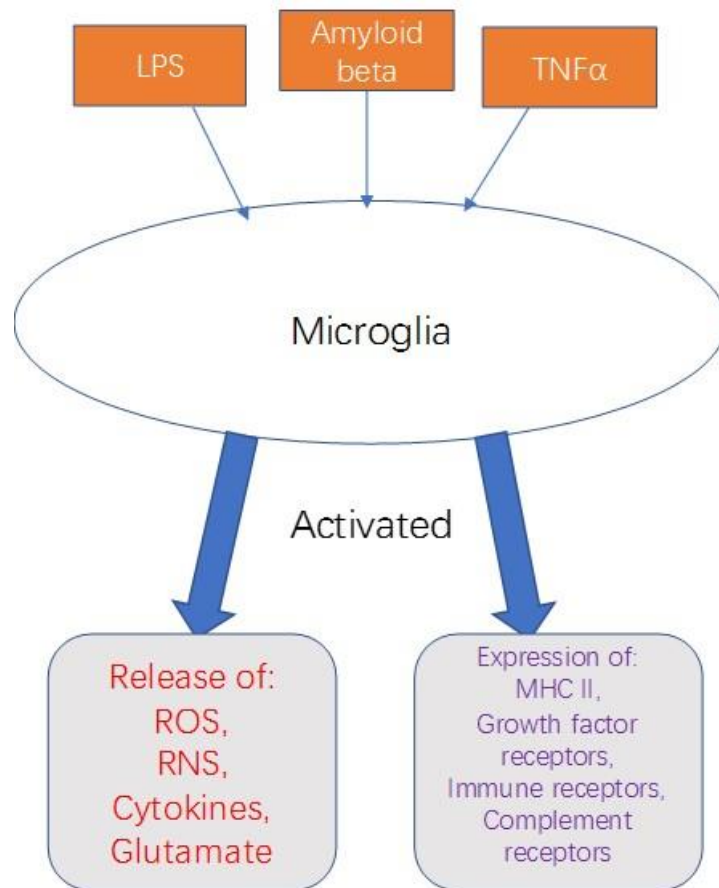


Figure 1.4. Microglia activation. Beta-amyloid, LPS and TNF $\alpha$  can activate microglia. Activation induces the expression of immune receptors, and also induces the release of mediator substances. Activated microglia can become migratory and move to the sites of neuronal injury, or phagocytic, enabling them to engulf pathogens and toxic proteins

Microglial cells are activated by a variety of stimuli released from damaged or dying neurons, and other cells of the CNS. Structurally, microglial activation is a process with cells changing from a ramified morphology to a hyper-ramified morphology, followed by becoming amoeboid, which facilitates migration to sites of neuronal injury (Raivich, 2005). It was demonstrated (Booth and Thomas, 1991) that the adenosine tri-phosphate (ATP) acts as one of the signals released from damaged neurons for microglia to respond. Microglial cells were shown to be unable to respond to CNS damage after

blockage of ATP signalling whereas addition of ATP to microglia can induce the activation to levels seen during CNS injury (Davalos et al., 2005). Furthermore, physical damage to CNS tissue through the formation of lesions or damage to blood vessels or the blood-brain barrier, which results in an influx of immune cells from the periphery also promotes microglial activation and the damage of blood vessels specifically may induce this activation through exposure of microglia to blood-derived factors such as thrombin (Moller et al., 2000), albumin or leukocytes (Nimmerjahn et al., 2005). Activated microglia are characterised by a number of phenotypic and morphological changes. A hallmark of microglial activation is the retraction of processes and enlargement of the cell body and nucleus. Activated microglia also express several immune receptors and immunomodulatory proteins such as the major histocompatibility complex II (MHC II), complement factors, and growth factors (Rimaniol et al., 2000). Importantly, microglial activation promotes the release of mediator substances such as reactive oxygen species (ROS), cytotoxic proteases, reactive nitrogen species (RNS) and glutamate (Block and Hong, 2007). Microglial activation can be either protective or toxic (Streit, 2002). Activated microglia can maintain and support neuronal survival by releasing trophic and anti-inflammatory molecules, such as transforming growth factor- $\beta$  (TGF- $\beta$ ) and interleukin-6 (IL-6) (Boche et al., 2006), removing invading pathogens or toxic products (Liu et al., 2002), and facilitating the guidance of stem cells to lesion sites to promote neurogenesis (Walton et al., 2006). However, microglial activation can also release cytotoxic substances such as NO or ONOO- (Colton and Gilbert, 1987), superoxide (Cheret et al., 2008), and pro-inflammatory cytokines such as interleukin-1 $\beta$  (IL-1 $\beta$ ) and tumour necrosis factor- $\alpha$  (TNF- $\alpha$ ) (Bruce et al., 1996). Furthermore, microglial activation can

be perpetuated by autocrine pathways, in which cytokines released from microglia may enhance microglial activation (Walter and Neumann, 2009).

#### **1.6.4 Microglial Nox2 activation**

Microglia activation can be induced when exposed to stimuli and subsequently produce excessive ROS production following the activation of NADPH oxidase. It is believed to be harmful to both the microglia themselves and surrounding neurons. Thus, the activation of the microglial NADPH oxidase can lead to CNS damage and is associated with several neurodegenerative diseases. Nox2 is widely believed as one of the key enzymes responsible for the production of ROS. It was reported that Nox2 can mediate intracellular signalling procedures and regulate TNF receptor associated factor 2 (TRAF2) binding to the TNF-receptor1/TNF receptor associated death domain (TNFR1/TRADD) complex, promoting NF- $\kappa$ B translocation and cell death (Shen et al., 2004). Nox2-derived ROS in microglia promote microglial activation and proliferation. Neurotoxicity caused by Nox2-derived ROS can also lead to oxidative burst in conditions such as stroke (Jekabsone et al., 2006, Barger et al., 2007, Block and Hong, 2007).

Superoxide production, through activation of the microglial NADPH oxidase, plays an important role in regulating the expression of pro-inflammatory factors. The superoxide is also implicated in the oxidative burst and the removal of invading pathogens. According to the literature, intracellular superoxide production from microglia acts as a second messenger to regulate down-stream signaling pathways, such as PKC, MAPK and NF- $\kappa$ B (Mander and Brown, 2005, Guyton et al., 1996, Schreck et al., 1991). The activation of these signalling pathways modulates microglial reactivity, which promotes microglial mediated neurotoxicity. Importantly, the superoxide released from

microglia can be induced by toxins such as rotenone (Gao et al., 2002) and A $\beta$  (Qin et al., 2002) and this superoxide plays a critical role in inflammation related neurotoxicity. A $\beta$  can either promote or enhance neurotoxicity through the generation of superoxide and microglial activation. Furthermore, SOD or catalase mimetics, which remove superoxide or H<sub>2</sub>O<sub>2</sub> respectively, reduces (lipopolysaccharide) LPS-induced dopaminergic neurotoxicity, which therefore provides evidence that superoxide and H<sub>2</sub>O<sub>2</sub> play a central role in microglial mediated neurotoxicity (Wang et al., 2004).

Most research into microglial NADPH oxidase has focussed on the activity and expression of Nox2, which is implicated in many neurodegenerative conditions. Microglial Nox2 is up-regulated in Alzheimer's disease (Block, 2008), Parkinson's disease (Gao et al., 2003), ischaemia (Hur et al., 2010) and traumatic brain injury (Dohi et al., 2010). Several studies have shown that LPS significantly increases Nox2 induced superoxide production in microglia which is correlated with an increase in IL-6, IL-1 $\beta$  and TNF $\alpha$  production (Clement et al., 2010). Other studies also have shown that promoted superoxide production through Nox2 signalling initiates intracellular signalling cascades through the activation of NF- $\kappa$ B and subsequent cytokine release (Zhang et al., 2010). Additionally, LPS also stimulates iNOS expression and NO production, which cooperates with microglial NADPH oxidase-derived superoxide to produce the potent neurotoxin ONOO<sup>-</sup> (Brown, 2007). It was seen in Alzheimer's disease transgenic mice (the mice overexpresses the Swedish mutant (K670N M671I) human APP695 driven by hamster prion protein promoter) where NO production and Nox2 activation promotes neurotoxicity (Park et al., 2008).

Microglial Nox2 is heavily implicated in the neurotoxicity associated with neurodegenerative diseases and promotes the pathogenesis of inflammatory

degenerative conditions such as Alzheimer's disease and Parkinson's disease. A $\beta$  was reported to activate Nox2 and promotes assembly of the functional enzyme, leading to an inflammatory phenotype associated with the production of superoxide (Akiyama et al., 2000). Nox2 activation was also found to contribute to cytokine release resulting in neuronal apoptosis, which further promotes Alzheimer's disease progression (Combs et al., 2001). Nox2 activated by A $\beta$  leads to the production of intracellular ROS, which acts as a signalling molecule to promote the expression and release of pro-inflammatory cytokines, in particular TNF $\alpha$  (Forman and Torres, 2002). The released TNF $\alpha$  can be abolished by the NADPH oxidase inhibitor apocynin when microglial cells were exposed to A $\beta$  (Jekabsone et al., 2006). Furthermore, the release of cytokines such as TNF $\alpha$  from A $\beta$  activated microglia can act on TNF $\alpha$  receptors on microglia in an autocrine manner, promoting further activation of Nox2, and increased microglial reactivity in Alzheimer's diseases (Mander et al., 2006). Furthermore, the mouse model of Alzheimer's disease was created by transferring yeast artificial chromosomes which contains the entire genomic copy of human APP and/or PS-1 genes harboring FAD mutations into transgenic mice (Lamb et al., 1993) (Lamb et al., 1997). It was documented that a mutant APP YAC transgenic mouse develops A $\beta$  deposits and that this deposition is accelerated when the animals are mated to homozygosity and/or to mutant PS-1 YAC transgenic mice (Lamb et al., 1999). Studies have linked the inflammatory microglial response and Nox2 mediated superoxide production in Alzheimer's diseases with neuronal damage in this mouse model (Wilkinson et al., 2012), thereby suggesting that Nox2 is an important mediator of Alzheimer's disease progression.

## **1.7 Endothelial dysfunction and blood-brain barrier damage**

The blood-brain barrier is a special structure between the blood circulation and the brain tissues. It regulates and controls the entry of blood-borne molecules and cells into the brain and protects the brain from bacterial and virus invasion and to preserve brain microenvironment homeostasis (Pardridge, 2007, Davson, 2012). Therefore, the cerebral endothelium has a fundamental role in maintain brain homeostasis. It serves also a mean of communication between the circulating blood cells and underlying brain tissues (Pardridge, 2007) (Rubin and Staddon, 1999) (Ueno, 2007). As I have discussed above (1.4 Ageing-related oxidative stress and endothelial dysfunction) that endothelial dysfunction and oxidative stress due to Nox2 activation is important in the development of ageing-related cardiovascular and metabolic diseases, therefore it is important to investigate a role of endothelial Nox2 in ageing-associated brain oxidative stress and neuronal dysfunction.

## **1.8 Hypothesis and aim**

There was extensive evidence supporting the role of Nox2-derive oxidase stress in ageing-related vascular diseases and neurodegeneration. The deletion of Nox2 in mice have been widely used to investigate the role of Nox2 in various disease pathologies. However, the exact role of Nox2 in ageing-associated cerebrovascular damage and neurodegeneration is not fully elucidated. The hypothesis of the thesis is that Nox2-derived ROS is increased with ageing which causes an accumulation of oxidative stress and therefore leads to the development of cerebral endothelial damage and brain dysfunction.

Therefore, the aim of this PhD research project is to investigate the role of Nox2 in brain oxidative stress, cerebral endothelial damage and brain dysfunction. According to the literature (Flurkey et al., 2007), the mouse age groups used are comparable with human ageing with young mice aged 3-4 months comparable to a 20-25-year-old “young” adult human and ageing mice of 21-22 months old are comparable to an over 60-year-old elderly human. In addition, the endothelium-specific Nox2 overexpression in mice in young (3-4 months) and early ageing (12-14 months) were also used to uncover the role of Nox2 in ageing-related endothelial dysfunction.

## Chapter 2

### Materials and methods

#### 2.1 Animal and sample information

All animal experimental procedures were conducted with protocols approved by the Guidance on the Operation of the Animals (Scientific Procedures) Act, 1986 (UK Home office). Experiments were performed with male wild-type (WT) and Nox2 knockout (Nox2<sup>-/-</sup>) mice on a C57BL/6 background at young (3-4 months old) and ageing (21-22 months old). Nox2<sup>-/-</sup> mice were generated by Pollock et al. by insertion of an expression cassette for neomycin resistance into exon 3 of the Nox2 gene (Cybb) and attaching a flanking herpes thymidine kinase gene insertion of a neomycin resistant gene (Pollock et al., 1995). All mice were initially purchased from the Jackson Laboratory (<https://www.jax.org/strain/002365>) and were subsequently bred at the animal unit in the university. All mice were housed at 18-23 °C and 45-55 % humidity in a 12:12 hour light dark cycle with lights on at 7 am. Nox2<sup>-/-</sup> mice were kept in sterile cages with sterile food and bedding and autoclaved water. The brain samples of young (3-4 months) and early ageing (12-14 months) Nox2 transgenic mice were kindly provided from Prof. Channon's group (Bendall et al., 2007). The Nox2 overexpression mice were created by constructing a human Nox2 transgene incorporating the murine Tie2 promoter and intronic enhancer, which then underwent pronuclear microinjection into fertilized eggs from superovulated C57BL/6xCBA mice. The brain samples of young (20-40 years old) and old (over 60 years old) human were kindly provided by Prof. Smith (MRC Brain Bank, University of Edinburgh).

## 2.2 Genotyping

Genotyping was performed on mice with an age of 10-15 days by polymerase chain reaction (PCR) and gel electrophoresis to identify *Nox2*<sup>-/-</sup> hemizygous male mice for scientific use. The tail of each mouse was marked with permanent marker for identification and a tail (~ 2mm) was cut and placed into a pre-labelled DNase-free 1.5 ml Eppendorf tube. After, each tail sample was digested with 150 µl of tail lysis buffer (10 mM Tris HCl pH 7.5, 50 mM KCl, 1.5 mM MgCl<sub>2</sub>, 0.01% Gelatin, 0.45% Nonidet P-40, 0.45% Tween-20, 200 µg/ml Proteinase K) in a water bath at 55 °C with gentle agitation. To deactivate proteinase K, all samples were heated at 95 °C for 5 minutes at the following morning. Next, the samples were briefly mixed by a vortex mixer, followed by centrifuging at 13000 x g for 5 minutes to pellet the debris. The supernatant containing genomic DNA was then used for PCR analysis. Alternatively, the supernatant can be stored at - 20 °C for future use.

Table 2.1 Thermal cycling parameters.

| Step | Temperature | Time   | Comments                       |
|------|-------------|--------|--------------------------------|
| 1    | 94 °C       | 3 min  |                                |
| 2    | 94 °C       | 20 sec |                                |
| 3    | 64 °C       | 30 sec | -0.5 °C per cycle              |
| 4    | 72 °C       | 35 sec | Repeat steps 2-4 for 12 cycles |
| 5    | 94 °C       | 20 sec |                                |
| 6    | 58 °C       | 30 sec |                                |
| 7    | 72 °C       | 35 sec | Repeat steps 5-7 for 25 cycles |
| 8    | 72 °C       | 2 min  |                                |
| 9    | 10 °C       |        | Hold                           |

A common forward primer (5'-AAG AGA AAC TCC TCT GCT GTG AA-3'), a wild-type reverse primer (5'-CGC ACT GGA ACC CCT GAG AAA GG-3') and a Nox2<sup>-/-</sup> reverse primer (5'-GTT CTA ATT CCA TCA GAA GCT TAT CG-3') synthesised by Eurofins MWG Operon were designed to amplify the areas of interest. The PCR mix (each mixture contains 1x GoTaq Flexi Buffer, 2.5 mM MgCl<sub>2</sub>, 0.2 mM dNTP mix, 1 μM common forward primer, 1 μM WT reverse primer, 1 μM Nox2<sup>-/-</sup> reverse primer and 0.3 Units of GoTaq Hot Start polymerase) was prepared on ice and 10 μl together with 2 μl of DNA sample from the digested tail tissue were added to PCR tubes. PCR reactions were performed on a PCR thermal cycler (Techne, UK) according to the thermal cycling parameters in table 2.1.

While the PCR was running, a 3% agarose gel was made up in a glass duran bottle by adding 3 g of agarose to 100 ml tris-acetate-EDTA (TAE) buffer containing 40 mM Tris-acetate and 1mM ethylenediaminetetraacetic acid (EDTA), and heating in a microwave until fully dissolved. 5 μl of Gel-Red (Biotium, USA) was added into the cooled (~ 55 °C) agarose solution before being poured into a gel rack. Then the rack containing the set gel was transferred to an electrophoresis chamber (Fisher Scientific, UK) with chilled 1x TAE buffer. Next, samples and a 100 bp DNA ladder were loaded onto the gel and the electrophoresis was carried out at 120 V for around 45 minutes. A GeneGenius bio imaging system (Syngene, UK) with the GeneSnap (Syngene, UK) software was applied to visualise and to capture bands. The presence of a 240-base pair (bp) band in the gel represents the wild-type allele and a 195 bp band represents the Nox2 allele. Heterozygote mice were identified by the presence of both bands.

### **2.3 Collection of mouse organs and tissues**

Animals were euthanised by an intraperitoneal (IP) injection of over-dose sodium pentobarbital (100mg/kg). After the mouse was confirmed dead, the body was sprayed with 70% ethanol. The skin below the ribs was lifted up using forceps and scissors were applied to make a small cut. Then, scissors were inserted into the cut made and opened. This was repeated until the skin was separated from the abdominal and thoracic cavities. After, the skin was cut along the midline of the body up to the neck and down to the legs. Once the cut was made to open the midline and cross the body below the ribs, the abdominal region was opened up. The handle of the scissors was used to gently push the intestines to the side until the inferior vena cava was clearly visible. A 25-gauge needle was carefully inserted into the vein to slowly draw the blood into a syringe and transferred into a 1.5ml Eppendorf tube with no anticoagulant. The stomach and intestines were removed after the blood collection. The fat, pancreas, spleen, kidneys and liver were collected afterwards. The rib cage was then removed by cutting along the sternum towards the head, through the ribs down to the diaphragm and through the diaphragm to give access to the heart and lungs which were collected. By cutting the connective tissue underneath the vessel, the aorta was then collected from the heart down to the iliac bifurcation. The brain was collected by cutting and peeling away the skull and then gently lifting out with a thin spatula. The muscle was collected by cutting through the femur close to the pelvis and then pulling the leg free allowing the muscle to be easily removed. All organs were firstly washed in ice-cold PBS and were then dried by soft tissues. The whole part of each organ was used to determine the organ weight expect muscle collected only from upper legs. Each organ was subsequently

measured by an analytical balance (Kern, UK) and was finally fixed in formalin or frozen at -80 °C for future use for the research group.

## **2.4 Isolation of coronary microvascular endothelial cell (CMEC)**

This method had been described in details by our group in previous publications (Li et al., 2001, Teng et al., 2012). For doing that, five to six hearts from 11-12 months old mice were excised and were immersed in ice cold calcium-free phosphate buffered saline (PBS). Hearts were then briefly dipped into 70% ethanol to devitalize epicardial mesothelial cells and re-immersed in PBS. The ventricular cavities were opened and washed carefully with PBS before minced into 1mm<sup>3</sup> pieces in calcium-free Hank's balanced salt solution (HBSS) supplemented with glucose 2 mM, taurine 2.5 mg/ ml, bovine serum albumin (BSA) 0.1%, and MgCl<sub>2</sub> 1.4 mM. The tissue pieces must be small enough to pass through a 10-ml pipette. Tissues were then transferred into a 50 ml Falcon tube and centrifuged at 25×g for 3 minutes. The tissue pellet was pre-digested for 5 minutes in 10 ml of pre-warmed collagenase (1 mg/ml), dissolved in modified HBSS at 37°C, and sheared by passing 10 times through a 10-ml pipette. The supernatant was discarded, and the collagenase digestion was repeated another twice with shearing every 3 min. The tissue pellet remaining at this stage was added with 8 ml EC isolation buffer containing 0.05% trypsin, 1 µg/ml DNase, 0.1 mM EDTA and 2 mg/ml glucose dissolved in HBSS, followed by 10 minutes incubation at 37°C with shearing every 3 min. At the end of this period, the supernatant was removed into a 12 ml Falcon tube containing 1 ml FBS. Cells were then separated from tissue debris and remaining myocytes by centrifuging at 25×g for 3 min. The supernatant was then spun at 120×g (4°C) for 7 min to sediment endothelial cells. A total of three 10 min digestion periods were required. After, cells were re-suspended in 10 ml growth medium

containing Dulbecco's modified Eagle's medium (DMEM) supplemented with 20% FBS, EC growth supplement (50 g/ml), 2-mercaptoethanol (5  $\mu$ M), L-glutamine (2 mM), penicillin (50 U/ml) and streptomycin (50 g/ml). Cells were seeded onto a gelatin-coated T-25 flask and cultured at 37°C with 5% CO<sub>2</sub>. After 2 hours, the medium containing debris and non-attached cells was replaced with fresh medium. After 24 hours, cells were washed twice with pre-warmed PBS and the medium was renewed.

## **2.5 Cell culture**

A mouse microglial cell line (BV-2) derived from raf/myc-immortalised murine neonatal microglia was purchased from Banca Biologica e Cell Factory, Italy. BV-2 cells were grown in RPMI1640 medium containing 10% (v/v) heat-inactivated fetal bovine serum (FBS), 100 U/ml ampicillin, 100  $\mu$ g/ml streptomycin and 2 mM L-glutamine. Cells were grown on non-coated flasks and continuously cultured in a humidified atmosphere at 37 °C, 95% O<sub>2</sub> and 5% CO<sub>2</sub>. BV-2 from passage 2-10 were used for all experiments. For all the cell culture work in this thesis, cells (BV-2, CMEC) were serum starved before stimulations occur.

### **2.5.1 Thawing cells**

Cells preserved in liquid nitrogen cryo-storage facility were removed and thawed at 37 °C in a water bath until small ice crystals were observed. Cryovials were decontaminated with 70% alcohol and placed in a class II tissue culture cabinet. Cells were then transferred to a 15ml falcon tube and washed with 9 ml phosphate buffered saline (PBS; Sigma), followed by centrifugal collection at 800 rpm for 7 minutes. After discarding the supernatant, cells were thoroughly re-suspended in 1 ml complete cell culture medium and transferred into a cap-vented T75 cell cultured flask containing 7

ml complete cell culture medium. Cells were cultured and maintained in an incubator with 5% CO<sub>2</sub>, at 37°C until reaching ~90% confluence.

### **2.5.2 Passaging cells**

After cells had reached 85 – 90% confluence, culture medium was discarded from the cell culture flask and the remaining cells were washed with 5 ml PBS. Next, 3 ml of Trypsin (0.5 g/l)-EDTA (0.2 g/l; Sigma) was added to coat the whole flask (for T25 flask: 1 ml of Trypsin-EDTA, for 10cm culture dishes; 1.5 ml of T rypsin-EDTA) and cells were incubated with the presence of Trypsin-EDTA at 37°C for 1-2 minutes. Trypsin-EDTA has the function to detach cells by inhibiting cell to cell contact and it also dislodges cells from the surface of the tissue culture flask. 5 ml of 10% FBS cell culture medium was immediately added into the flask and mixed well to neutralise the trypsin action. Cell suspension from the flask was transferred into a 15 ml falcon tube and cells were pelleted at 800 rpm for 5 minutes. 20 µl of suspended cell aliquot was taken to determine cell number and cell viability and processed as in section 2.3.3.

### **2.5.3 Cell count and cell Viability**

To determine cell number, viability and structure, cells were counted using a haemocytometer with trypan blue (0.4% w/v; Sigma), a negatively charged impermeable dye which enters the cells upon loss of membrane integrity. Trypan blue stained cells are considered dead or non-viable cells. After 1 minute, diluted cells were loaded onto the haemocytometer counting chamber and immobilised by using a coverslip. Cells in their physical state (alive or dead) were identified by their uptake of the dye. Observation and counting were done under a Zeiss light microscope at 20x magnification. The ratio of dead and alive cells as well as total number of cells was

taken from all four corners of a 4x4, 1/25 mm<sup>2</sup> quadrant. Cell viability was determined by the percentage of dead cells in the total cell count. Cells with a total viability of >95% were used in all experiments. The structure of cells was also observed and captured by light microscope.

#### **2.5.4 Freezing cells**

Both primary and immortalised cells can be frozen, preserved and stored in liquid nitrogen for stocks and long-term storage. To preserve quality frozen cells, a freezing mixture containing sterilized DMSO and FBS was initially prepared by adding one volume of DMSO into four volumes of FBS (20% DMSO/ 80% FBS solution). The mixture was thoroughly mixed by inversion and was cooled down and placed on ice for a minimum of 20 minutes before use (maximum 2 hours). Cultured cells were collected and a 0.5 ml (containing 1 x 10<sup>6</sup> or 2 x 10<sup>6</sup> cells) aliquot of cell suspension in complete (10% FBS) culture medium was transferred to a 2 ml cryovial followed by the addition of an equal volume of pre-cooled 20% DMSO/FBS freezing mixture drop-wise using a 1 ml pipette with constant agitation. Finally, the cryovial was placed in a room temperature cryo-freezing container containing isopropanol and immediately placed at -80 °C. Isopropanol has a valuable property for freezing cells, it enables temperature to decrease by 10 °C per minute to prevent cell damage by rapid freezing and formation of large ice crystals. After 24 hours, the frozen cells were removed and stored in a liquid nitrogen cryo-storage facility.

## **2.6 Beta-amyloid stimulation**

An excess of beta-amyloid (A $\beta$ ) accumulating into toxic fibrillar deposits within extracellular areas of the brain is believed to be the central pathological cause of

Alzheimer disease. These deposits ultimately destroy neural and synaptic function and lead to neuronal degeneration and dementia (Bell and Claudio, 2006). Beta-amyloid (A $\beta$ ) (1-42), a major component of amyloid plaques, accumulates in neurons of Alzheimer's disease brains. A $\beta$  (1-42) is reported to be resistant to degradation. It can accumulate as insoluble aggregates in late endosomes or lysosomes (Glabe, 2001). The intracellular accumulation of this insoluble amyloid is thought to be associated with many of the key pathological events of Alzheimer's disease. This intracellular amyloid induces the production of ROS (Glabe, 2001).

A $\beta$  (1-42) was purchased from Ana Spec, USA, with a sequence of H-Asp-Ala-Glu-Phe-Arg-His-Asp-Ser-Gly-Tyr-Glu-Val-His-His-Gln-Lys-Leu-Val-Phe-Phe-Ala-Glu-Asp-Val-Gly-Ser-Asn-Lys-Gly-Ala-Ile-Ile-Gly-Leu-Met-Val-Gly-Gly-Val-Val-Ile-Ala-OH (3-letter code). 1.0% NH<sub>4</sub>OH was directly added to resolve the lyophilized peptide power, followed by using 1x PBS as solvent to sub-dilute the solution to a concentration of 1 mg/mL.

A $\beta$  (1-42) was prepared following the guidance from the manufacturer. Oligomers were prepared by diluting the A $\beta$  (1-42) to 25  $\mu$ M with phenol red free DMEM-F12 and incubating for 24 h at 4 °C without shaking. Fibrils were similarly prepared by incubating 25  $\mu$ M A $\beta$  (1-42) in PBS at 37 °C for 24 h with vigorous shaking. Reconstituted peptide was aliquoted into several freezer vials and stored at -20°C.

BV-2 cells were cultured to 85-90% confluence on tissue culture flasks or 6-well plates. A $\beta$  (1-42) alone was kept at 37°C for at least an hour before use. After confluence, cells were subsequently incubated with 0.1-5  $\mu$ M A $\beta$  (1-42) in serum-free medium for 30 minutes at 37°C according to either acute or chronic stimulation. Cells were then scheduled for harvest accordingly as below.

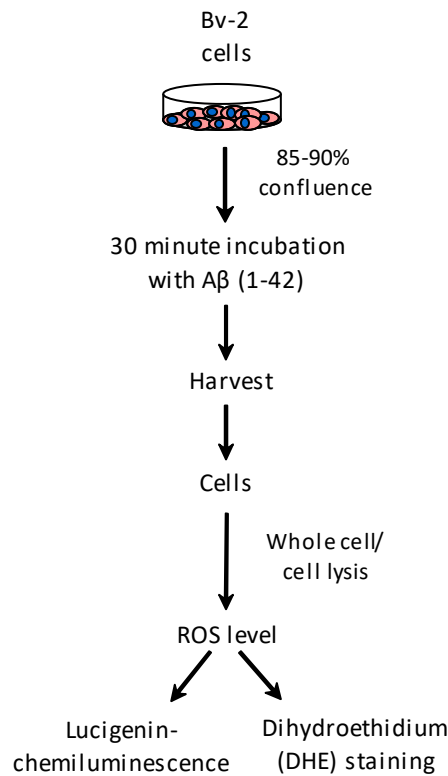


Figure 2.1. The procedures of examining ROS from BV-2 microglial cells stimulated by Aβ (1-42).

## 2.7 Tissue homogenisation, protein extraction and quantification

Approximately 3mm<sup>3</sup> cube was separated from each organ tissue (only mid-brain was used for the homogenisation of brain samples) and grinded with liquid nitrogen. Then the tissue was suspended in ice cold Hank's Balanced Salt Solution (HBSS). Next, the suspension was homogenised for approximately 1 minute. on ice with an ergonomic handheld homogeniser (Polytron, UK). The procedures were repeated 3 times. An additional one round is applicable if the mixture is not properly homogenised. For cell disruption, an ultrasonic processor (Sonic & Materials Inc, USA) was applied to release biological molecules from inside a cell. Sonication was processed twice (20% amplitude, 20 seconds each) with 1-minute intervals on ice. To acquire cellular

constituents, cells were re-suspended in an appropriate volume of harvesting buffer and homogenised for 30 seconds on ice using the hand-held homogeniser followed by 2 pulses of 10 seconds sonication on ice using ultrasonic processor at half of maximal amplitude. Cell homogenates were then analysed for their protein concentration.

Protein concentration was measured by the Bradford protein assay (Bradford, 1976) using Bio-Rad Dye (Bio-Rad Laboratories GmbH # 109219). Milli-Q water was used to dilute Bio-Rad Dye 1 in 5 and transferred into 1.6 semi-micro plastic disposable cuvettes in order to blank the spectrophotometer (WPA UV1101). 2µl of tissue homogenates was added to 1mL of the diluted Bradford reagent and absorbance was measured at 595nm. Protein concentration (µg/µl) was calculated according to the following equation from known bovine serum albumin (BSA) protein standards equation:

$$Y = (17.44X - 0.428) / V$$

Where Y= protein concentration (µg/µl); X= absorbance; and V= volume injected (µl).

## **2.8 Measurement of ROS production by lucigenin chemiluminescence**

### **Assay**

O<sub>2</sub><sup>-</sup> production was measured using lucigenin-enhanced chemiluminescence in a 96-well microplate luminometer (Molecular Devices, UK). Lucigenin (bis-N-methylacridinium) is first reduced by one electron to produce the lucigenin cation radical. Superoxide then reduces this cation radical to produce lucigenin dioxetane, which decomposes creating two molecules of N-methylacridone. When one of them relaxes to its ground state from the excited state, the light was emitted (Guzik and Channon, 2005) and detected by the microplate reader.

Tissue homogenates and cell samples were prepared as described (section 2.2). All measurements were carried out in the luminometer which was set to 37°C. Firstly, the amount of protein used from each sample was normalised to 50µg in lucigenin buffer (0.8mM MgCl<sub>2</sub>, 1.8mM CaCl<sub>2</sub> in HBSS). Secondly, the lucigenin was injected by the microplate reader to achieve a low concentration (5µM) that minimizes the artifactual superoxide production via redox cycling. To obtain a basal reading, omitted light expressed as relative light units (RLU) was recorded for 11 cycles with 3 second intervals per well. 100µM NADPH was then added manually to each well before 21 cycles of readings with 3 second intervals per well were recorded. To confirm specificity of superoxide, tiron (10mM), a cell-permeable superoxide scavenger, was added to each well and another 21 cycles were repeated. All studies were performed in duplicate.

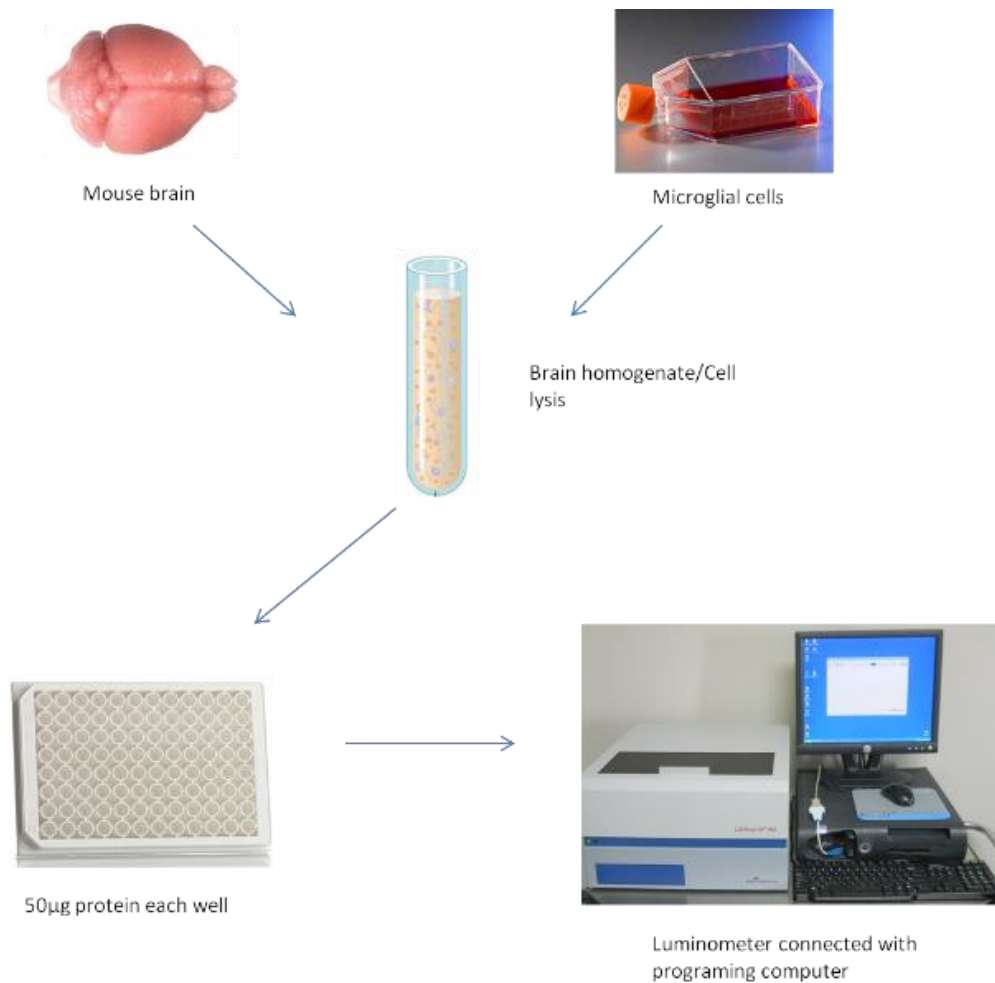


Figure 2.2. Illustration of lucigenin-chemiluminescence technique. Lucigenin buffer: Hank's balanced salt solution plus freshly added  $MgCl_2$  0.8 mM and  $CaCl_2$  1.8 mM. Lucigenin (final concentration 5  $\mu M$ ) and NADPH (final concentration 100  $\mu M$ ) were injected into the wells through the auto-dispensers in the dark chamber of the luminometer just before reading. The final volume was 200  $\mu l$ /well.

To investigate the enzymatic sources of superoxide using NADPH as a substrate, samples were incubated in a 96 well plate with the following inhibitors: 100 $\mu M$  NOS inhibitor (N $\omega$ -Nitro-L-arginine methyl ester, L-NAME), 100  $\mu M$  xanthine oxidase inhibitor (oxypurinol), 20  $\mu M$  flavoprotein inhibitor (diphenyleneiodonium) and 10

mM tiron. The measurements were performed as described above after a 10-minute incubation period.

## **2.9 *In situ* Dihydroethidium (DHE) detection of superoxide production by tissue sections**

Dihydroethidium (DHE) staining was performed to measure intracellular superoxide levels in brains. DHE can freely permeate cell membranes and react with superoxide inside cells to produce a red fluorescent product (2-hydroxyethidium) and therefore be used to monitor superoxide production (Owusu-Ansah et al., 2008). Frozen sections of brain were cut (10 $\mu$ m) by a cryostat (Carl Zeiss Ltd, UK) and thawed onto superfrost plus slides (VWR, UK). Cells were seeded into chamber slides and kept in the incubator overnight to allow cells to attach.

The slides were incubated with 100  $\mu$ l of DHE buffer (50 $\mu$ M in HBSS) per section and dried by tapping off the excess buffer. Then 20  $\mu$ l of DHE buffer was added to each section and the slides were incubated at 37°C for 15 minutes. 20 $\mu$ l of DHE staining solution (2 $\mu$ M in DHE buffer) was then added onto each section for 5 minutes in the dark before images were captured under a Euromex fluorescent microscope (Euromex, The Netherlands) equipped with a Hamamatsu Camera (C8484-05G01, Hamamatsu, Japan) at 20x magnification with a minimum of 10 images taken per section. The excitation wavelength is 530-560nm while the emission wavelength is 575-650nm. All images were quantified by using Simple PCI imaging software (Hamamatsu, UK).

## **2.10 DCF (5-(and 6)-chloromethyl-2',7'-dichlorodihydrofluorescein diacetate) detection of intracellular superoxide production**

CMECs were collected when they reached 90% confluency. Cells were then counted and  $1 \times 10^4$  cells were seeded into cell culture degree 96-well plate until the next day. After, CMECs were stimulated with buffer, high glucose alone (25 mM), insulin alone (1.2 nM) or high glucose plus insulin for 24 hours. Cells were then washed with PBS twice before applying 5  $\mu$ M of DCF (Invitrogen, UK) in BPS. Cells were incubated for 30 minutes at room temperature, followed by 5 minutes incubation of 1xDAPI at dark. Cells were washed with BPS twice and was then proceeded for acquiring images under an Olympus BX61 fluorescent microscope equipment equipped with FTIC (excitation/emission: 470-495/510-550nm) and DAPI (excitation/emission: 360-370/420-460nm) filters.

## **2.11 SOD-inhibitable cytochrome c reduction assay for the measurement of superoxide production by tissue homogenates**

Cytochrome c is reduced by reaction with superoxide, producing ferrocytochrome c, which has a detectable absorbance at 550 nm. Tissue homogenates were prepared and the concentration was determined as described in section 2.5. The assay buffer containing 0.8 mM  $MgCl_2$  and 1.8 mM  $CaCl_2$  in HBSS and superoxide dismutase solution (2 U/ $\mu$ l) were prepared freshly. Protein samples (40 $\mu$ g protein dissolved in 70  $\mu$ l of assay buffer) were added into the well of a transparent, flat-bottom 96-well plate. Next, 20  $\mu$ l of HBSS or SOD (2 U/ $\mu$ l) was added into the wells accordingly. The plated was then shaken gently for a few times and incubated for 15 minutes at 37°C. While waiting, the cytochrome c solution (10mg cytochrome c in 10ml HBSS) and NADPH

solution (0.8 mg/ml) were prepared in wrapped foil. After, 100 µl of cytochrome c solution was added into each well and the plate was shaken gently. Finally, 20µl of NADPH was added into each well before detection. To conclude, in each well, the total volume is 210µl, containing 0.1 mM cytochrome c, 100 µM NADPH and 200U/ml SOD if required. The whole plate was measured by an absorbance reader (Molecular Devices, UK) at 550nm wavelength. A 150-minute running time was performed. Superoxide production was quantified in picomoles per microgram of protein from the difference between absorbance values obtained from sample wells with or without SOD. Each value was normalized using the equation:  $\text{nmol superoxide/ min / well} = \Delta\text{mAbs}_{550 \text{ nm}} / \text{min} \times 0.047619 \times \text{reaction volume (in mL)} / \text{path length (in cm)}$  (Molshanski-Mor et al., 2007). Therefore, the equation  $(\text{nmol O}_2 / \text{min} / \text{well} = \Delta\text{mAbs}_{550 \text{ nm}} / \text{min} \times 0.047619 \times 0.21 / 0.6)$  was applied.

## **2.12 Catalase-inhibitable amplex red assay for the measurement of hydrogen oxide production by tissue samples**

Amplex Red is a colourless and non-fluorescent compound that is used as a probe for the measurement of extracellular H<sub>2</sub>O<sub>2</sub>. Basically, Amplex Red reacts with H<sub>2</sub>O<sub>2</sub> at 1:1 stoichiometric ratios catalysed by horseradish peroxidase (HRP) to form the coloured and highly fluorescent compound resorufin. A small piece of the mid brain was obtained from the whole brain and mixed with 200 µl of HBSS into an Eppendorf tube. Each sample was homogenized for three times (1 minute each time, max speed) followed by sonication for twice (20% amplitude, 15 seconds each time). All samples were kept in ice during all steps. Protein concentration of each protein sample is determined as described in section 2.5. In advance, 10 mM stock solution of Amplex Red was prepared by dissolving Amplex Red reagent in DMSO and aliquot in 25 µl

vials. All stocks were kept in  $-20^{\circ}\text{C}$  with foil wrapped until further use. NADPH solution (0.8 mg/ml), 1 U/ $\mu\text{l}$  stock solution HRP and 1000 U/ml were also prepared in PBS with foil wrapped prior to experiments. To prepare standard concentrations of  $\text{H}_2\text{O}_2$ , 33%  $\text{H}_2\text{O}_2$  stock was diluted to 10x 0, 0.0625, 0.125, 0.25, 0.5, 1, 2  $\mu\text{M}$  in 50 mM potassium phosphate buffer (pH 7.7 containing diethylenetriaminepentaacetic acid). It should be aware that the commercial PBS cannot be used here as 500 mM potassium phosphate (pH 7.0) was contained. A black, transparent flat-bottom 96-well plate was applied. In the standard curve well, 10  $\mu\text{l}$  of various concentrations of  $\text{H}_2\text{O}_2$  were loaded together with 40  $\mu\text{l}$  PBS and 50  $\mu\text{l}$  Amplex Red (AR) solution containing 25 mM HEPES, pH 7.4, 0.12 M NaCl, 3 mM KCl, 1 mM  $\text{MgCl}_2$ , 25  $\mu\text{M}$  Amplex Red and 0.3 U/ml HRP). For the sample wells, 20  $\mu\text{l}$  of protein samples containing 20  $\mu\text{g}$  protein and 50  $\mu\text{M}$  glucose 6-phosphate were loaded together with 10  $\mu\text{l}$  of 1000 U/ml of catalase/PBS in the parallel wells. The plate was then incubated for 5 minutes at  $37^{\circ}\text{C}$ . Next, 50  $\mu\text{l}$  of Amplex Red solution was added to all sample wells. Finally, 20  $\mu\text{l}$  of NADPH (final concentration 0.1 mM) was applied to sample wells. The plate reader (FLUOstar OPTIMA, BMG, Germany) was set at  $37^{\circ}\text{C}$  before inserting the plate to the machine. The fluorescence filter was set up to 530 nm excitation and 587 nm emission. The plate was read for 90 minutes with 60 cycles. The standard curve of  $\text{H}_2\text{O}_2$  was generated using the fluorescent units obtained from standard  $\text{H}_2\text{O}_2$  wells.  $\text{H}_2\text{O}_2$  production was quantified using the differences between fluorescent units obtained from sample wells with and without catalase. The concentrations of  $\text{H}_2\text{O}_2$  of each sample was calculated according to the standard curve.

## 2.13 Immunofluorescence

The expression and location of antigens of interest in brains were investigated by indirect antibody labelling immunofluorescence. Frozen samples of brain tissues were cut into 10µm thickness sections via a cryostat (Carl Zeiss Ltd, UK) and thaw mounted onto superfrost plus slides (VWR, UK). All slides were fixed in 50:50 (v/v) methanol/acetone for 10 minutes at -20°C and then fan dried for 15 minutes before being stored at -80°C for further use. Cells were seeded into chamber slides and fixed with 2% paraformaldehyde (PFA) solution the next day. The fixing can be performed for either 10 to 20 minutes at room temperature or overnight at 4°C. The slides were then used for staining or stored at -80°C for further use.

Slides were taken out of the -80°C freezer and were fan dried at room temperature for 15 minutes. Then, slides were washed with ice cold 1x PBS prior to blocking with 50µl 2% bovine serum albumin (BSA) in 1x PBS with 0.5% Triton X-100 for 30 minutes at room temperature. Subsequently, sections were washed three times in ice cold 1x PBS and incubated with primary antibody (1:100 diluted in 0.2% BSA) for 1 hour at room temperature. Then, sections were washed with 1x PBS to remove excess antibody, followed by incubation with fluorescein isothiocyanate (FITC) or cyanin-3 (Cy3) fluoreochrome conjugated secondary antibodies (1:250 diluted in 0.2% BSA) for 45 minutes at room temperature. The secondary antibodies were then drained from the slides which were rinsed and washed three times in ice cold 1 x PBS. The above procedure was repeated using a second primary antibody and second fluoreochrome conjugated secondary antibody. 1x DAPI (4, 6-diamidino-2-phenylindole chloride) was added to each section and incubated for the final 5 minutes. 1x ice cold PBS was then used to wash off excess DAPI and secondary antibody, followed by dipping in MilliQ

water to remove excess salt. Finally, antifade solution (0.1% p-phenylenediamine: Mowiol=1:9) was applied on each section and coverslips were placed over the top without producing bubbles. Slides were kept at 4°C overnight in dark until the next day.

All slides were visualised by an Euromex fluorescent microscope (Euromex, The Netherlands) equipped with a Hamamatsu Camera (C8484-05G01, Hamamatsu, Japan) to investigate FTIC (excitation/emission: 470-495/510-550nm), Cy3 (excitation/emission: 530-560/575-650nm) and DAPI (excitation/emission: 360-370/420-460nm) fluorescence, expect that CMEC slides were captured under an Olympus BX61 fluorescent microscope equipment with the same camera and filters. Images were captured at 10x, 20x or 40x magnification with a minimum of 10 images taken per section. The fluorescence of each image is quantified using the HC ImageLive software, following the procedures provided by the manual (available at <https://hcimage.com/assets/pdfs/HCImageLiveGuide.pdf>)

## **2.14 Western blotting**

Western blotting aims to investigate into the relative expression of proteins of interest in mouse brain. Tissue homogenates were prepared and the protein concentration of each sample was determined using the Bradford assay as described above (section 2.2). All samples containing equal protein concentration (3 µg/µl) were prepared with 3X sample buffer and were boiled at 95°C for 5 minutes before storing.

To prepare for sodium dodecyl sulphate polyacrylamide gel electrophoresis (SDS-PAGE) separation, Mini-Gels were prepared using the Bio-Rad Mini-protein IITM (Bio-Rad, UK) according to the manufacturer's instructions. A 10% separating gel containing 5 ml of H<sub>2</sub>O, 2.5 ml of separating buffer, 2.5 ml of 40% acrylamide, 60 µl

of 10% ammonium persulfate and 6  $\mu$ l of TEMED was prepared and allowed to set before a 5% stacking gel containing 1.85 ml of H<sub>2</sub>O, 0.75 ml of stacking buffer, 0.375 ml of 40% acrylamide, 40  $\mu$ l of 10% ammonium persulfate and 4  $\mu$ l of TEMED was overlaid. The protein marker (Precision Plus Protein™ Standards, Bio-Rad, UK) was loaded into the first well of the gel and 10  $\mu$ l of samples were loaded into subsequent wells. The gel was run at 80 V for 30 minutes and then 110 V for about 100-120 minutes (The time depends on when the blue dye reached the bottom of the gel) in running buffer.

To transfer separated proteins from the gel onto a Millipore® Immobilon-P Polyvinylidene Difluoride (PVDF) transfer membrane (Sigma), a Bio-Rad Trans-Blot® Semi-Dry Transfer Cell (Bio-Rad), UK) was used. A unit of Bio-Rad Semi-Dry Transfer Cell is able to transfer 4 gels at a time. Filter papers (Whatman, UK) were soaked in transfer buffer for 10-15 minutes and the PVDF membranes were soaked in absolute methanol for 30 seconds followed by 2 minutes in distilled water and left in transfer buffer for 10 minutes. The transfer 'sandwich' was prepared by stacking the PVDF membranes with the separating gel on top between two layers of rectangular filter papers (four either side). The semi-dry transfer process was run constantly at 15V for 1 hour to enable larger molecular weight (>90kDa) protein transfer across from the gel onto the membrane. After, the membranes containing the transferred proteins were blocked with 2.5% non-fat milk/Tris-buffered saline-0.1% Tween 20 (TBST, recipe see table 2.6) on an orbital shaker for 1 hour at room temperature. Membranes were then incubated with primary antibodies diluted to their optimal concentrations with 2.5% non-fat milk in 1 X PBS over night at 4°C with orbital shaking. The next day, the membranes were left shaking at room temperature for 1 hours before being washed with 1 X TBST for 10 minutes then 1 X TBS for 10 minutes and finally 1 X PBS for 10

minutes. The membranes were then incubated with horseradish peroxidase (HRP)-conjugated secondary antibodies diluted to their optimal concentrations with 2.5% non-fat milk in 1 X PBS for 2 hours at room temperature on a orbital shaker. Following another set of 10 minutes washes with TBST, TBS and PBS, the membrane was exposed to Clarity Western Enhanced-Chemiluminescence Plus (ECLplus) reagent according to the manufacturer's instructions (Bio-Rad, UK) and antigen detection was carried out by a BioSpectrum AC Imaging System (UVP, UK). 60 images were captured in 20 minutes of exposure and each band was assayed for their optical density (OD) from the resulting image and normalised to alpha-tubulin as the loading control.

## **2.15 Assessment of locomotor activity**

WT and Nox2 knockout male mice of two age groups: young (3-4m) versus ageing (21-22m) were housed in wheel-running cages (ClockLab, Actimetrics, Wilmette, IL) in light-tight, sound-attenuated cabinets. Mice were entrained to a 12h: 12h light-dark (LD) cycles for 10 days and subsequently changed to a 10-day period of constant darkness (DD). After that, the animals were re-entrained to a 12h: 12h LD cycle. Temperature was maintained between 19 to 22°C and the relative humidity was kept at 50% ± 10%. Nox2 knockout mice were provided with autoclaved food and water and placed in sterilised cabinets while WT mice were kept in normal circumstance and supplied with normal food and water. The mouse movements in the wheel-running cage were detected by passive infrared (PIR) apparatus (RISCO Ltd, UK) and were recorded in 1-min bins. Data were collected on the last 8 days of LD cycle and the first 8 days of DD cycle. Entrainment to the LD and DD period was verified by using the  $\chi^2$  periodogram analysis (Sokolove and Bushell, 1978), which results in Qp values indicating the strength of the periodicity for specific period lengths. The activity data of PIR are averaged into 30

minutes bins. Fourier analysis was performed with Circwave (Hut, University of Groningen) to plot a fitted curve with number of harmonic set at 3.

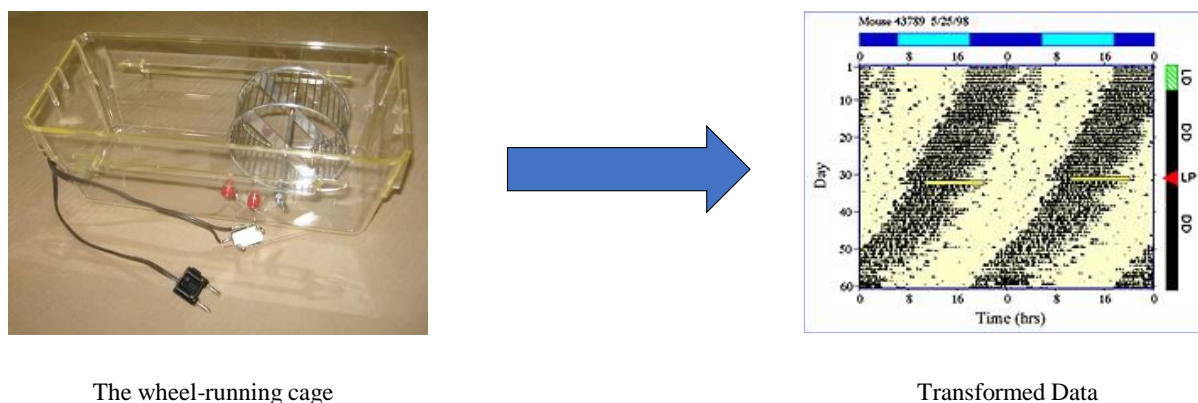


Figure 2.3. Photoshoot of a wheel-running cage (left) for mouse circadian assessment and a digital electronic record of the mouse movement shown on computer screen (right).

## 2.16 Statistical analysis

All the data used in this thesis are presented as mean  $\pm$  standard deviation (SD) and plotted and analysed using the GraphPad Prism 6 software. ANOVA is used to access the differences in a scale-level dependent variable by a nominal-level variable having 2 or more categories. Comparisons of results were made by either one-way or two-way ANOVA followed by a bonferroni *post-hoc* test depending either one or two independent variables existed in samples. A p-value of less than 0.05 was denoted as statistical significance. For the in vivo animal work, a number of at least 9-12 mice per group were used. For the ex vivo experiments using tissues from WT and Nox2<sup>-/-</sup> mice, a number of at least from 9 mice were used. For the ex vivo work based on Nox2 overexpression mice, a number of at least 6 mice were used. For the ex vivo work on

human brain samples, a number of at least 9 individual samples were used. For the in vitro CMEC work, cells from at least 3 independent isolation were used and each CMEC isolation used 6 mouse hearts. For the BV-2 cell culture experiments, with a number of at least 6 flasks per group were used.

## Appendix

Table I: List of materials and reagents

| <b>Materials</b>             | <b>Supplier</b>   | <b>Catalogue Number</b> |
|------------------------------|-------------------|-------------------------|
| 2-mercaptoethanol            | Sigma Aldrich     | M7154                   |
| Acetone                      | Fisher Scientific | A/0606/17               |
| Acetylcholine                | Sigma Aldrich     | A6628                   |
| Acrylamide                   | Fisher Scientific | BPE1410-1               |
| Ammonium persulphate         | Sigma Aldrich     | A9164                   |
| Ampicillin                   | Fisher Scientific | BPE1760-5               |
| Beta-amyloid 1-42            | Ana-spec          | AS-24224                |
| Bio-Rad Bradford Protein Dye | Bio-Rad           | 500-0006                |
| BSA                          | Sigma Aldrich     | A2153                   |
| Bromophenol blue             | Bio-Rad           | 161-0404                |
| Calcium Chloride             | Sigma Aldrich     | C5670                   |
| DHE                          | Invitrogen        | D11347                  |
| Diphenyleneiodonium Chloride | Sigma Aldrich     | D2926                   |
| DMSO                         | Sigma Aldrich     | D2650                   |
| DAPI                         | Sigma Aldrich     | D9542                   |
| ECL <sup>Plus</sup> reagent  | GE Healthcare     | NA                      |

|                                  |                     |             |
|----------------------------------|---------------------|-------------|
| EDTA                             | Fisher Scientific   | D/0700/53   |
| ECGS                             | Sigma Aldrich       | E2759       |
| Ethanol (100%)                   | Fisher Scientific   | E/0650DF/17 |
| FBS                              | Sigma Aldrich       | F2442       |
| Glucose                          | Sigma Aldrich       | G8270       |
| Glycerol                         | Sigma Aldrich       | G5516       |
| Glycine                          | Fisher Scientific   | G/0800/60   |
| Hanks' Buffered Salt Solution    | Gibco, Thermofisher | 14175-137   |
| Heparin                          | Sigma Aldrich       | H0135       |
| HEPES                            | Acros organics      | 7365-45-9   |
| Isopentane                       | Fisher Scientific   | 9/1030/17   |
| Insulin                          | Sigma Aldrich       | I6634       |
| KCl                              | Sigma Aldrich       | P3911       |
| KH <sub>2</sub> PO <sub>4</sub>  | Fisher Scientific   | P/4800/53   |
| L-Glutamine                      | Sigma Aldrich       | G3126       |
| L-NAME                           | Sigma Aldrich       | N5751       |
| M199 medium                      | Sigma Aldrich       | M4530       |
| Magnesium chloride               | Sigma Aldrich       | M8266       |
| Membrane filter (0.22 μm)        | Milipore            | SLGP033RS   |
| Methanol                         | Fisher Scientific   | M/4056/17   |
| Mowiol                           | Sigma Aldrich       | 81381       |
| Na <sub>2</sub> HPO <sub>4</sub> | Fisher Scientific   | N7785       |
| NADPH                            | Sigma Aldrich       | N7785       |
| Non-fat milk                     | Marvel              | N/A         |

|                               |                   |              |
|-------------------------------|-------------------|--------------|
| OCT                           | CellPath          | KMA-0100-00A |
| Oxypurinol                    | Sigma Aldrich     | O4502        |
| PBS                           | Sigma Aldrich     | P4417        |
| Paraformaldehyde              | Sigma Aldrich     | P6148        |
| Protease inhibitor cocktail   | Sigma Aldrich     | P8340        |
| PVDF                          | Sigma Aldrich     | P2813        |
| Propidium iodide              | Sigma Aldrich     | P4170        |
| Protein marker                | Bio-Rad           | 161-3074     |
| Rotenone                      | Sigma Aldrich     | R8875        |
| Sodium chloride               | Fisher Scientific | 10112640     |
| Sodium dodecylsulphate        | Sigma Aldrich     | 71725        |
| Sodium orthovanadate          | Sigma Aldrich     | S6508        |
| Sodium pyrophosphate          | Sigma Aldrich     | P8010        |
| Streptomycin/Penicillin (10X) | Sigma Aldrich     | P7539        |
| TEMED                         | Sigma Aldrich     | 87689        |
| Tiron                         | Sigma Aldrich     | 89460        |
| Triton X-100                  | Sigma Aldrich     | X100         |
| Tris-acetate                  | Sigma Aldrich     | T8280        |
| Tris Base                     | Fisher Scientific | T/3710/60    |
| Tris HCl                      | Sigma             | T5941        |
| Trypan blue                   | Sigma Aldrich     | T8154        |
| Trypsin-EDTA                  | Sigma Aldrich     | T3924        |
| Tween-20                      | Fisher Scientific | BPE337       |

Table II: List of antibodies used

| Antibodies            | Species | Dilution | Company         |
|-----------------------|---------|----------|-----------------|
| p47 <sup>phox</sup> * | Rabbit  | 1:500    | Santa Cruz      |
| CD31                  | Goat    | 1:500    | Santa Cruz      |
| Iba-1*                | Goat    | 1:500    | Santa Cruz      |
| NeuN                  | Mouse   | 1:500    | Millipore       |
| $\alpha$ -tubulin     | Mouse   | 1:1000   | Santa Cruz      |
| $\beta$ -actin*       | Rabbit  | 1:1000   | Bioss           |
| Nox1*                 | Goat    | 1:500    | Santa Cruz      |
| Nox2*                 | Rabbit  | 1:500    | Santa Cruz      |
| Nox4*                 | Rabbit  | 1:500    | Santa Cruz      |
| p22 <sup>phox</sup>   | Rabbit  | 1:500    | Santa Cruz      |
| p40 <sup>phox</sup>   | Rabbit  | 1:500    | Santa Cruz      |
| p53*                  | Rabbit  | 1:500    | Santa Cruz      |
| p67 <sup>phox</sup>   | Goat    | 1:500    | Santa Cruz      |
| Rac-1                 | Rabbit  | 1:500    | Santa Cruz      |
| Total-p38MAPK         | Rabbit  | 1:500    | Santa Cruz      |
| p-p38 MAPK            | Rabbit  | 1:1000   | Cell Signalling |
| Total-ERK1/2*         | Rabbit  | 1:500    | Santa Cruz      |
| p-ERK1/2*             | Mouse   | 1:1000   | Santa Cruz      |
| Total-JNK             | Mouse   | 1:1000   | Santa Cruz      |
| p-JNK                 | Rabbit  | 1:500    | Santa Cruz      |
| Total-Akt             | Rabbit  | 1:500    | Santa Cruz      |
| p-Akt                 | Rabbit  | 1:500    | Santa Cruz      |

\*Antibodies used for human samples

Table III: RPMI 1640 media constituents

| <b>Components</b>  | <b>Molecular Weight</b> | <b>Concentration (mg/L)</b> |
|--|-------------------------|-----------------------------|
| Glycine  | 75.0                    | 10.0                        |
| L-Arginine hydrochloride   | 211.0                   | 240.0                       |
| L-Asparagine   | 132.0                   | 50.0                        |
| L-Aspartic acid  | 133.0                   | 20.0                        |
| L-Cystine  | 240.0                   | 50.0                        |
| L-Glutamic Acid  | 147.0                   | 20.0                        |
| L-Glutamine  | 146.0                   | 300.0                       |
| L-Histidine  | 155.0                   | 15.0                        |
| L-Hydroxyproline   | 131.0                   | 20.0                        |
| L-Isoleucine   | 131.0                   | 50.0                        |
| L-Leucine  | 131.0                   | 50.0                        |
| L-Lysine hydrochloride   | 183.0                   | 40.0                        |
| L-Methionine   | 149.0                   | 15.0                        |
| L-Phenylalanine  | 165.0                   | 15.0                        |
| L-Proline  | 115.0                   | 20.0                        |
| L-Serine   | 105.0                   | 30.0                        |
| L-Threonine  | 119.0                   | 20.0                        |
| L-Tryptophan   | 204.0                   | 5.0                         |
| L-Tyrosine   | 181.0                   | 20.0                        |
| L-Valine   | 117.0                   | 20.0                        |
| Biotin   | 244.0                   | 0.2                         |
| Choline chloride   | 140.0                   | 3.0                         |
| D-Calcium pantothenate   | 477.0                   | 0.25                        |
| Folic Acid   | 441.0                   | 1.0                         |
| Niacinamide  | 122.0                   | 1.0                         |
| Para-Aminobenzoic Acid   | 137.0                   | 1.0                         |
| Pyridoxine hydrochloride   | 206.0                   | 1.0                         |
| Riboflavin   | 376.0                   | 0.2                         |
| Thiamine hydrochloride   | 337.0                   | 1.0                         |
| Vitamin B12  | 1355.0                  | 0.005                       |
| i-Inositol   | 180.0                   | 35.0                        |
| Calcium nitrate  | 236.0                   | 100.0                       |
| Magnesium Sulfate  | 246.0                   | 100.0                       |
| Potassium Chloride   | 75.0                    | 400.0                       |
| Sodium Bicarbonate   | 84.0                    | 2000.0                      |
| Sodium Chloride  | 58.0                    | 6000.0                      |
| Sodium Phosphate dibasic (Na <sub>2</sub> HPO <sub>4</sub> ) anhydrous | 142.0                   | 800.0                       |
| D-Glucose (Dextrose)   | 180.0                   | 2000.0                      |
| Glutathione (reduced)  | 307.0                   | 1.0                         |
| Phenol Red   | 376.4                   | 5.0                         |

## Chapter 3

### **Knockout of Nox2 attenuates the increased oxidative stress in multiple organs and preserves locomotor function in ageing mice**

#### **3.1 Introduction**

It is well known that ageing is one of the causes for oxidative stress and is a potential risk factor for developing vascular diseases. During ageing, ROS is accumulated in the organism, mostly owing to direct damage of sensitive and biologically significant targets, and thus becomes a major cause of oxidative stress. The free radical theory of ageing also suggests that accumulated damage caused by free radicals and ROS accelerates the ageing process (Harman, 1956). Among all the sources of ROS, the NADPH oxidases generating ROS act as important contributors to the oxidative stress and a link between risk factors and vascular diseases (Drummond et al., 2011).

The brain may be particularly vulnerable to oxidative stress, depending on its high oxygen metabolic rate (consumes approximately 20% of the total consumption of oxygen of a mammal); high dependence on oxidative metabolism for obtaining energy; high content of iron, an endogenous catalyser for the generation of ROS and reactive nitrogen species (RNS) and lower content of antioxidant enzymes compared with other organs (Floyd and Hensley, 2002, Mattson et al., 2002). Attention has been focused on the involvement of oxidative stress in brain dysfunction and neurodegenerative disorders. The production of ROS and subsequent oxidative stress have also been implicated in a final common pathway for the toxicity caused by a number of environmental neurotoxicants. In higher organisms, the brain has a very high energy demand which makes it more susceptible to the impact of metabolic by-products,

particularly to ROS. In ageing, increases in the concentration of oxidised macromolecules (Finkel and Holbrook, 2000) and upregulation of genes involved in the oxidative stress response are detected (Yankner et al., 2008). The relationship between oxidative stress and age-related changes in the brain has been examined in the senescent population. Many of these studies measured the consequent damage induced by ROS. For instance, increased ROS production found in 24 months age of mice compared with 3 months age was associated with endothelium dependent relaxation and neurovascular coupling induced by ageing (Park et al., 2007).

Numerous literatures have reported the increasing Nox activity with ageing. Along with the ageing-related increases of bodyweights, the Nox activities and Nox subunit expressions were found to increase in older mice (24 months) compared with young mice (4 months), fed with either Western diet (41% calories from fat) or very high fat lard diet (60% calories from fat) (Bruce-Keller et al., 2010). Along with the increase in bodyweight, increased NADPH oxidase activity and increased expression of cytosolic subunits p47<sup>phox</sup> and p67<sup>phox</sup> was observed in ageing rat (26 months) in comparison with young controls (5 months) (Erdos et al., 2011). In ageing human subjects (55-80 years) compared with young humans (18-30 years), increased bodyweight has also been seen to be associated with increased oxidative stress along with increased p47<sup>phox</sup> expression (Donato et al., 2007). The above findings strongly suggest a role for NADPH oxidase derived oxidative stress with ageing. However, to what extent and which isoform of NADPH oxidase is involved remain unclear. Due to the fact that p47<sup>phox</sup> and p67<sup>phox</sup>, found increased in ageing, are important regulatory subunits of the Nox2 isoform and as Nox2 is highly expressed in the vascular system, this study was carried out to identify the role of Nox2 in ageing-related oxidative stress.

Oxidative damage and changes result in a loss of brain function (Lovell et al., 2001, Halliwell, 2006). Increased Nox2 expression and activity and subsequent increased superoxide production were found in the brain of ageing mice in association with cognitive decline (Dugan et al., 2009). Ageing has also been shown to be associated with a decline in locomotor activity in rats (Salvatore et al., 2009). Furthermore, during ageing, circadian regulation is disrupted which affects more than 80% of humans over 65 years old and this percentage is even higher in patients with neurodegenerative diseases, particularly Alzheimer's diseases (van Someren et al., 2000, Wu and Swaab, 2007). Recent studies have involved oxidative stress as one of the factors regulating circadian rhythms (Zheng et al., 2007, Wilking et al., 2013). However, detailed investigation of how Nox2 is involved in the reduction in the activity with ageing is still missing.

The exact mechanisms behind ageing-related oxidative stress in the brain are not fully understood. However, increasing evidence suggests that NADPH oxidase derived superoxide may play a substantial role. More information is required to further understand the significance of Nox2 in the ageing-related oxidative stress in the brain and therefore this study focuses on uncovering the role of Nox2 in ageing-associated superoxide production in the brain and ageing-related locomotor activity. Groups of young (3-4 months) and ageing (21-22 months) Nox2KO mice and their WT controls were used to investigate ageing-related differences in superoxide production and total activity.

### **3.1.1 Aims and objectives**

The aim of this chapter was to discover the role of Nox2-derived oxidative stress in multiple organs, particularly in the brain with ageing and therefore the objectives were:

1. To measure the levels of ROS production in each organ homogenates from WT and Nox2KO mice and to determine if the knockout of Nox2 may be protective.
2. To use different methods to measure the level of brain superoxide production and to determine the role of Nox2.
3. To investigate the locomotor activity with ageing and determine the effect of Nox2 deletion.

## 3.2 Results

### 3.2.1 The global effect of ageing on multiple organ oxidative stress and the role of Nox2

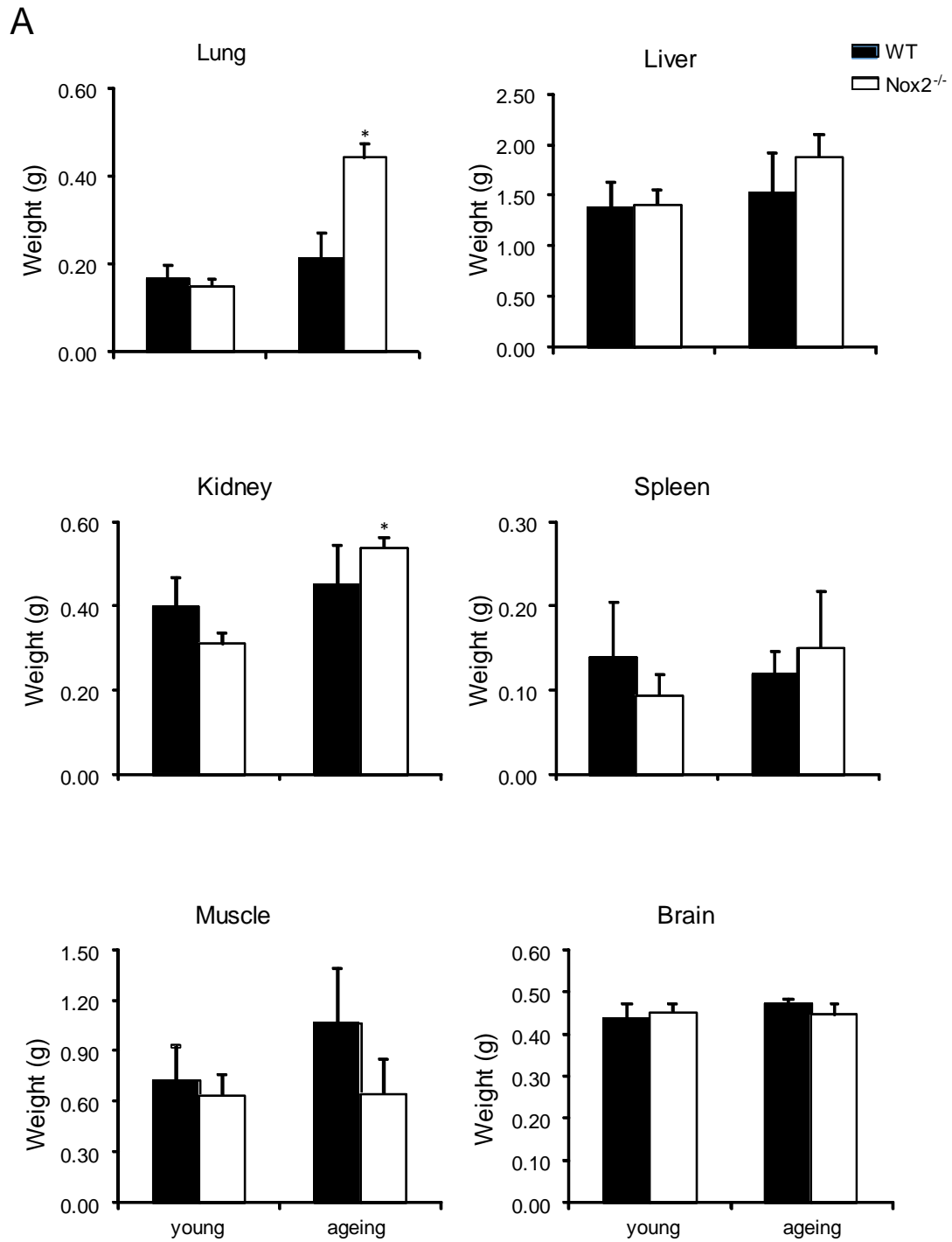
The lung, liver, kidney, spleen, muscle and mid-brain were collected from young (3-4 months) and ageing (21-22 months) WT and Nox2KO mice. The weight of each organ was measured immediately after taken out of mice to investigate the effect of ageing on organ mass and the role of Nox2. There were no significant differences in organ weight between the young (3-4 months) and ageing (21-22 months) for both WT and Nox2KO mice, except that the weight of lungs and kidneys was significantly higher in Nox2KO ageing mice compared to young controls (figure 3.1A).

The measurements of ROS production were carried out using organ homogenates assessed by lucigenin (5 $\mu$ M) chemiluminescence (figure 3.1B). In WT mice, the levels of O<sub>2</sub><sup>-</sup> production in different organs varied with the highest level found in the liver. There was a significant increase in ROS production in ageing WT heart homogenates compared with ageing Nox2KO samples (159.0  $\pm$  32.1 versus 47.2  $\pm$  18.7 MLU \*p<0.05). Oppositely, there was no difference between WT and Nox2KO heart homogenate at young age. At old age, there was significant greater ROS production in WT lung homogenates compared with Nox2KO lung homogenates (112.3  $\pm$  51.0 versus 30.6  $\pm$  16.2 MLU \*p<0.05). However, there was again no significant difference between WT and Nox2KO lung samples. The ageing WT liver homogenates produced significantly higher ROS production compared with Nox2KO liver at the same age (717.6  $\pm$  176.1 versus 263.8  $\pm$  131.6 MLU \*p<0.05). There was also a decrease in ROS production by Nox2KO liver samples compared with WT controls at young age but the difference was not statistically significant. When investigating the brain samples, there

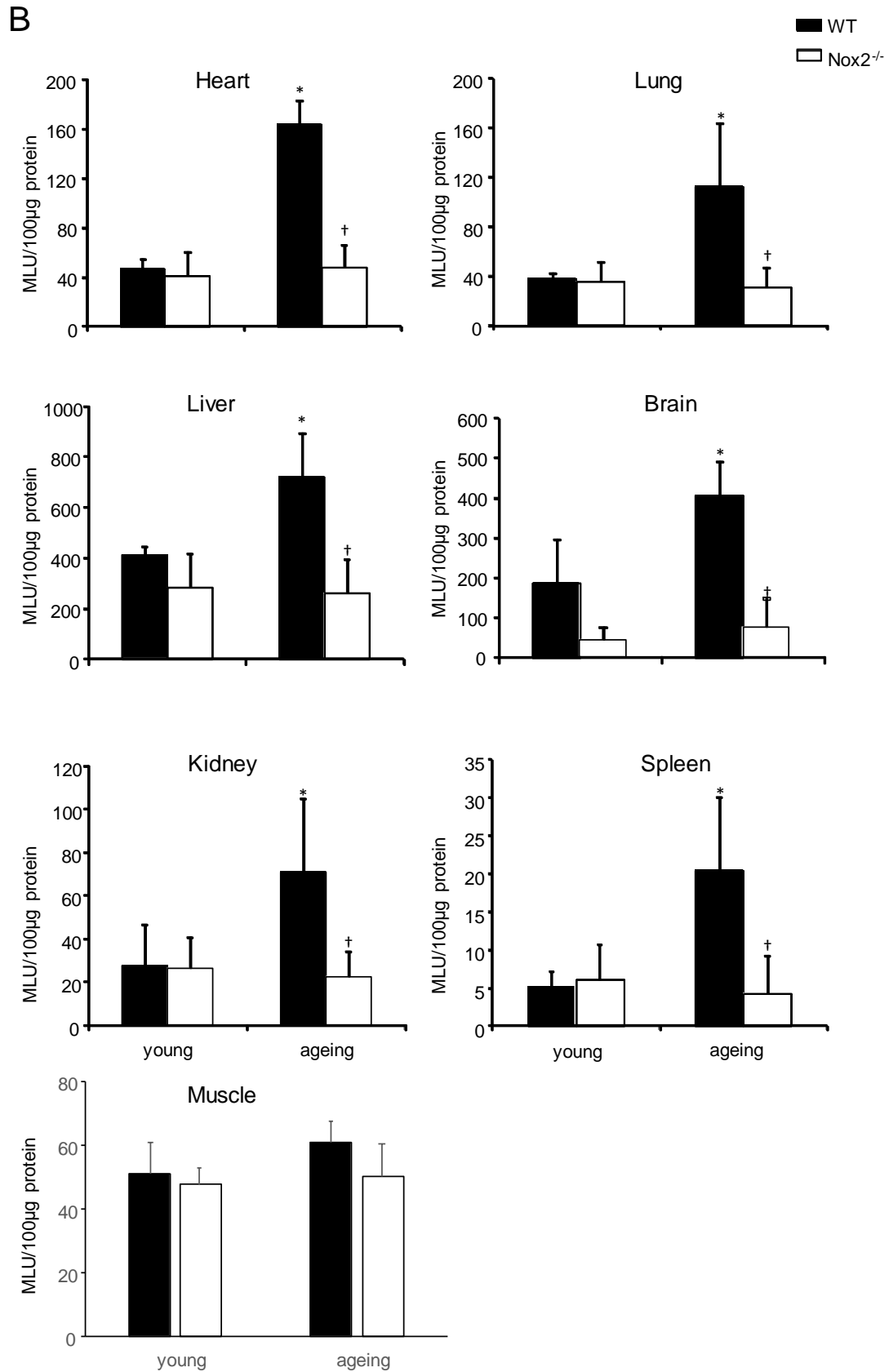
was a significant decrease found in Nox2KO brain homogenates compared with WT samples at young age ( $185.6 \pm 109.4$  versus  $45.0 \pm 30.1$  MLU \* $p < 0.05$ ). However, WT ageing brain homogenates were found to produce significantly larger amount of ROS production compared with the Nox2KO aging brain homogenates ( $405.8 \pm 86.8$  versus  $76.5 \pm 70.9$  MLU \* $p < 0.05$ ). The ageing WT kidney homogenates produced significantly higher ROS compared with Nox2KO kidneys ( $70.6 \pm 33.7$  versus  $22.6 \pm 11.2$  MLU \* $p < 0.05$ ). However, in the early stage of age, there were almost the same amount of ROS produced between WT and Nox2KO kidney samples. There was relatively small amount of ROS detected from the spleen samples. Despite this, at old age WT spleen homogenates had significantly higher ROS production than Nox2KO spleen samples ( $20.5 \pm 9.4$  versus  $5.2 \pm 4.7$  MLU \* $p < 0.05$ ) but this was not found at young age. The muscle produced low levels of ROS production without significant difference between age groups of both WT and Nox2KO mice.

In summary, compared to WT young controls, there were significant increases in the levels of  $O_2^-$  production in ageing heart, lung, liver, brain, kidney and spleen. There was a significant decrease in the levels of  $O_2^-$  production in Nox2KO organs compared with WT organs at old age. There was however also a significant decrease in the levels of  $O_2^-$  production in Nox2KO samples compared with WT samples at young age which was found only in brain homogenates.

Figure 3.1 A. The effects of ageing on multiple organ weight



B. ROS production detected by NADPH-dependent lucigenin chemiluminescence



### Legend to Figure 3.1

A) Organ weight measurements of WT and Nox2KO C57Bl/6 mice. Data was expressed as mean  $\pm$  SD with a number of 6-12 mice per group. The whole part of each organ was used to determine the organ weight except muscle collected only from upper legs. (The weight of hearts was not recorded due to the immediate use for CMEC isolation). Comparisons were made by two-way ANOVA with bonferroni *post-hoc* test. \* $p < 0.05$  versus young mice. Lung: WT ageing vs. young,  $p = 0.054$ ; KO ageing vs. young,  $p = 0.01$ . Liver: WT ageing vs. young,  $p = 0.73$ ; KO ageing vs. young,  $p = 0.09$ . Kidney: WT ageing vs. young,  $p = 0.28$ ; KO ageing vs. young,  $p = 0.01$ . Spleen: WT ageing vs. young,  $p = 0.25$ ; KO ageing vs. young,  $p = 0.06$ . Muscle: WT ageing vs. young,  $p = 0.50$ ; KO ageing vs. young,  $p = 0.89$ . Brain: WT ageing vs. young,  $p = 0.83$ ; KO ageing vs. young,  $p = 0.90$

B) ROS production was detected in organ homogenates by NADPH-dependent lucigenin ( $5\mu\text{M}$ ) chemiluminescence at young (3-4 months) and ageing (21-22 months) WT/Nox2KO mice. Data was expressed as mean  $\pm$  SD with a number of 9 mice per group. Comparisons were made by two-way ANOVA with bonferroni *post-hoc* test. \* $p < 0.05$  versus young mice. † $p < 0.05$  versus age-matched WT mice.

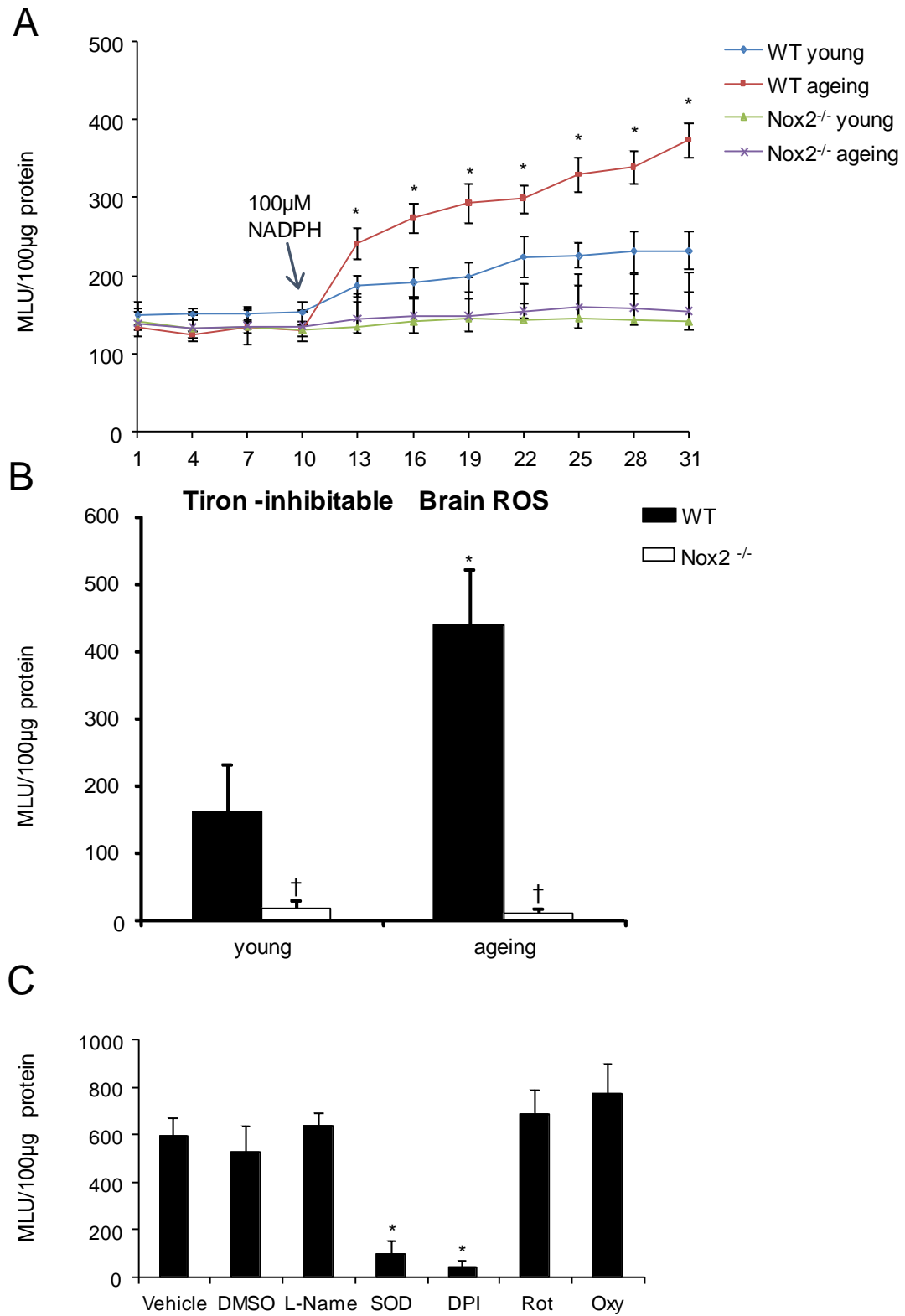
### **3.2.2 The effect of ageing and the role of Nox2 on brain ROS production detected by lucigenin chemiluminescence**

Brain homogenates were used to detect the superoxide production by lucigenin chemiluminescence. A representative figure was shown in figure 3.2 A which demonstrated the kinetic ROS production with the increasing cycles. The measurements of both WT young and ageing samples immediately increase after adding the 100  $\mu$ M of NADPH on 10<sup>th</sup> cycle, indicating that the superoxide production is NADPH-dependent. However, this was not found in the measurements of Nox2KO young and ageing samples.

To confirm that the superoxide is the major type of ROS being produced, each lucigenin chemiluminescence assay was performed in the presence or absence of 10 mM tiron, the superoxide scavenger. The values of the differences between the ROS production before and after adding tiron were used as tiron-inhibitable ROS production. There was very little superoxide produced in the brain homogenates of Nox2KO mice. The WT brain homogenates had significantly greater amount of superoxide compared with Nox2KO mice on both young and ageing.

An inhibitor assay was carried out to determine the source of superoxide in ageing WT mice. Brain homogenates were incubated with either buffer, 0.1% DMOS, 100  $\mu$ M of the nitric oxide synthase (NOS) inhibitor N(G)-Nitro-L-arginine Methyl Ester (L-NAME), 100  $\mu$ M of the xanthine oxidase inhibitor oxypurinol (oxy), 20  $\mu$ M of the NADPH oxidase inhibitor diphenyleneiodonium (DPI), 50  $\mu$ M of the mitochondrial complex-1 enzymes rotenone (Rot) or 200U/ml of superoxide dismutase (SOD). There was a significant decrease in ROS production in the presence of SOD or DPI but not in the presence of DMOS, L-NAME, rotenone or oxypurinol.

Figure 3.2 The effect of ageing on NADPH derived ROS production detected by lucigenin chemiluminescence in WT and Nox2KO mice brains



### Legend to Figure 3.2

A) Representative example of kinetic ROS measurements by NADPH-dependent lucigenin (5 $\mu$ M) chemiluminescence in brain homogenates of WT and Nox2KO young (3-4 months) and ageing (21-22 months) mice.

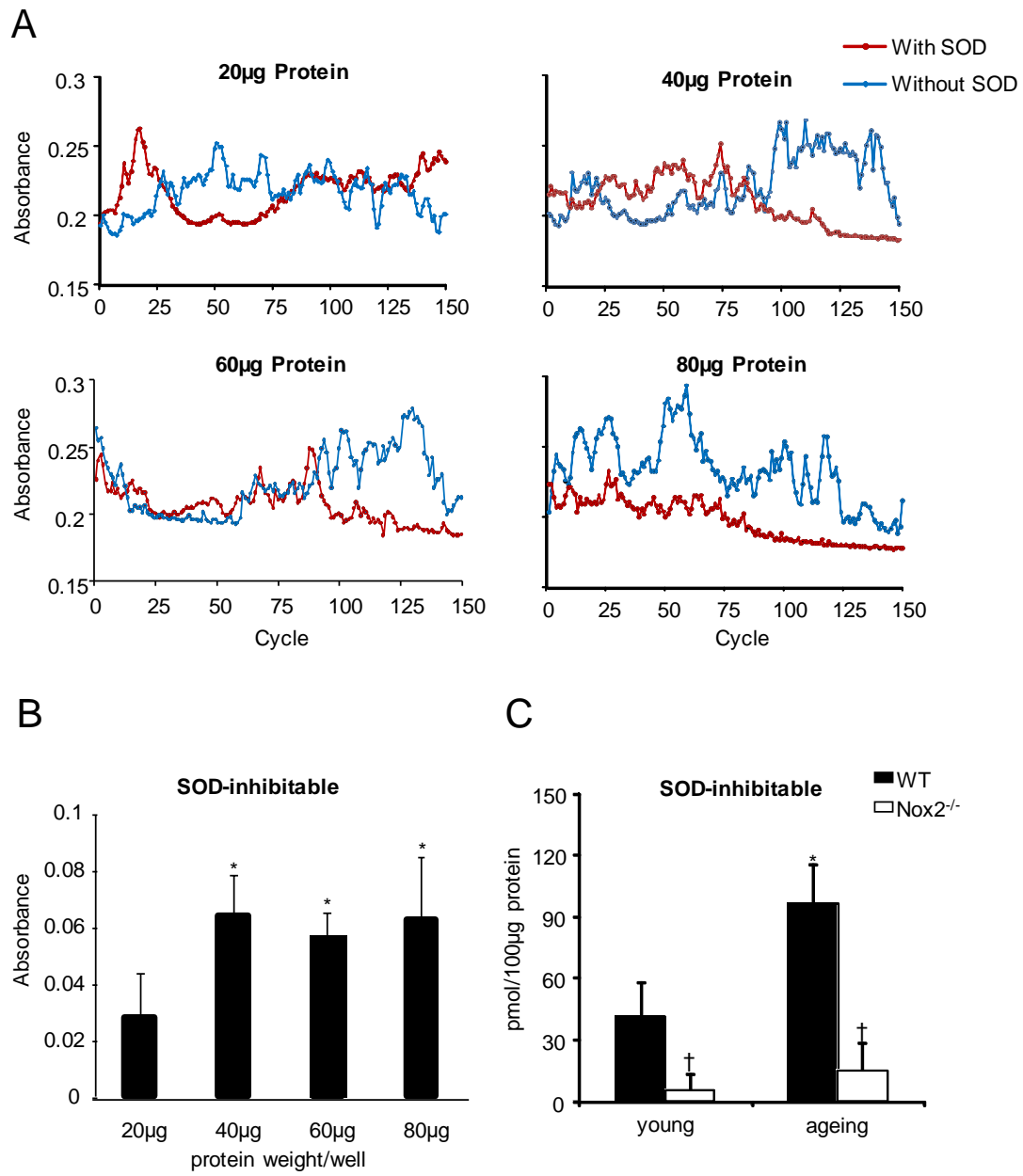
B) Tiron-inhibitable ROS production was detected in brain homogenates by NADPH-dependent lucigenin (5 $\mu$ M) chemiluminescence from young (3-4 months) and ageing (21-22 months) WT/Nox2KO mice. Measurements were continued after adding 10mM of the superoxide scavenger tiron. Data was expressed as mean  $\pm$  SD with a number of 9 mice per group. Comparisons were made by two-way ANOVA with bonferroni *post-hoc* test. \* $p$ <0.05 versus young mice. † $p$ <0.05 versus age-matched WT mice.

C) Inhibitor assay in ageing (21-22 months) WT mice to confirm the source of superoxide in ageing brains. Homogenates were incubated with 0.1% DMSO (the initial solvent for the inhibitor), 100  $\mu$ M L-NAME, 200 U/mL superoxide dismutase (SOD), 20  $\mu$ M diphenyleneiodonium (DPI), 50  $\mu$ M rotenone (Rot) or 100  $\mu$ M oxypurinol (Oxy) for 15 minutes before measurement of superoxide production by NADPH-dependent lucigenin (5 $\mu$ M) chemiluminescence. Data was expressed as mean  $\pm$  SD with a number of 9 mice per group. Comparisons were made by one-way ANOVA with bonferroni *post-hoc* test. \* $p$ <0.05 versus vehicle.

### **3.2.3 The effect of ageing and the role of Nox2 on brain ROS production detected by cytochrome c reduction assay**

The SOD-inhibitable ROS production in brain homogenates of young (3-4 months) and ageing (21-22 months) WT and Nox2KO mice was examined by cytochrome c reduction assay. Different concentrations of protein samples were firstly used to carry out the assay, and the kinetic curve of each experiment was indicated in figure 3.3A. There was a difference of absorbance between the presence and absence of SOD around cycle 50 and 70 when loading 20  $\mu\text{g}$  protein in each well. There was also a difference found around cycle 100 when loading 40  $\mu\text{g}$  protein, which was also shown in the figure of applying 60 and 80  $\mu\text{g}$  protein. This was further compared between different concentrations of protein samples at the same time (cycle 98-102) (figure 3.3B). The difference of absorbance between the present and absence of SOD when applying 40  $\mu\text{g}$  protein was significantly higher than 20 $\mu\text{g}$  protein and the same result was found when applying 60 and 80  $\mu\text{g}$  protein. Thus, 40  $\mu\text{g}$  protein in each brain homogenate from young and ageing WT and Nox2KO mice was used to determine the SOD-inhibitable ROS production (figure 3.3C). Compared with WT young brains, there was significantly greater ROS produced in the WT ageing brains ( $41.1 \pm 16.5$  versus  $96.3 \pm 18.8$  pmol/100 $\mu\text{g}$  protein). However, the Nox2KO brain at both young and ageing had significantly lower ROS production compared to age-matched WT brains.

Figure 3.3 The effect of ageing on NADPH dependent ROS production detected by cytochrome c reduction assay in WT and Nox2KO mice brains



### Legend to Figure 3.3

A) Kinetic curves of the absorbance in cytochrome c reduction assay of WT mice using 20 µg, 40 µg, 60 µg and 80 µg protein from brain homogenates (n=6 mice per group). The absorbance values were used to plot the kinetic curves with increasing cycle (20 seconds between cycles).

B) The mean values of absorbance between cycle 98-102 were used to determine the ROS production when applying different amount of protein samples per well. The differences of the absorption values between the presence and absence of SOD was calculated. Data was expressed as mean ± SD with a number of 6 mice per group. Comparisons were made by one-way ANOVA with bonferroni *post-hoc* test. \*p<0.05 versus 20µg protein per well.

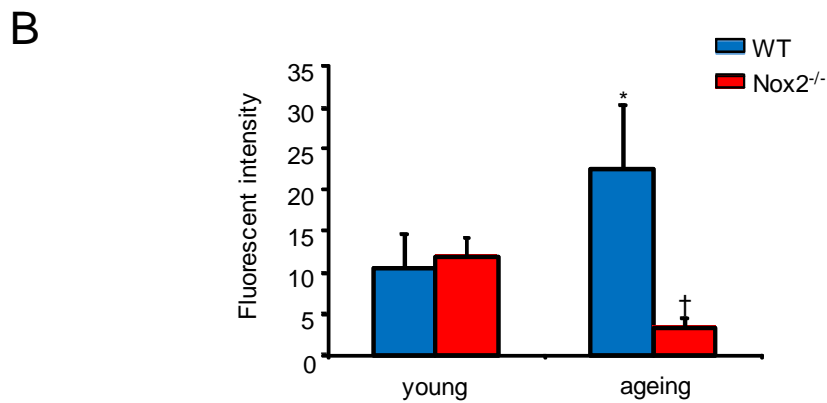
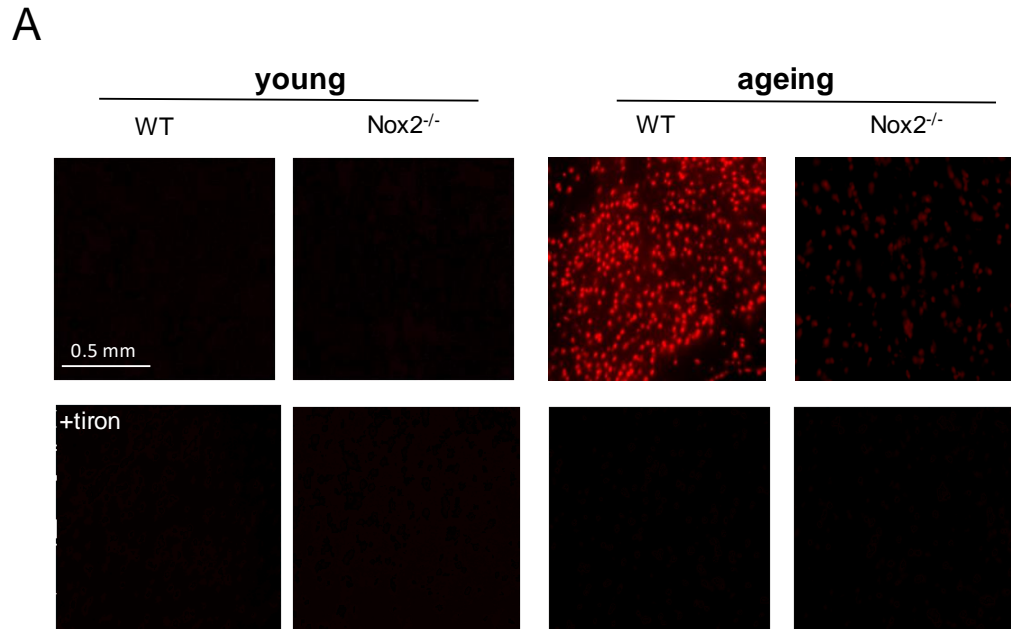
C) SOD-inhibitable ROS production was detected in brain homogenates by NADPH-dependent cytochrome c reduction at young (3-4 months) and ageing (21-22 months) WT/Nox2KO mice. The difference of the absorption values between the presence and absence of SOD was used to determine the ROS production. Data was expressed as mean ± SD with a number of 9 mice per group. Comparisons were made by two-way ANOVA with bonferroni *post-hoc* test. \*p<0.05 versus young mice. †p<0.05 versus age-matched WT mice.

### **3.2.4 The effect of ageing and the role of Nox2 on brain ROS production detected by DHE fluorescence**

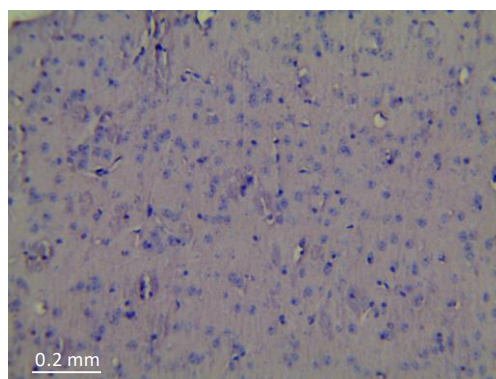
The ROS production in brains of young (3-4 months) and ageing (21-22 months) WT and Nox2KO mice was carried out by dihydroethidium (DHE) fluorescence using brain sections (figure 3.4A). The red DHE fluorescence increased with ageing in WT mice but reduced in Nox2KO mice. With the presence of tiron, a non-enzymatic  $O_2^-$  scavenger, the fluorescence was significantly decreased. These were further confirmed by quantification of the fluorescent intensities (figure 3.4B).

There was a significant increase in fluorescent intensity in ageing WT brains compared with young brains ( $10.6 \pm 4.1$  versus  $22.5 \pm 7.9$ ). Fluorescent intensity decreased significantly in ageing Nox2KO brain sections compared to age-matched WT brains ( $3.4 \pm 1.2$  versus  $22.5 \pm 7.9$ ). However, there was no significant difference in fluorescent intensity between WT and Nox2KO brains at young age. Moreover, in Nox2KO brains, ageing did not have significantly increased fluorescent intensity compared with young age.

Figure 3.4 The role of Nox2 in ageing-related oxidative stress on WT and Nox2KO brain sections detected by DHE fluorescence



H&E staining image of WT young mid-brain section



#### Legend to Figure 3.4

10 $\mu$ m frozen brain sections from young (3-4m) and ageing (21-22m) WT and Nox2KO mice were incubated with 2 $\mu$ M of DHE for 5min. A fluorescent microscope with a Cy3 filter (excitation: 530-560 nm; emission: 575-650 nm) was used to measure the intracellular ROS production.

A) Representative fluorescent images of *in situ* brain ROS production detected by DHE fluorescence. Images were captured at 10X magnification. 10mM of tiron was applied prior to DHE staining and incubated for 10min.

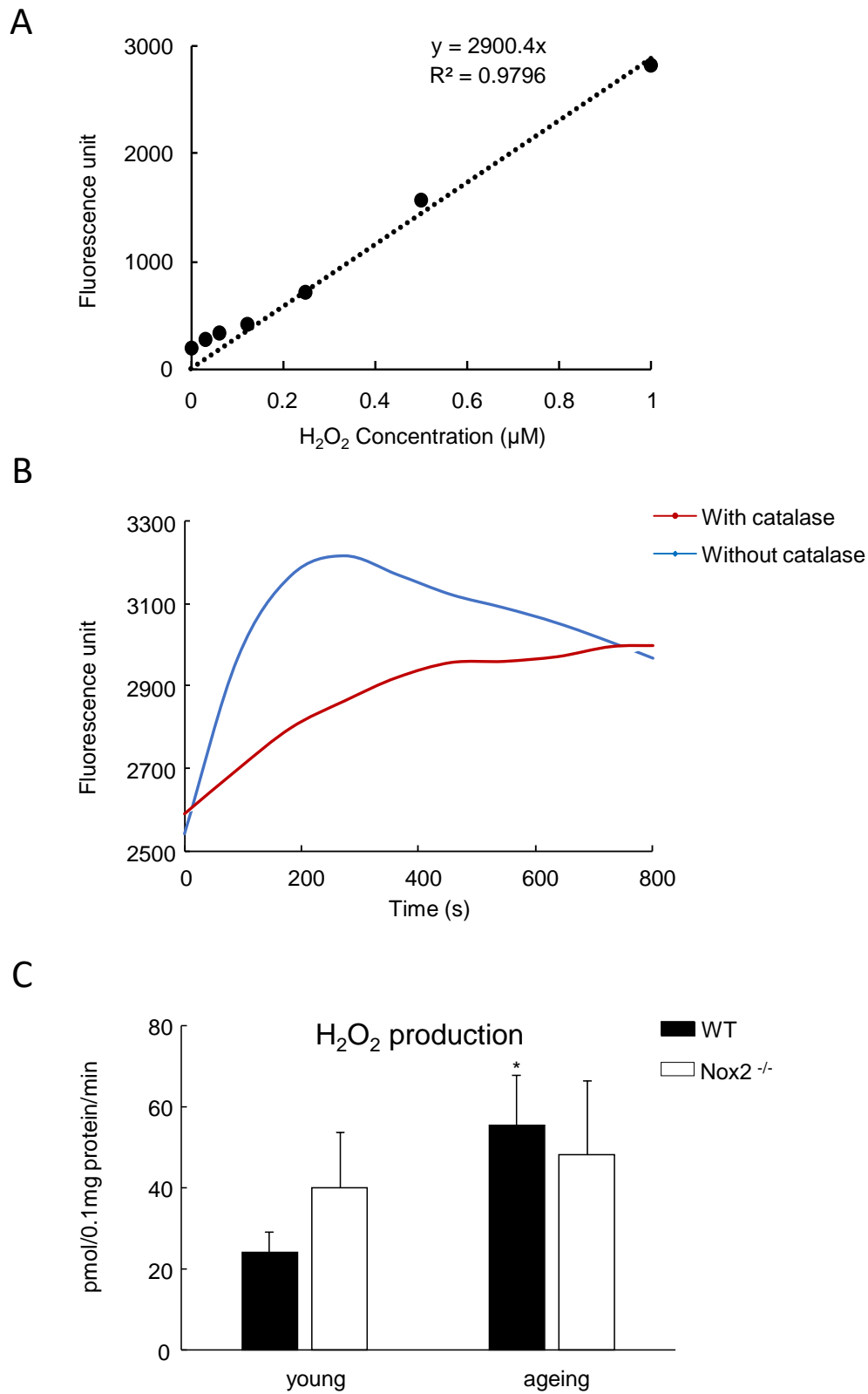
B) Quantitative analysis of DHE fluorescent intensities of brain images from WT and Nox2KO young and ageing mice. Data was shown as mean  $\pm$  SD from 6 mouse brains (3 sections from each brain and 15-20 images were taken per section). Comparisons were made by two-way ANOVA with bonferroni *post-hoc* test. \* $p < 0.05$  versus young mice.  $\dagger p < 0.05$  versus age-matched WT mice.

### **3.2.5 The effect of ageing and the role of Nox2 on brain hydrogen peroxide production detected by Amplex Red assay**

Apart from the increasing superoxide production derived from Nox2, it is also interesting to investigate the other type of ROS, hydrogen peroxide (H<sub>2</sub>O<sub>2</sub>) in the ageing brain. H<sub>2</sub>O<sub>2</sub> is dismuted from superoxide by SOD. Nox4 is thought to contribute to H<sub>2</sub>O<sub>2</sub> generation under pathological conditions and during aging (Vendrov et al., 2015). H<sub>2</sub>O<sub>2</sub> production in brain homogenates of young (3-4 months) and ageing (21-22 months) WT and Nox2KO mice was accessed by Amplex Red assay. As the determination of H<sub>2</sub>O<sub>2</sub> by the Amplex Red method is not direct, the fluorescence unit was extrapolated to the amounts of H<sub>2</sub>O<sub>2</sub> produced using appropriate calibration standards (Figure 3.5A). To confirm the specificity of the assay, 1000 Units/ml of catalase, which catalyses the reaction by which hydrogen peroxide is decomposed to water and oxygen was added in parallel wells. A representative example of the difference in fluorescence units between the presence and absence of catalase was shown in figure 3.5B.

Compared with WT young mice, there was a significant increase in the H<sub>2</sub>O<sub>2</sub> production in WT ageing mice (55.4 ±12.1 versus 24.0 ±5.0), there was also an increase in Nox2KO young mice but was not significant (40.0 ±13.6 versus 24.0 ±5.0). On the contrast, at the ageing group, the H<sub>2</sub>O<sub>2</sub> production was dropped in Nox2KO mice compared with WT mice but it was not significant (48.3 ±18.0 versus 55.4 ±12.1). Furthermore, no significant difference was found in H<sub>2</sub>O<sub>2</sub> production between young and ageing brains in Nox2KO mice (40.0 ±13.6 versus 48.3 ±18.0).

Figure 3.5 The hydrogen peroxide production detected by Amplex Red assay in WT and Nox2KO mice



### Legend to Figure 3.5

A) The standard curve of the fluorescence unit values corresponding to different concentrations of H<sub>2</sub>O<sub>2</sub>.

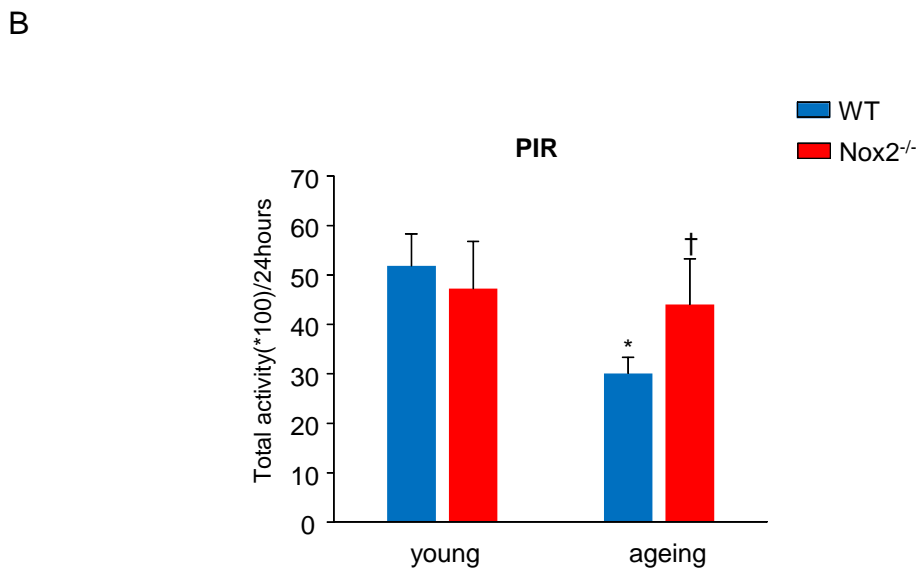
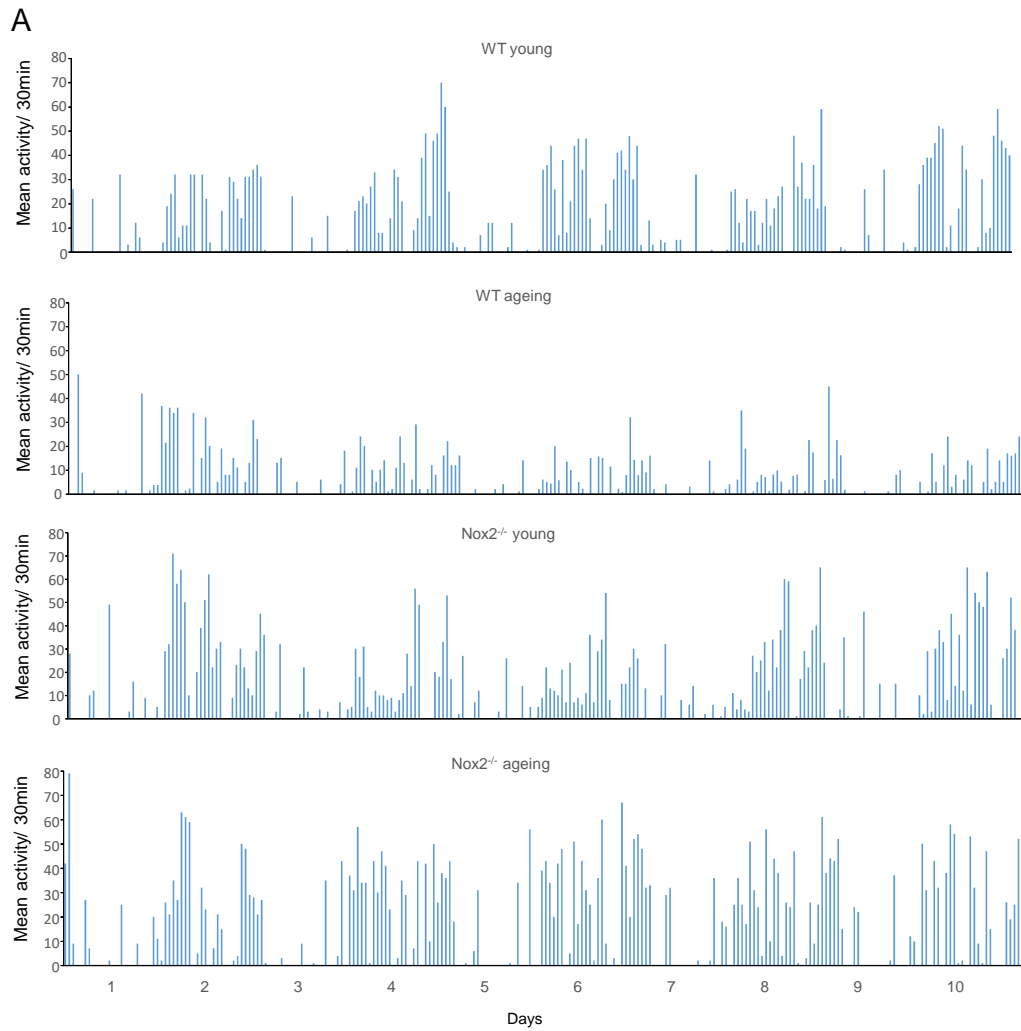
B) Representative curves plotted from kinetic fluorescence values of WT control samples pre-incubated with and without catalase.

C) Catalase-inhibitable H<sub>2</sub>O<sub>2</sub> production was detected in brain homogenates by NADPH-dependent amplex red assay at young (3-4 months) and ageing (21-22 months) WT/Nox2KO mice. The difference between the absorption values in the presence and absence of catalase was used to determine the H<sub>2</sub>O<sub>2</sub> production. Data as expressed as mean  $\pm$  SD with a number of 9 mice per group. Comparisons were made by two-way ANOVA with bonferroni *post-hoc* test. \*p<0.05 versus WT young mice.

### **3.2.6 Difference in total activities between WT and Nox2 knockout mice detected by PIR (passive infrared) sensor**

The exact mechanisms behind decreased locomotor activity with ageing are unknown. Our hypothesis is that Nox2-derived oxidative stress plays an important role in ageing-related reduction of locomotor activity. Knockout of Nox2 may reserve the locomotor activity in ageing. To explore this, the spontaneous activity of WT/Nox2KO mice at young (3-4 months) and ageing (21-22 months) was investigated using chamber cages with PIR sensor for 10 days in 12h: 12h light-dark cycle. There was no difference in the activity between WT and Nox2KO young mice which both displayed high activity during the darkness and much lower activity during the light period. However, there was a significant decrease in the total activity of WT ageing mice in comparison with young mice. There was also significant difference in the activity found in WT aging mice compared with Nox2KO ageing mice. This was further confirmed by the quantification of the total activity detected by PIR in figure 3.6B.

Figure 3.6 Difference in total activities between WT and Nox2 knockout mice detected by PIR (passive infrared) sensor



### Legend to Figure 3.6

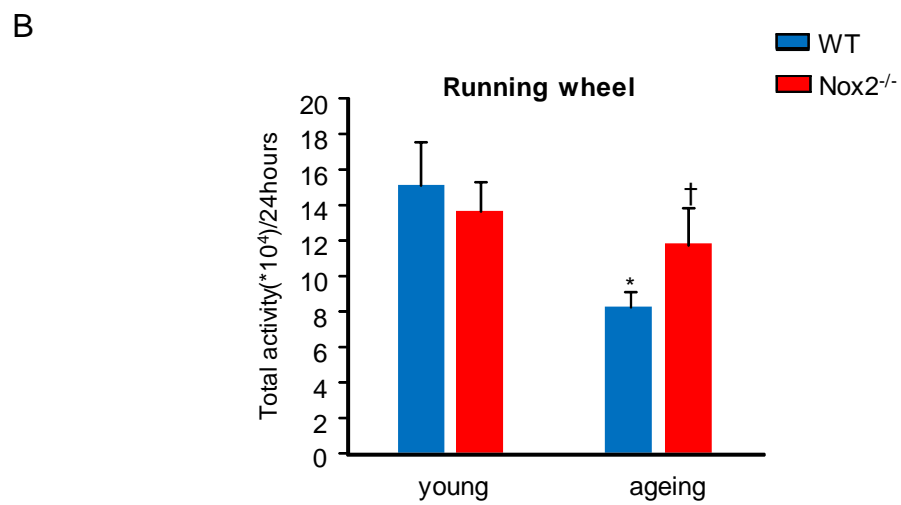
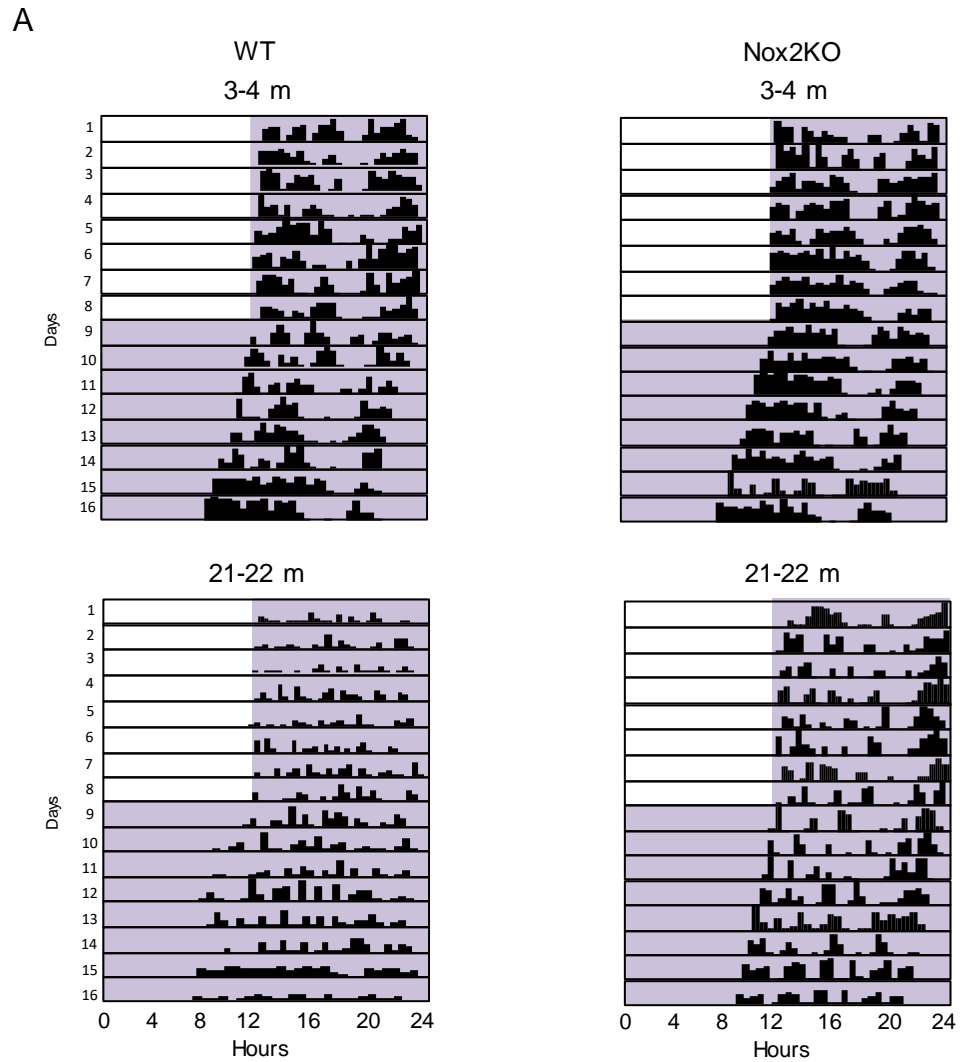
A) The representative curves of mice activity measured in young (3-4 months) and ageing (21-22 months) mice using chamber cages equipped with PIR sensor for 10 days of 12 hour: 12 hour light-dark (LD) cycle. The Data were collected in 30-minutes bins for 10-day period beginning at 09:00 a.m. Each pick represents the movement times of individual mouse passing the PIR detector above the cage.

B) The total activity per 24 h during LD cycle was quantified using the PIR data at young and ageing WT/Nox2KO mice. Data was expressed as mean  $\pm$  SD with a number of 6 mice per group. Comparisons were made by two-way ANOVA with bonferroni *post-hoc* test. \* $p < 0.05$  versus age-matched WT mice, †  $p < 0.05$  versus age-matched WT mice.

### **3.2.7 Difference in total activities between WT and Nox2 knockout mice detected by running wheel**

The actogram is a graph of activity from a single mouse where consecutive days are plotted on the y-axis, and time is plotted on the x-axis. During the LD cycle, the mouse started running at the offset of lights and consolidates its activity to the dark phase. During the light phase, activity was minimal. On day 9, the lights were turned off, leaving the mouse in constant darkness. Without a light cycle, there was no input to the circadian clock, which resulted in the clock running on its endogenous time. In the figure 3.7A, activity starts earlier each day indicating that the endogenous clock of Nox2KO ageing mouse was less than 24 hours, which was similar to WT and Nox2KO mice at young age. However, the shift in the activity during constant darkness was not found in the WT ageing mouse. The total activity of mice was also quantified according to the running wheel (figure 3.7B). Compared to WT young mice, ageing mice had a significant decrease in total activity. There was also a decrease in Nox2KO mice between ageing and young age but it was not significant.

Figure 3.7 Difference in total activities between WT and Nox2 knockout mice detected by running wheel



### Legend to figure 3.7

A) The representative actograms of young (3-4 months) and ageing (21-22 months) WT/Nox2KO mice housed in cages equipped with running wheel for 8 days of 12 hour: 12 hour light-dark (LD) cycle, followed by 8 days of 12 hour: 12 hour dark-dark (DD) cycle for measuring the spontaneous activity. The data was collected continuously over 24 hours for 16 consecutive days. The black bars represent the number of wheel revolutions, and the background is shaded to give an indication of the light/dark cycle.

B) The total activity per 24 h during LD cycle was quantified using the running wheel data at young and ageing WT/Nox2KO mice. Data was expressed as mean  $\pm$  SD with a number of 6 mice per group. Comparisons were made by two-way ANOVA with bonferroni *post-hoc* test. \* $p < 0.05$  versus WT young mice, †  $p < 0.05$  versus age-matched WT mice.

### 3.3 Discussion

In this chapter, the ageing-related ROS production and overall activity of mice have been investigated with particular focus on the role of Nox2. WT and Nox2KO mice were grouped into young (3-4 months) and ageing (21-22 months) to assess the organ weight, superoxide production and total activity.

The weight of each organ from WT and Nox2KO mice at different ages was firstly measured. There was no difference between either different age groups or different genotypes except the lungs and kidneys from Nox2KO group. Despite that several studies have reported that the increase Nox activity with ageing were associated with bodyweight, we demonstrated that the difference of weight between young and ageing were not from multiple organs in WT mice (Figure 3.1A). Moreover, ROS have been well known to increase with age and therefore accelerate ageing (Balaban et al., 2005). We have demonstrated that superoxide production was significantly increased with ageing in WT heart, lung, liver, kidney, spleen and brain, and this ageing-related increase in superoxide production was attenuated in the Nox2KO mice (figure 3.1B). This provides evidence that Nox2 is a major source of superoxide in these organs with ageing. Interestingly, there was little superoxide in spleen that was just detectable in lucigenin-chemiluminescence, suggesting that there were other sources of ROS produced in the spleen, for example, Nox5 (Fulton, 2009).

ROS consist of radical and non-radical oxygen species formed by the partial reduction of oxygen, including such as superoxide anion ( $O_2^-$ ), hydroxyl radical ( $\cdot OH$ ), hydrogen peroxide ( $H_2O_2$ ) and singlet oxygen ( $^1O_2$ ). In this chapter, brain sections from WT and Nox2KO mice at young and ageing were used to investigate the role of Nox2-derived superoxide on ageing-related oxidative stress in the brain. Intracellular ROS levels in

the brain were examined by DHE fluorescence. The WT brains had an ageing-related increase in ROS production which was not found in the Nox2KO mice, suggesting that Nox2 is a major source of ROS in the ageing brain. To confirm the DHE fluorescence results, superoxide production in brain homogenates were also assessed by lucigenin-chemiluminescence. Similarly, there was an ageing-related increase in superoxide production in WT brains but was attenuated in the Nox2KO brains. For both DHE fluorescence and lucigenin-chemiluminescence, experiments were carried out in the presence of the superoxide scavenger tiron and there was a significant decrease in the level of superoxide production in WT and Nox2KO mice at all age, which convinces that rather than other types of ROS, superoxide was detected. An inhibitor assay was then performed in the WT ageing brain homogenates to validate that Nox2 is the major source of superoxide. There was no difference in superoxide production in the presence of mitochondrial inhibitor rotenone, the NOS inhibitor L-NAME or the xanthine oxidase inhibitor oxypurinol. However, there was a significant decrease in the superoxide production in the presence of DPI which is a flavoprotein inhibitor for NADPH oxidase. These results further support that Nox2 is a major source of ROS in the brain with ageing.

The chemiluminescent compound lucigenin has been widely used to detect superoxide production in neutrophils, macrophages, vascular cells and tissues. There was concern about the validity of lucigenin for detection of  $O_2^-$  because lucigenin itself can generate  $O_2^-$ . However, 5  $\mu$ M of lucigenin was proved to be a sensitive and valid probe for detecting  $O_2^-$  production in vascular tissues (Li et al., 1998, Skatchkov et al., 1999, Fan and Li, 2014). Moreover, we have also used cytochrome c reduction assay to further validate the superoxide assessment. As with DHE fluorescence and lucigenin-chemiluminescence results, there was an ageing-related increase in superoxide

production in the WT mice that was attenuated in the Nox2KO mice, which supports the previous findings. And again, Nox2 was further confirmed as a major source of ROS in the brain with ageing.

Apart from the superoxide, the production of H<sub>2</sub>O<sub>2</sub> was also assessed in the brain homogenates of WT and Nox2KO mice at young and old age. Experiments were performed in the presence or absence of catalase, proving that H<sub>2</sub>O<sub>2</sub> was detected instead of other types of ROS. There was a significant increase in WT ageing brains compared with young brains, suggesting that H<sub>2</sub>O<sub>2</sub> production accelerates with ageing brain and supplying more evidence for the accumulation of ROS with ageing. In ageing, there was no difference in the H<sub>2</sub>O<sub>2</sub> production between WT and Nox2KO mice, providing evidence that Nox2 acts as a source of superoxide rather than H<sub>2</sub>O<sub>2</sub> during ageing. The increase of H<sub>2</sub>O<sub>2</sub> production in ageing brains compared to young controls in Nox2KO mice indicates that other sources of H<sub>2</sub>O<sub>2</sub> might contribute to ROS accumulation with ageing in the brain.

The total activities recorded by PIR were not different between WT and Nox2KO mice at young age, however in ageing there was significant decrease in activities of WT mice which was not seen in the Nox2KO mice. Similarly, the total activity assessed by running wheel also exhibited a significant decrease with ageing, but this effect was not found in Nox2KO mice. Interestingly, we observed that the shift of circadian rhythms activity during the change from LD cycle to DD cycle retained in the Nox2KO mice with ageing, which was not seen in the WT mice. Although circadian rhythm was not our primary interest, the results showed that Nox2 may play a role in the circadian rhythm disruption with ageing.

Overall these findings support a major source of superoxide, Nox2, plays an important role in the oxidative damage in the brain and the deletion of Nox2 has been shown in this study to protect the ageing brain from ageing-related ROS accumulation and to prevent a reduction in total activity.

## Chapter 4

### **Knockout of Nox2 reduces cerebral endothelial damage, neuronal death and oxidative signalling in the brain**

#### **4.1 Introduction**

Increasing evidence had shown that ROS are important molecules in the control of vascular reactivity, particularly the superoxide anion, which increases vascular tone via the inactivation of endothelium-derived nitric oxide (Droge, 2002). It has been proved by investigators that NADPH oxidase derived superoxide production increases during various challenges in the cerebral arteries (Didion and Faraci, 2002, Paravicini et al., 2004, Park et al., 2004). Many studies have focused on the importance of NADPH oxidase in vascular disease. Recent studies have pointed out that cerebrovascular disease was not only a primary cause of cognitive impairment, but also contributing to the dementia caused by other factors, including Alzheimer's diseases and other neurodegenerative pathologies (Gorelick et al., 2011, Toledo et al., 2013). The catalytic domain of NADPH oxidase exists in its Nox subunit. Depending on species, cell type, and condition, different homologs of Nox are expressed in vascular cells, including Nox1, Nox2, Nox4, and Nox5 (Chrissobolis and Faraci, 2008, Montezano et al., 2011). Impairment of endothelial function and neurovascular coupling is restored to normal with scavengers of superoxide, genetic deletion of the Nox2 component of NADPH oxidase in models of ageing and Alzheimer's disease, while the mice overexpressing the Swedish mutation of the amyloid precursor protein (Tg2576) were used as a model of Alzheimer's disease (Park et al., 2007, Park et al., 2008). In short, these findings

support the concept that NADPH oxidases are key promoters of oxidative stress in ageing-related cerebrovascular diseases.

Besides vascular tissue, the central nervous system (CNS) also expresses Nox isoforms, particularly Nox2 and Nox4 being the most prominent isoforms detected in a variety of cell types in the brain, including neurons, microglia and astrocytes (Cahill-Smith and Li, 2014). In microglial cells, Nox2 is highly expressed in microglial cells (Harrigan et al., 2008). Nox2 was found to be activated when responding to neurotoxic stimulation in microglial cells, and subsequently produces excessive ROS production, causing neuronal damage (Block, 2008). Microglial cells can also respond to neuronal damage and become further activated, which can be long-lived and eventually kill the neuron (Block, 2008). In ageing-related neurodegeneration, Nox2 activation and Nox2-derived oxidative damage in the brain have appeared to be an important mechanism in the development of Alzheimer's disease (Zekry et al., 2003). It has been well known that Alzheimer's disease is strongly associated with accumulation of the protein  $\beta$ -amyloid ( $A\beta$ ). Additionally, increase levels of  $A\beta$  were found in Down syndrome and a number of cancers, including esophageal, colorectal, lung, and hepatic (Hartley et al., 2017; Jin et al., 2017). Recent studies have indicated a close relationship between the levels of  $A\beta$  and Nox2 activity, and increased expression of Nox2 were also found in activated microglia surrounding  $\beta$ -amyloid-laden capillaries from patients with capillary cerebral amyloid angiopathy (Carrano et al., 2011, Carrano et al., 2012). Increased ROS production activates downstream signaling pathways, such as ERK1/2 (Sung et al., 2007). Other redox-sensitive MAP kinases, such as p38 MAPK, have also been found to be upregulated in the brains of patients with Alzheimer's disease (Hensley et al., 1999).

Although it has been recently established that NADPH oxidase is expressed and active in the vascular circulation and CNS, the exact mechanisms behind the cerebral vascular damage and neurodegeneration with ageing are still unclear. Therefore, this study focuses on elucidating the role of Nox2 in ageing-related cerebral vascular damage, microglia activation and neuronal death with ageing. Brains from groups of young (3-4 months) and ageing (21-22 months) WT and Nox2KO mice were used to assess the cerebral endothelial, neuronal and microglial cells. The brain homogenates were used to investigate the expression of NADPH oxidase subunits and MAPK and Akt phosphorylation. The microglial cells were further assessed for superoxide production under multiple stimuli.

#### **4.1.1 Aims and objectives**

The aim of this chapter was to investigate whether Nox2-derived oxidative stress cause damages to cerebral microvasculature, microglial function and neuronal death in ageing.

The specific objectives are listed below:

1. To compare the endothelial and neuronal cells in the mid-brain sections of WT and Nox2 KO mice between young mice versus ageing mice. To investigate the brain expression of NADPH oxidase subunits and MAPK and Akt phosphorylation between young versus ageing to determine the role of Nox2.
2. To explore the Nox2 and microglial activation with ageing and to further measure the level of superoxide production from microglial cells in the presence of A $\beta$  and other stimuli.

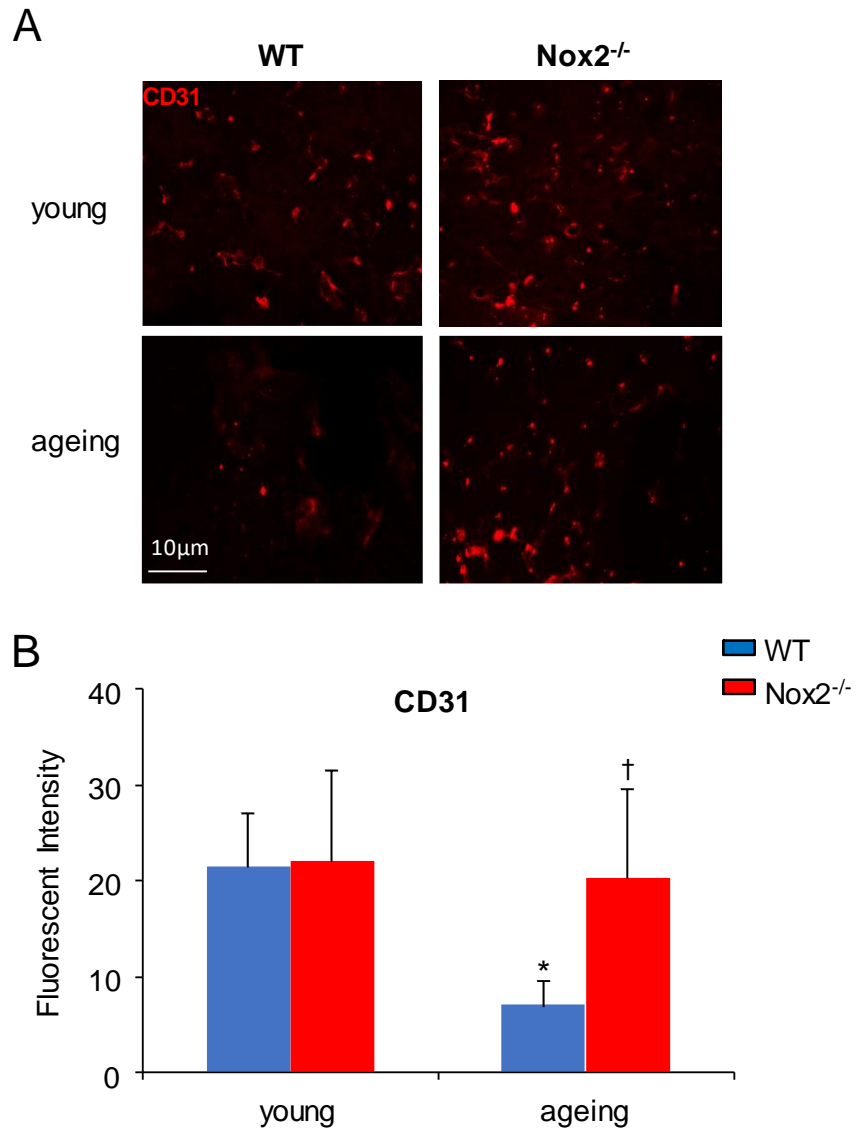
## **4.2 Results**

### **4.2.1 The effect of ageing on cerebral endothelial cells detected by immunofluorescence**

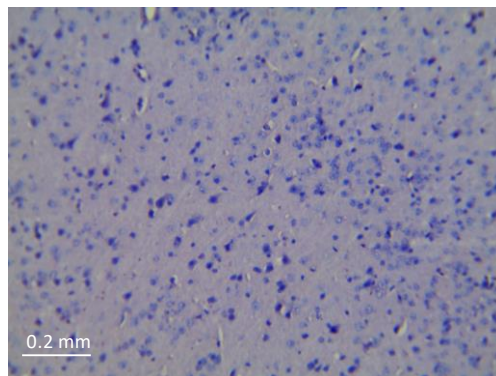
Immunofluorescence was performed to detect the expression of CD31 (the endothelial cell marker) in the brain sections in WT and Nox2KO mice at young (3-4 months) and old (21-22 months) age (figure 4.1A). In WT brains, the red fluorescence showed a decrease with ageing that was not seen in the Nox2KO brains. Furthermore, there was no difference in the CD31 fluorescence intensity between WT and Nox2KO mice at young age. However, the CD31 fluorescence intensity increased in Nox2KO mice compared with WT mice at old age.

The above findings were confirmed by the quantification of the fluorescent intensity (figure 4.1B). A 2-fold reduction of fluorescent intensity of CD31 staining in WT ageing mice was demonstrated, compared with WT young mice. However, there was no significant difference between young and ageing in Nox2KO mice.

Figure 4.1 The effect of ageing on cerebral endothelial cells detected by immunofluorescence



H&E staining image of WT young mid-brain section



#### Legend to figure 4.1

Frozen sections of brains (10 $\mu$ m thickness) were from young (3-4 months) and ageing (21-22 months) WT and Nox2<sup>-/-</sup> mice. Sections were stained with the endothelial cell marker CD31 (red). Fluorescent labelled antigens were investigated with an Euromex fluorescent microscope to measure Cy3 (excitation: 530-560 nm; emission: 575-650 nm) fluorescence.

A. Representative fluorescent images were captured at 40X magnification to visualize endothelium in brain sections.

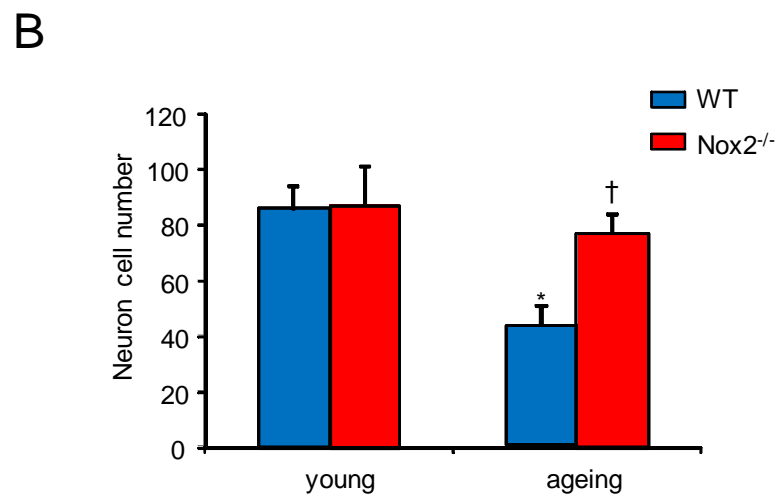
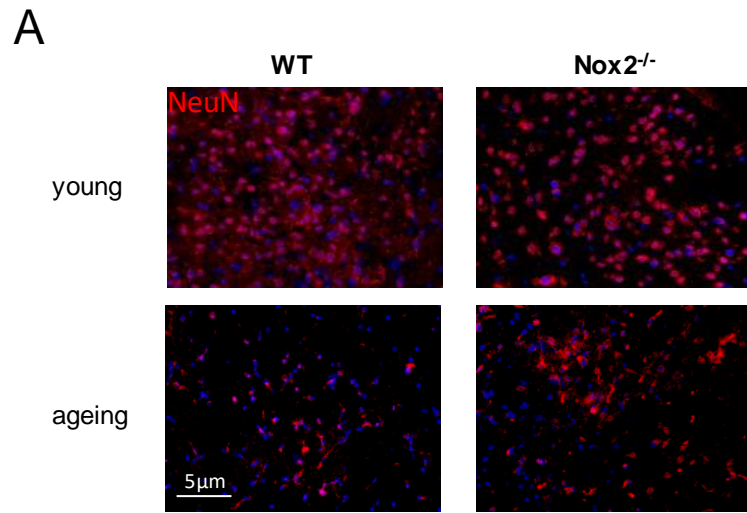
B. Quantitative analysis results of fluorescent intensity in images of brain sections from WT and Nox2<sup>-/-</sup> mice. Data was shown as mean  $\pm$  SD from 6 mouse brains (more than 10 images were taken per brain). Comparison were made by two-way ANOVA with bonferroni *post-hoc* test. \*p<0.05 versus young mice, †p<0.05 versus age-matched WT mice.

#### **4.2.2 The effect of ageing on neuronal cells detected by immunofluorescence**

Immunofluorescence was carried out to investigate the effect of ageing on neurons using the neuronal cell marker NeuN in mid-brain sections of WT and Nox2KO mice at young (3-4 months) and old (21-22 months) age (figure 4.2A). There were no differences between any of the groups in blue fluorescence. However, in WT brains, the red fluorescence showed a significant decrease with ageing that was not seen in the Nox2KO brains.

The above findings were confirmed by the quantification of the fluorescent intensity. An over 2-fold reduction of neurons in WT ageing mice was showed in figure 4.2B compared with WT young mice. In Nox2KO mice, there was also a decrease in the number of neurons between young and ageing however the difference was not significant.

Figure 4.2 The effect of ageing on neuron cell population detected by immunofluorescence



## Legend for Figure 4.2

A) Immunofluorescence images of 10 $\mu$ m thickness frozen brain sections from young (3-4 months) and ageing (21-22 months) WT and Nox2<sup>-/-</sup> mice. Sections were stained with the neuron cell marker NeuN (red) and the nuclear stain DAPI (blue). Fluorescent labelled antigens were examined with an Euromex fluorescent microscope under 20X magnification to investigate fluorescence.

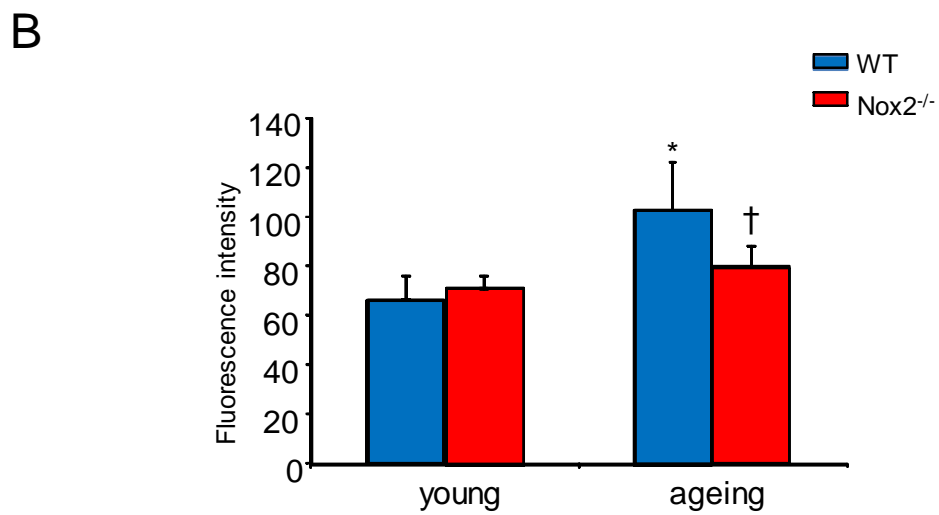
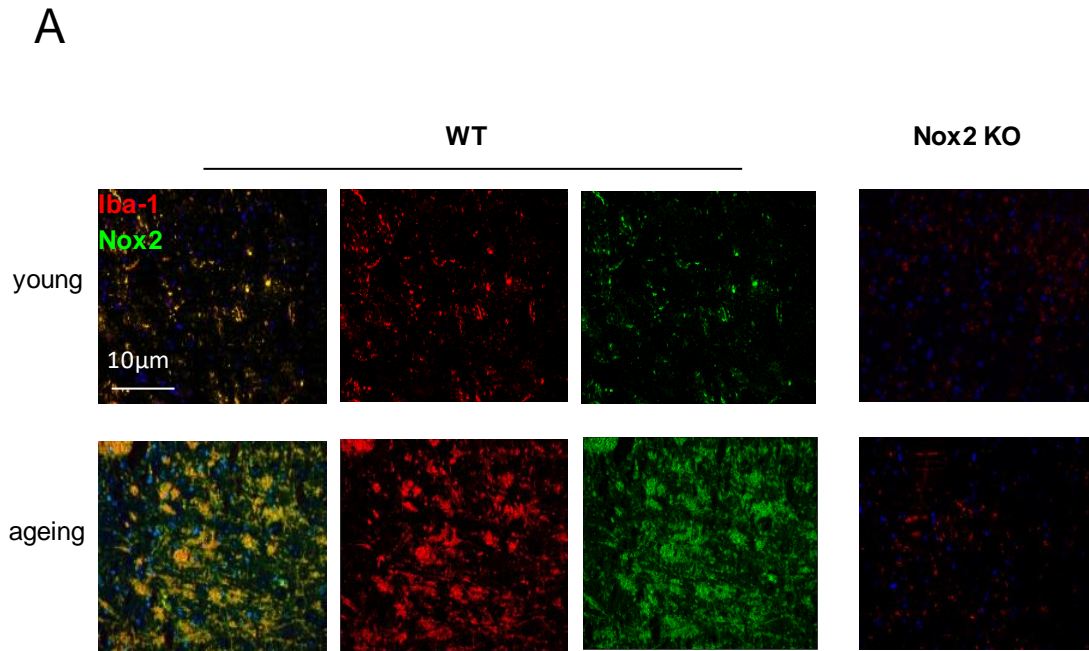
B) Quantitative analysis results by counting neuron amounts using Image J software in images of brain sections from WT and Nox2<sup>-/-</sup> mice. Data was shown as mean  $\pm$  SD from 6 mouse brains (3 sections from each brain and 15-20 images were taken per section). Comparisons were made by two-way ANOVA with bonferroni *post-hoc* test. \*p<0.05 versus young mice. †p<0.05 versus age-matched WT mice.

### **4.2.3 The effect of ageing on microglial Nox2 expression detected by immunofluorescence**

The expression of Nox2 in the microglia cells of the brain in young (3-4 months) and ageing (20-22 months) WT and Nox2KO mice was investigated by immunofluorescence (figure 4.3A). The microglial Nox2 expression in brains was indicated by the yellow fluorescence (red fluorescence merged with green fluorescence). The blue fluorescence of the nuclear stain DAPI was not changed in any of the groups. The red fluorescence of the microglial cell marker Iba-1 was increased with ageing in WT mice which was not seen in Nox2KO mice. Furthermore, in WT mice the green Nox2 fluorescence was increased with ageing and was absent in Nox2KO mice.

The quantification of the fluorescent intensity of Iba-1 staining was performed and the co-localization area (yellow colour area) was selected for quantification (figure 4.3B). Compared to WT young brains, there was a nearly 2-fold increase of Iba-1 expression in WT ageing mice, however there was no significant difference between young and ageing in Nox2KO brains.

Figure 4.3 The effects of ageing on microglial Nox2 expression detected by immunofluorescence



### Legend for Figure 4.3

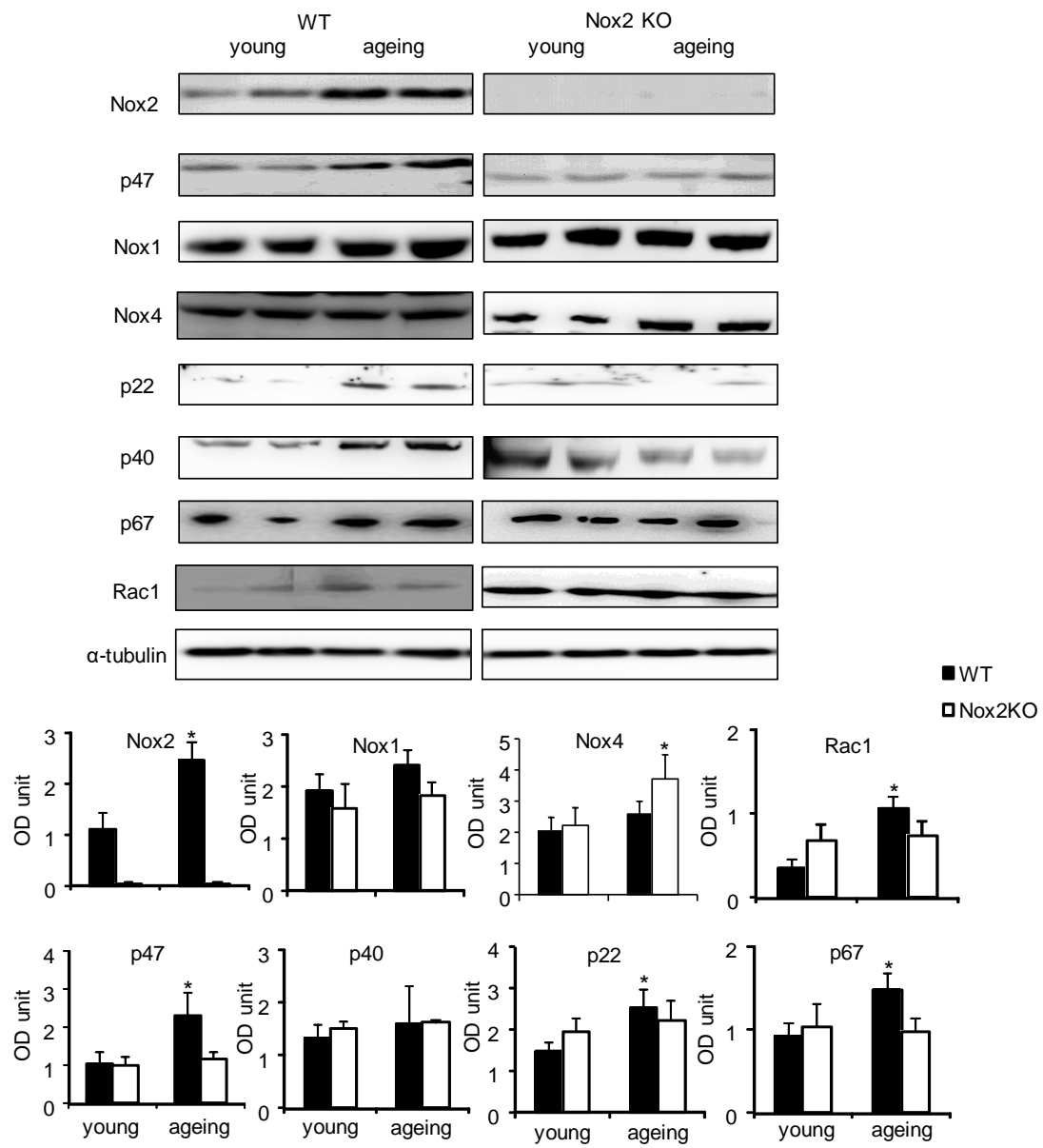
A) Immunofluorescence images of 10 $\mu$ m frozen brain sections from young (3-4 months) and ageing (21-22 months) WT and Nox2<sup>-/-</sup> C57Bl/6 mice. Sections are stained with Nox2 (green), the microglial cell marker Iba-1 (red) and the nuclear stain DAPI (blue). Fluorescent labelled antigens were observed with a Euromex fluorescent microscope under 40X magnification to investigate fluorescence.

B) Quantitative analysis results of fluorescent intensities of Iba-1 staining (on co-localization area) from images of brain sections from WT and Nox2<sup>-/-</sup> mice. Data was shown as mean  $\pm$  SD from 6 mouse brains (3 sections from each brain and 15-20 images were taken per section). Comparisons were made by two-way ANOVA with bonferroni *post-hoc* test. \*p<0.05 versus young mice. †p<0.05 versus age-matched WT mice.

#### **4.2.4 The effect of ageing on NADPH oxidase subunit expression in the brain detected by Western blot**

To further define a role for Nox2 in the oxidative regulation of ageing brain function, the expression of Nox subunit was examined by Western blot using brain homogenates from WT/Nox2KO young and ageing mice (Figure 4.4). There was no significant difference in the expression of these molecules at the young age between WT and Nox2KO brains. However, compared to young WT brains, there were significant increases in the levels of Nox2, p22<sup>phox</sup>, p47<sup>phox</sup>, p67<sup>phox</sup> and rac1 expressions. There was an ageing-related increase in the levels of Nox4 and p40<sup>phox</sup> between young and ageing brain in WT mice however it was not statistically significant. In Nox2KO brains, there was no significant difference in the levels of expressions of p22<sup>phox</sup>, p40<sup>phox</sup>, p47<sup>phox</sup>, p67<sup>phox</sup> and rac1 between young and ageing; instead, ageing Nox2KO brains had a significant increase in Nox4 expression as compared to young Nox2KO controls. Although the levels of Nox1 expression showed a pattern of age-related increase, the difference between young and ageing groups was not statistically significant for both WT and Nox2KO mice.

Figure 4.4 The effects of ageing on NADPH subunits expression detected by western blots



#### Legend for Figure 4.4

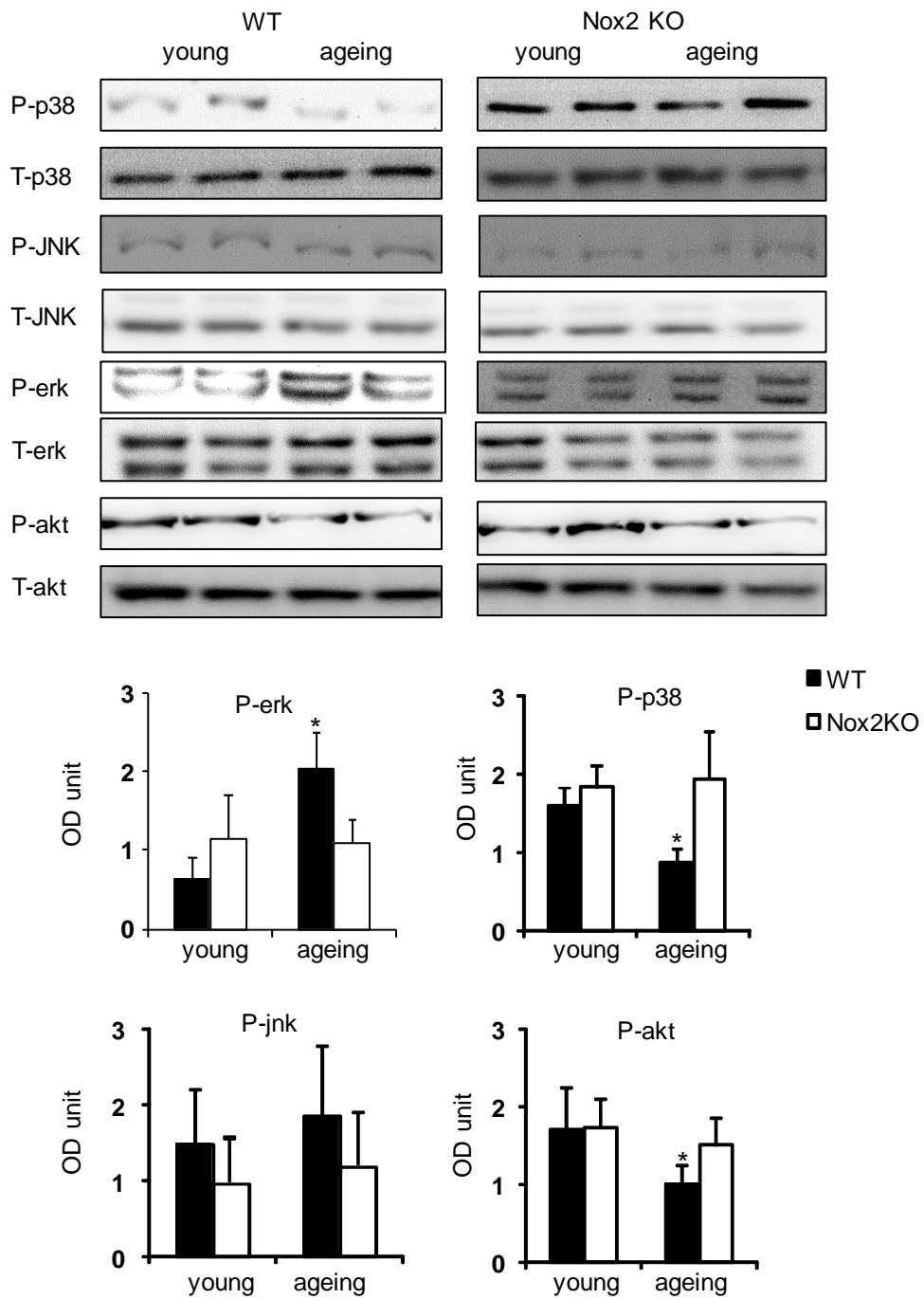
The brain homogenates from WT and Nox2KO mice at young (3-4 months) and ageing (21-22 months) groups were used for detecting the levels of expression of NADPH subunits by Western blot. Levels of protein expressions of Nox1, Nox2, Nox4, p22<sup>phox</sup>, p40<sup>phox</sup>, p47<sup>phox</sup>, p67<sup>phox</sup> and Rac1 were investigated.  $\alpha$ -tubulin detected in the same sample was used as a loading control. The optical densities (OD) of Nox subunit bands were quantified digitally and normalized to the  $\alpha$ -tubulin levels. Data was shown as mean  $\pm$  SD from 6 mouse brains per group. Comparisons were made by two-way ANOVA with bonferroni *post-hoc* test. \* $p < 0.05$  versus young mice in the same genetic group.

#### **4.2.5 The effect of ageing on MAPK and Akt phosphorylation in the brain detected by Western blot**

Mitogen activated protein kinases (MAPK), including ERK1/2, p38 MAPK and JNK, are redox-sensitive signaling molecules which can respond to ageing progress via NADPH oxidase. To investigate the role of Nox2 during MAPK activation with ageing, WT/Nox2KO brain homogenates were used to examine the phosphorylation of ERK1/2, p38 MAPK and JNK by Western blot (figure 4.5). The levels of total protein detected in the same samples were used as loading controls. There was no significant difference in the expression of these molecules at the young age between WT and Nox2KO brains. Compared to young WT brains, the levels of ERK1/2 phosphorylation were increased significantly, which was accompanied by significant decreases in the levels of p38MAPK phosphorylation in ageing WT brains. However, there was no significant difference in ERK1/2 and p38 MAPK phosphorylation between young and ageing brains of Nox2KO mice. The levels of phosphorylated JNK were very low and showed no significant changes between young and ageing groups of WT and Nox2KO brains. According to the above data, we have provided evidence for a crucial role of age-associated Nox2 activation in the activation of redox signaling pathways

The levels of Akt phosphorylation, a key molecule involved in the insulin signaling pathway, were also examined in young and ageing WT/Nox2KO brain homogenates by Western blot (Figure 4.5). There was a significant decrease in Akt phosphorylation in the WT ageing brains in comparison to the levels in WT young brains. However, this change was absent between young and ageing groups in Nox2KO brains.

Figure 4.5 The effect of ageing on MAPK and Akt phosphorylation in the brain detected by Western blot



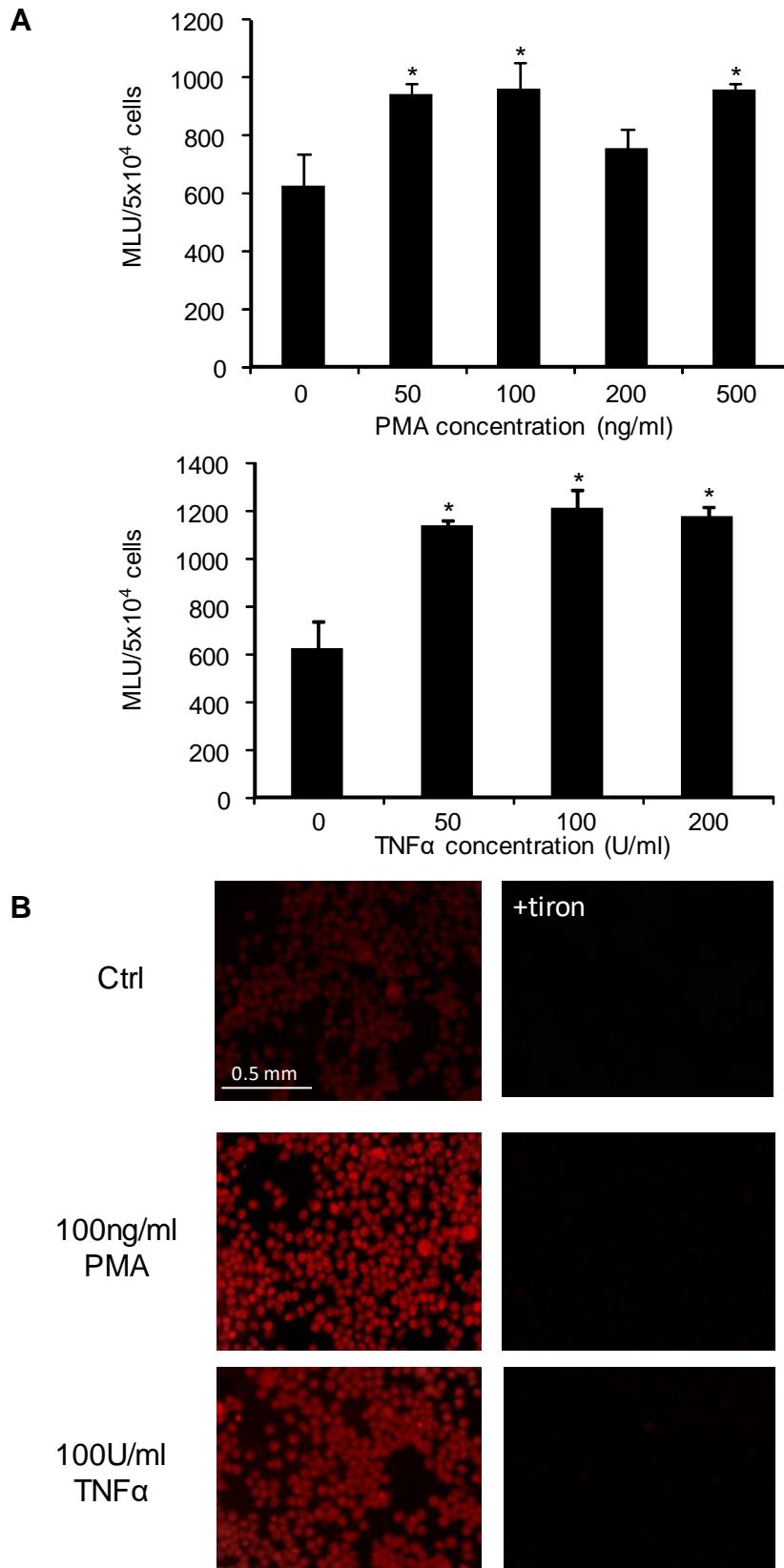
#### Legend for Figure 4.5

The brain homogenates from WT and Nox2KO mice at young (3-4 months) and ageing (21-22 months) groups were used for detecting the levels of expression of MAPK and Akt phosphorylation by Western blot. Levels of protein expressions of p-p38, p-JNK, p-erk, p-akt were detected. The phospho-bands were quantified and normalized to the total levels of the same protein detected in the same samples. Data was shown as mean  $\pm$  SD from 6 mouse brains per group. Comparisons were made by two-way ANOVA with bonferroni *post-hoc* test. \* $p < 0.05$  versus young mice in the same genetic group.

#### **4.2.6 The effects of PMA and TNF $\alpha$ on microglial cell ROS production measured by lucigenin chemiluminescence and DHE fluorescence**

To characterize the ROS production of BV-2 cells in response to PMA and TNF $\alpha$ , the dose response of both stimuli for acute stimulation on BV-2 cells was carried out and ROS levels of cells stimulated by difference concentrations of PMA and TNF $\alpha$  were examined using NADPH-dependent lucigenin chemiluminescence. In figure 4.6A, compared to other concentrations, 100 ng/ml of PMA stimulation can induce a relatively higher ROS production, which was significantly higher than the control group. 100 U/ml of TNF $\alpha$  was also able to induce a significant increase in BV-2 ROS production, demonstrating a relatively higher ROS production compared with other concentrations. Thus, 100 ng/ml of PMA and 100 U/ml of TNF $\alpha$  were applied for the assessment of BV-2 ROS production by DHE fluorescence in the absence or the presence of 100 ng/ml of PMA/ 100 U/ml of TNF $\alpha$ . The red DHE fluorescence significantly increased when cells were stimulated with either 100 ng/ml of PMA or 100 U/ml of TNF $\alpha$  compared with control group. However, in the presence of tiron, a superoxide scavenger, the red DHE fluorescence was almost undetectable in all groups.

Figure 4.6 The effects of PMA and TNF $\alpha$  on microglial cell (BV-2) ROS production measured by lucigenin chemiluminescence and DHE fluorescence



#### Legend for Figure 4.6

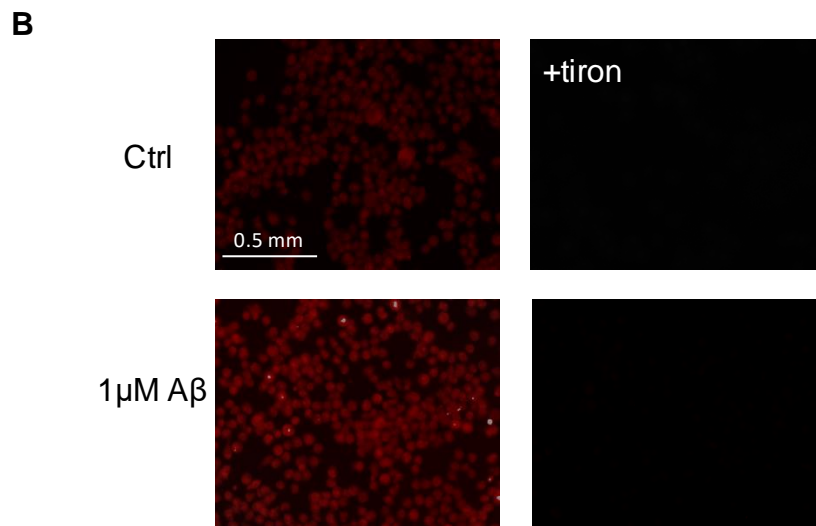
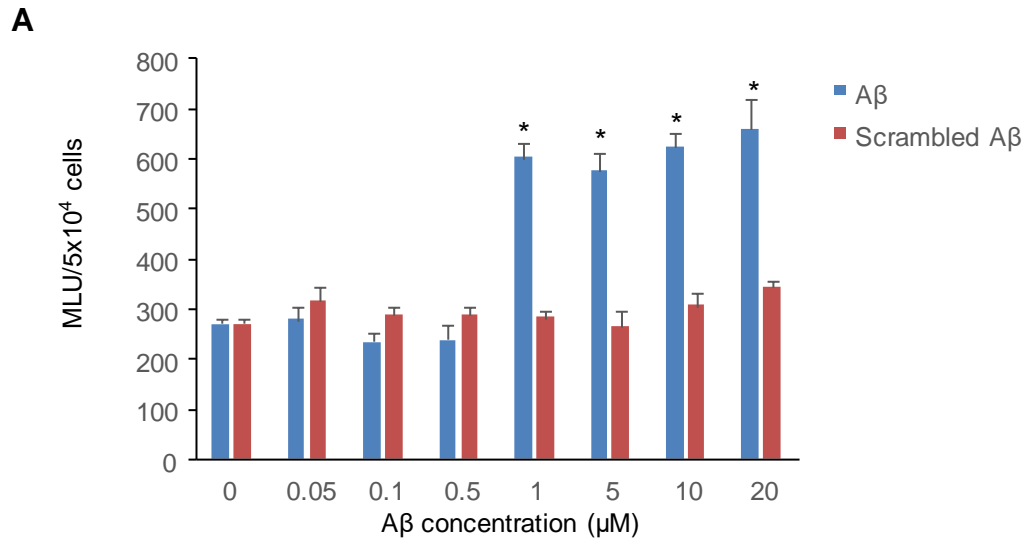
A) Dose responses of multiple stimuli on BV-2 cells measured by NADPH-dependent lucigenin (5  $\mu$ M) chemiluminescence. PMA and TNF $\alpha$  or BPS (same volume used as the solvent added to other groups) were incubated with BV-2 at 37°C for 30min and cells were then homogenised and detected. Data was shown as mean  $\pm$  SD from 6 independent experiments. Comparisons were made by one-way ANOVA with bonferroni *post-hoc* test. \* $p$ <0.05 versus control groups.

B) BV-2 cells were harvested and seeded on coverslips inside a 6-well cell culture plate overnight at 37°C in an incubator. Cells were then incubated with different stimuli for 30min at 37°C. Coverslips was then put on glass slides and incubated with 0.5 $\mu$ M of dihydrothedium (DHE). Parallely, 10mM tiron (a ROS scavenger) was applied for 15min before adding DHE. Intracellular ROS production was detected under a fluorescent microscope with a Cy3 filter (excitation: 530-560 nm; emission: 575-650 nm).

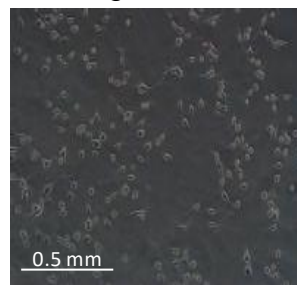
#### **4.2.7 The effects of A $\beta$ (1-42) on microglial cell (BV-2) ROS production measured by lucigenin chemiluminescence and DHE fluorescence**

To characterize the ROS production of BV-2 cell line in response to A $\beta$  (1-42), the dose response of A $\beta$  (1-42) for acute stimulation on BV-2 cells was carried out (Liu et al., 2015; Pan et al., 2011). ROS levels of cells stimulated by difference concentrations of either A $\beta$  (1-42) or scrambled A $\beta$  (1-42) were examined using NADPH-dependent lucigenin chemiluminescence. As shown in Figure 4.7A, there was no significant difference found in the ROS production from BV-2 cells between all doses of scrambled A $\beta$ . 1  $\mu$ M of A $\beta$  (1-42) was able to induce a significant increase in ROS production. This rise in ROS production lasted until cell treated with 20  $\mu$ M of A $\beta$  (1-42) at which point there was an over two-fold increase of ROS production compared to control group (unstimulated cells). Though a slight drop of ROS production was observed when cells were stimulated by 5  $\mu$ M of A $\beta$  (1-42), the increase in ROS production was still significantly higher than control group. The levels of ROS were relatively stable starting from 1  $\mu$ M of A $\beta$  (1-42) stimulation. Therefore, these results demonstrated that BV-2 cell line was a good cell model to study the mechanism of A $\beta$  (1-42)-induced microglial ROS production, and 1  $\mu$ M of A $\beta$  (1-42) stimulation was applied for subsequent experiments. Furthermore, to confirm the above results, superoxide production in BV-2 cells was assessed by DHE fluorescence in the absence or presence of 1  $\mu$ M of A $\beta$  (1-42). Similarly, the red DHE fluorescence dramatically increased when BV-2 cells were stimulated with 1  $\mu$ M of A $\beta$  (1-42) compared with control group. However, in the presence of tiron, a superoxide scavenger, the red DHE fluorescence was almost undetectable in both groups.

Figure 4.7 The effects of A $\beta$  (1-42) on microglial cell (BV-2) ROS production measured by lucigenin chemiluminescence and DHE fluorescence



Bright field image of untreated BV2 cells



#### Legend for Figure 4.7

A) Various dose of A $\beta$  (1-42) and its scrambled protein on BV-2 cells measured by NADPH-dependent lucigenin (5  $\mu$ M) chemiluminescence. A $\beta$  or scrambled A $\beta$  was incubated with BV-2 cells at 37°C for 30min before intracellular cell ROS measurements. Data was shown as mean  $\pm$  SD from 6 independent experiments. Comparisons were made by two-way ANOVA with bonferroni *post-hoc* test. \* $p$ <0.05 versus control groups.

B) BV-2 cells were harvested and seeded on coverslips inside a 6-well cell culture plate overnight at 37°C in an incubator. Cells were then incubated with 1 $\mu$ M of A $\beta$  (1-42) for 30min at 37°C. Coverslips was then put on glass slides and incubated with 0.5 $\mu$ M of dihydrothedium (DHE). Parallely, 10mM tiron (a ROS scavenger) was applied for 15min before adding DHE. intracellular ROS production was detected under a fluorescent microscope with a Cy3 filter (excitation: 530-560 nm; emission: 575-650 nm).

### 4.3 Discussion

In this chapter, the effect of ageing on cerebral endothelial, neuronal and microglia cells has been investigated with particular focus on the role of Nox2-derived oxidative stress. WT and Nox2KO mice were grouped into two age groups- young (3-4 months) and ageing (21-22 months) and the brain sections were used to assess the endothelial, microglial and neuronal cells. BV-2, a mouse microglial cell line, was also investigated for superoxide production with different stimuli.

To confirm the effect of ageing on the vascular dementia, the brain sections were investigated by immunofluorescence with CD31 as an endothelial cell marker. There was a significant decrease in the population of endothelial cells in WT ageing brains in comparisons with WT young controls, indicating that the ageing-related endothelial dysfunction contributes to vascular dementia in the brain. However, the decrease in the endothelial cell number was not seen in the Nox2KO ageing brains compared with Nox2KO young brains. There was also no difference in the endothelial cell numbers between the WT and Nox2KO brain at young age. These findings support that Nox2 acts as an important role in the vascular dementia and the deletion of Nox2 may help against the endothelial loss during ageing.

To investigate the effect of ageing on the neuronal cells and determine the role of Nox2, the brain sections were investigated by immunofluorescence with NeuN as a neuronal cell marker. It is well known that ageing is a major risk factor of neurodegenerative diseases, which is defined as the progressive loss of structure or function of neurons causing neuron cell death and therefore leading to dysfunction of the central nervous system (CNS) (Haass and Selkoe, 2007). This was confirmed by the significant decrease of neuronal cells found in the WT ageing brains compared with WT young

controls. Oppositely, in the Nox2KO brains, the significant difference in the neuronal cells between young and ageing groups was not seen. The above findings provide evidence for the role of Nox2 in the ageing-related neurodegeneration. Although the difference was not significant, there was a decrease of neurons in the Nox2KO ageing brains, compared with the Nox2KO young brains, indicating that, besides Nox2, there may be other factors involved in the ageing-related neurodegeneration. Interestingly, as described above, both endothelial cells and neuronal cells were decreased with ageing in WT mice. However, the brain weight was not seen to decline in figure 3.1. It may be because that Leukoariosis/white matter lesions were found to increase with age (Peters, 2006).

The microglial Nox2 expression in the brain with ageing was also investigated by immunofluorescence while Iba-1 was used as a microglial cell marker to inspect the microglial activation. In the WT brains, there was a significant increase of microglia expression with ageing, accompanied with a significant increase of Nox2 expression with ageing. However, this was not found in the Nox2KO ageing brains, compared with Nox2KO young mice. And as expected, no Nox2 was expressed in the Nox2KO mice. Together with the ageing-related neuron death and increased brain ROS production found previously, these results support that microglial Nox2 activation produces excessive ROS production and subsequently causes neuronal damage.

Western blot was carried out to confirm the increasing Nox2 expression with ageing, together with p22<sup>phox</sup>, p40<sup>phox</sup>, p47<sup>phox</sup>, p67<sup>phox</sup> and rac1. The significant increase was found in the levels of expressions of Nox2, p22<sup>phox</sup>, p40<sup>phox</sup>, p47<sup>phox</sup>, p67<sup>phox</sup> and rac1 with ageing. However, there was no significant difference in the levels of expressions of p22<sup>phox</sup>, p40<sup>phox</sup>, p47<sup>phox</sup>, p67<sup>phox</sup> and rac1 between young and ageing Nox2KO brains.

This has further confirmed Nox2-derived oxidative stress in the ageing brain. Furthermore, the levels of expression of other isoforms (Nox1 and Nox4) were also investigated using the brain homogenates from WT and Nox2KO mice at young and ageing groups. Although the levels of Nox1 expression showed an increase, the difference between young and ageing groups was not statistically significant for both WT and Nox2KO mice. There was no significant difference in the levels of expression in Nox4 between WT young and ageing mice. However, in Nox2KO mice, a significant increase of Nox4 expression was found in ageing, which might be a compensatory response. The reason might be that Nox4 acts as a protective role in vascular function (Schroder et al., 2012).

To examine the activation of redox signaling pathways with ageing, redox-sensitive ERK1/2, p38MAPK and JNK phosphorylation in brain samples were investigated using phosphorylation-specific monoclonal antibodies. The levels of expression of phosphorylated ERK1/2 and p38MAPK was found to be significantly increased with ageing, while there was no significant difference between young and ageing brains of Nox2KO mice. The levels of phosphorylated JNK showed no significant change between age groups of WT and Nox2KO brains. Together with the increased expression of Nox2 and other subunits with ageing, these findings have shown a crucial role for age-associated Nox2 activation in the activation of redox signaling pathways in the ageing brain.

Nox2 is expressed in the microglial cells in the brain, which was confirmed by immunofluorescence in the figure 4.3A. To uncover the Nox2-derive oxidative stress in the microglial activation, the intracellular superoxide production of BV-2 cells was detected by lucigenin-chemiluminescence in the presence of A $\beta$  which is associated with Alzheimer's diseases, and inflammatory factors such as PMA and TNF $\alpha$ . The dose

response experiment has demonstrated that 100 ng/ml of PMA, 100 U/ml of TNF $\alpha$  and 1  $\mu$ M of A $\beta$  (1-42) represent the best concentrations of each stimuli in BV-2 cells when examining the superoxide production. The increase in the superoxide production of BV-2 cells in the presence of 100 ng/ml of PMA, 100 U/ml of TNF $\alpha$  or 1  $\mu$ M of A $\beta$  (1-42) detected by DHE fluorescence has further confirmed that microglial is activated when challenged with different stimuli and produces excessive ROS.

Putting together, my data suggest that increased expression of Nox2 with ageing leads to capillary loss, microglial activation and neuron death in the brain. Age-associated Nox2 activation plays a crucial role in the activation of redox signaling pathways and Nox2-derived oxidative stress contributes to the cerebral vascular dementia and neurodegeneration. Elimination of Nox2 has been shown here to protect against the vascular ageing and neuron loss.

## Chapter 5

# **Overexpression of Nox2 increases brain oxidative stress and endothelial damage, studies using human Nox2 transgenic mice; and the clinical significance**

### **5.1 Introduction**

It was well documented that obesity and insulin resistance in an ageing population has led to a rapid increase in type-2 diabetes and cardiovascular diseases (Houston et al., 2009, Krause et al., 2007). The progressive endothelial dysfunction characterised by increased ROS production has been accepted as an early pathological change in the development of metabolic and cardiovascular diseases (Li and Shah, 2004, Sukumar et al., 2013). Importantly, mounting evidence suggests a role for a Nox2-containing NADPH oxidase in increased reactive oxygen species production in the endothelium that contributes to further deterioration of vascular function in ageing (Du et al., 2013, Fan et al., 2014, Fan et al., 2017). The endothelial cells form the blood-brain barrier between the blood circulation and the brain tissues and endothelial dysfunction would affect the function of other cells in the brain. Oxidative stress can cause DNA damage, alters transcriptional machinery and promotes inflammatory gene expressions. All these are key factors that further accelerate vascular ageing. In response to stimuli, such as high glucose and insulin, the endothelial Nox2 is activated and produces excessive levels of ROS, which outstrips the endogenous antioxidant defence and causes oxidative damage to the endothelium and the organs (Du et al., 2013, Fan et al., 2014). Transgenic mice with endothelial specific Nox2 overexpression had high levels of ROS production and ERK1/2 activation in the endothelium (Fan et al., 2014). Furthermore,

there is a close relationship between the levels of endothelial oxidative stress and the degree of insulin resistance and cardiovascular disorders found in experimental animals and in humans (Capell et al., 2007; Li et al., 2004; Sukumar et al., 2013). However, the mechanism of Nox2 activation in the cerebral vascular system and endothelial cells in normal ageing remains unclear.

In this study, we firstly used brain tissues from transgenic mice with endothelial specific Nox2 overexpression kindly provided by the research of Prof. Channon's group (Bendall et al., 2007) at Oxford in young (3-4 months) and early ageing (12-14 months) to examine ageing-associated endothelial Nox2 activation induced brain oxidative stress and endothelial damage in the brain. To generate this model, a human Nox2 transgene was constructed, incorporating the murine Tie2 promoter and intronic enhancer. The Tie2-Nox2 transgene underwent pronuclear microinjection into fertilized eggs from superovulated C57BL/6xCBA mice. Transgenic founders were then back-crossed on to the C57BL/6J strain. To further confirm the important role of endothelial Nox2 in response to age-related metabolic disorders, coronary microvascular endothelial cells (CMEC) was isolated from WT and Nox2KO mice at middle age (11-12 months old). We also examined high glucose and insulin-induced oxidative stress and Nox2 activation in endothelial cell using CMECs isolated from WT and Nox2KO mice. Finally, young (20-40 years old) and old (over 60 years old) human brains collected from MRC brain tissue bank and given to us by Prof. Colin Smith (the University of Edinburgh, Department of Pathology) were used to investigate the role of Nox2 derived ROS in ageing-related oxidative stress. In particular, the ageing-associated activation of Nox2 and redox-signalling, microglial activation and cell apoptosis in these human brain tissues were further evaluated confirmed by Western blots in human brains.

## 5.2 Results

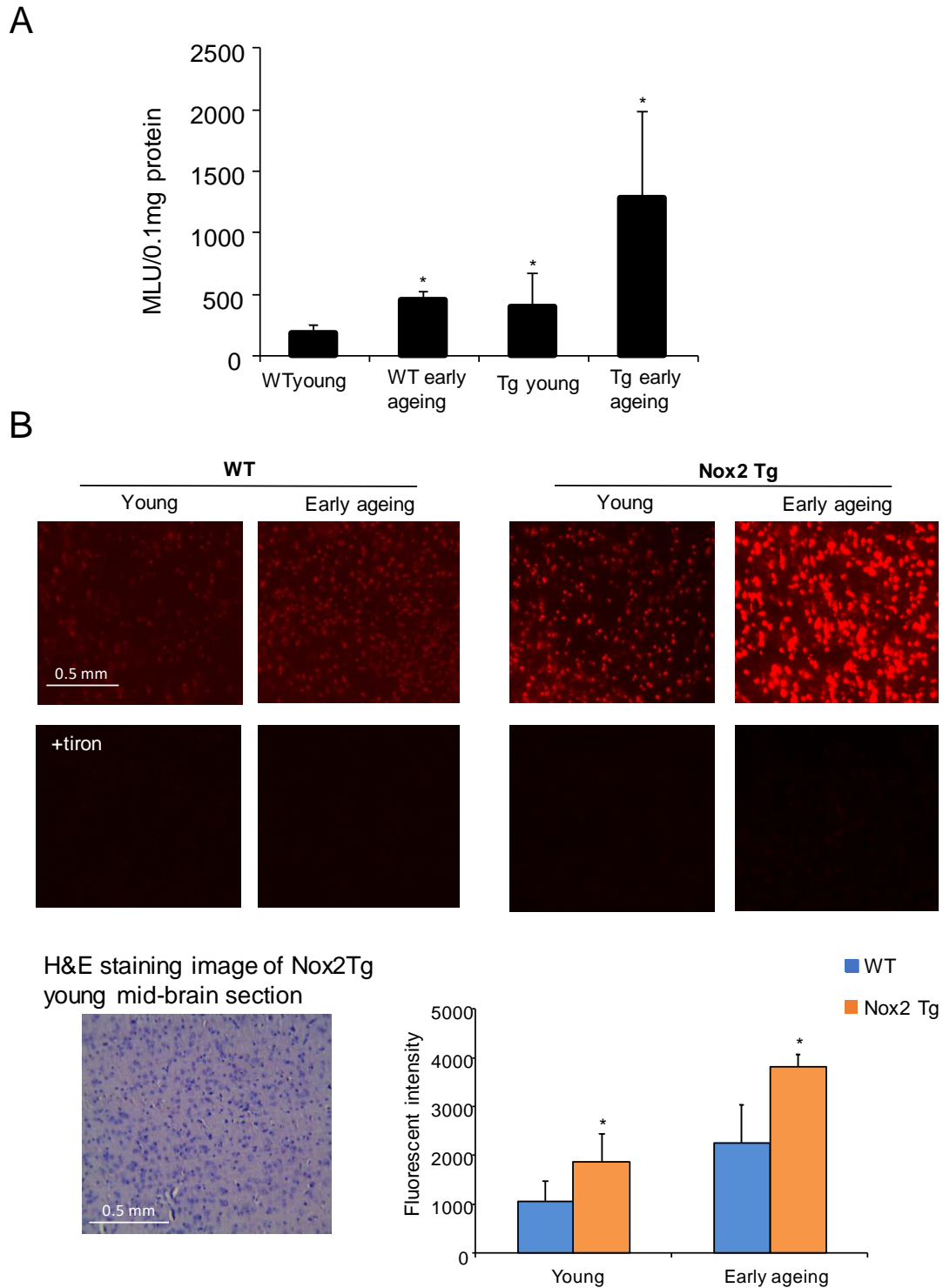
### 5.2.1 The effect of ageing and the role of Nox2 on superoxide production from Nox2 transgenic brain detected by lucigenin chemiluminescence and DHE fluorescence

The superoxide production in brain homogenates of young (3-4 months) and early ageing (12-14 months) WT and endothelial specific Nox2 overexpression transgenic (Nox2Tg) mice was assessed by lucigenin chemiluminescence (figure 5.1A). There was 2-fold increase in superoxide production in early ageing WT brain homogenates compared with young WT controls. Similarly, there was also a significant increase in superoxide production in young Nox2Tg brain homogenates compared with young WT controls. Regarding the effect of Nox2, there was nearly a 3-fold increase in superoxide production in Nox2Tg old mice compared with Nox2Tg young mice.

The superoxide production in brains of young (3-4 months) and early ageing (12-14 months) WT and Nox2 transgenic (Nox2Tg) mice was also assessed by DHE fluorescence (figure 5.1B). In Nox2Tg mice, the red DHE fluorescence increased with early ageing, and this was also found in WT group. Tiron, a non-enzymic superoxide scavenger was added to confirm that only the superoxide was detected rather than other species of ROS. The red DHE fluorescence was nearly undetectable in all groups.

The fluorescent intensities were quantified and there was a significant increase in fluorescent intensity between young and early ageing groups in WT brains. Fluorescent intensity also increased significantly in early ageing Nox2Tg mice compared with young Nox2Tg mice. In terms of the effect of Nox2, Nox2Tg brains had significant increase in superoxide production compared with WT brains at both young and early ageing groups.

Figure 5.1 The effect of ageing and the role of Nox2 on superoxide production from Nox2 transgenic brain detected by lucigenin chemiluminescence and DHE fluorescence.



## Legend to Figure 5.1

A) Tiron-inhibitable ROS production was detected in brain homogenates by NADPH-dependent lucigenin (5 $\mu$ M) chemiluminescence from young (3-4 months) and early ageing (11-12 months) WT/Nox2 overexpression (Tg) mice. Data was expressed as mean  $\pm$  SD with a number of 6 mice per group. Comparisons were made by a one-way ANOVA with bonferroni *post-hoc* test. \* $p < 0.05$  versus young mice.

B) 10 $\mu$ m thickness of frozen brain sections from young (3-4 months) and early ageing (12-14 months) age WT/Nox2 overexpression (Tg) mice were incubated with 2 $\mu$ M of dihydroethidium (DHE) for 5min. A fluorescent microscope with a Cy3 filter (excitation: 530-560 nm; emission: 575-650 nm) was used to measure the intracellular ROS production. Upper figure: representative fluorescent images of *in situ* brain ROS production detected by DHE fluorescence. Images were captured at 10X magnification. 10mM of tiron was applied prior to DHE staining and incubated for 10min. Lower figure: left, the representative bright field image of the mid-brain area applied in the experiment. Right, quantitative analysis of DHE fluorescent intensities of brain images from WT and Nox2 overexpression young and early ageing mice. Data was shown as mean  $\pm$  SD from 6 mouse brains (3 sections from each brain and 15-20 images were taken per section). Comparison were made by two-way ANOVA with bonferroni *post-hoc* test. \*  $p < 0.05$  versus age-matched WT mice.

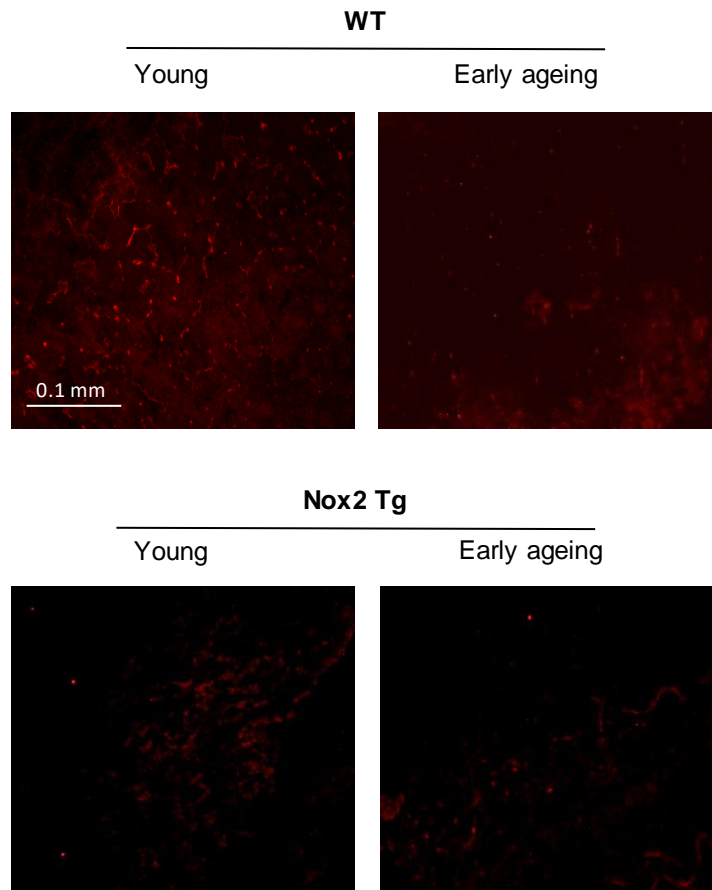
### **5.2.2 The effect of ageing and the role of endothelial Nox2 overexpression on cerebral endothelial cells detected by immunofluorescence**

Immunofluorescence was performed to detect the expression of CD31 (the endothelial cell marker) in the brain sections in the WT and Nox2Tg mice at young (3-4 months) and early ageing (12-14 months) (figure 5.2A). In WT brains, the red fluorescence showed a decrease with ageing. There was also a decrease in Nox2Tg early aged brains compared with Nox2Tg young brains. Furthermore, there was no significant difference in the fluorescence between WT and Nox2Tg mice at young age. In both young and early ageing groups, the Nox2Tg brains showed a decrease in the red fluorescence compared with WT brains at the same age.

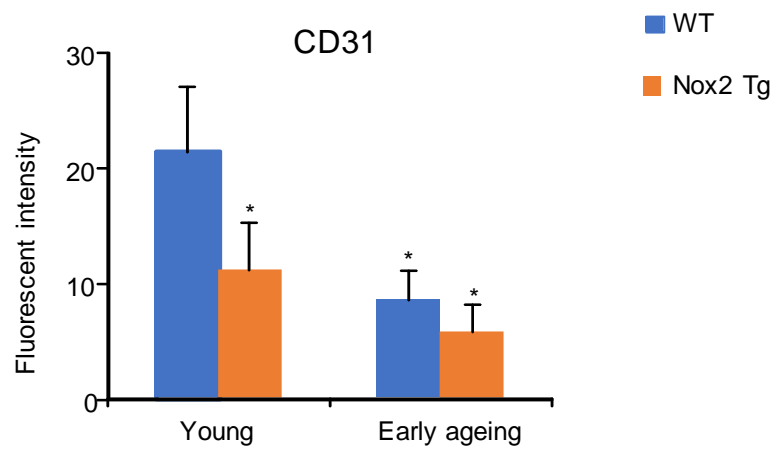
The above findings were confirmed by the quantification of the fluorescent intensity (Figure 5.2B). A significant reduction of the endothelial cell population in WT ageing mice was demonstrated compared with WT young mice. Similarly, there was over 2-fold decrease in the fluorescent intensity in Nox2Tg early aged brain compared with Nox2Tg young brains.

Figure 5.2 The effect of ageing and the role of endothelial Nox2 over expression on cerebral endothelial cells detected by immunofluorescence

A



B



## Legend to figure 5.2

Frozen sections of mid-brains (10 $\mu$ m thickness) were from young (3-4 months) and early ageing (11-12 months) WT/Nox2 overexpression (Tg) mice. Sections were stained with the endothelial cell marker CD31 (red). Fluorescent labelled antigens were investigated with an Euromex fluorescent microscope to measure Cy3 (excitation: 530-560 nm; emission: 575-650 nm) fluorescence.

A. Representative fluorescent images were captured at 40X magnification to visualize CD31 expression in different mid-brain sections.

B. Quantitative analysis results of fluorescent intensity in images of brain sections from WT and Tg mice. Data was shown as mean  $\pm$  SD from 6 mouse brains (more than 10 images were taken per brain section). Comparison were made by two-way ANOVA with bonferroni *post-hoc* test. \* $p < 0.05$  versus young mice.

### **5.2.3 The effect of high glucose and insulin on endothelial Nox2 activation and endothelial ROS production detected by DCF fluorescence**

In order to investigate if ageing associated metabolic disorders such as high glucose and insulin levels (insulin resistance) plays a role in endothelial Nox2 activation, isolated coronary microvascular endothelial cells (CMEC) from middle aged (11-12 months old) were isolated from WT and Nox2 KO mice. The ROS production was examined by DCF fluorescence after CMECs were challenged with high glucose (25 mM) plus insulin (1.2 nM) for 24 hours (figure 5.3A). The green fluorescence increased when WT CMECs were stimulated with high glucose plus insulin compared with WT CMEC controls. However, the green fluorescence was reduced in Nox2KO CMECs. This was confirmed by quantification of the fluorescent intensities (figure 5.3B).

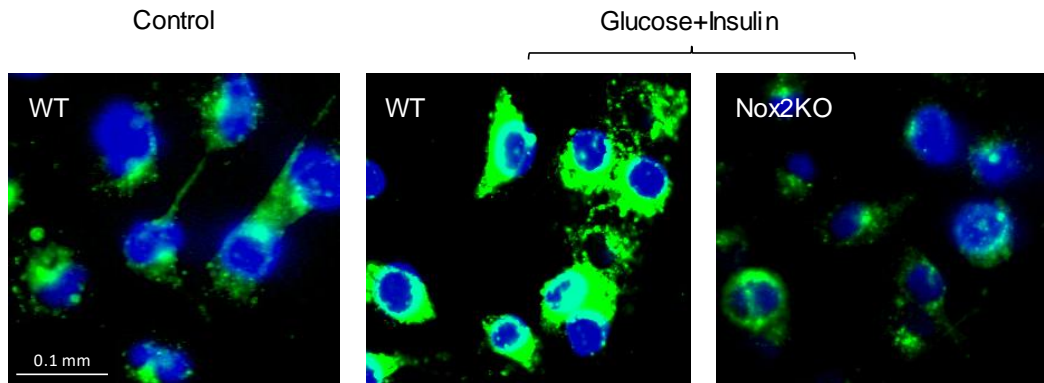
Fluorescent intensity significantly increased when WT CMECs stimulated with high glucose plus insulin compared with CMEC controls. However, this was not seen in the Nox2KO CMECs. There was a significant decrease in fluorescent intensity in Nox2KO CMECs compared with WT CMECs when challenged with glucose and insulin. However, no difference in fluorescent intensity was found between the presence and the absence of high glucose and insulin in Nox2KO CMECs. There was still detectable ROS in Nox2KO CMECs either the presence or the absence of high glucose and insulin, which suggests that there are still ROS produced by other sources apart from Nox2 in endothelial cells.

The ROS production was also assessed by lucigenin chemiluminescence when WT/Nox2KO CMECs were treated with either BPS, high glucose alone, insulin alone or high glucose plus insulin. When cells were stimulated with high glucose or insulin alone, the ROS production was significantly higher compared with control group

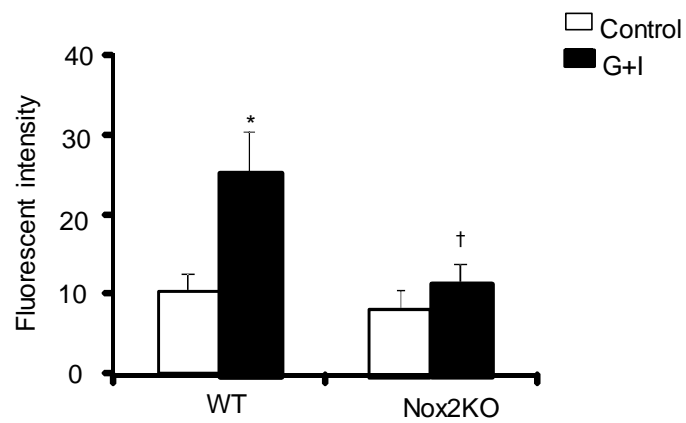
(figure 5.3C). The combination of high glucose and insulin led to a higher ROS production. However, these were not found in the Nox2KO CMECs, which further proves that high glucose and insulin are potent activators of the endothelial Nox2 enzyme.

Figure 5.3 The effect of high glucose and insulin on CMEC ROS production detected by DCF fluorescence

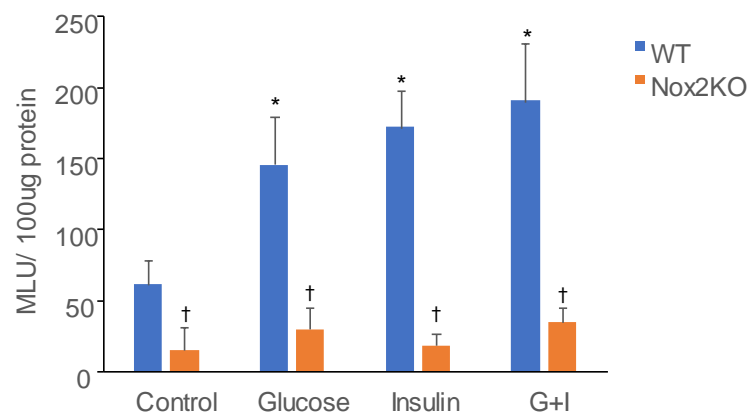
A



B



C



Legend to figure 5.3

A) Representative fluorescent images of intracellular ROS production detected by DCF fluorescence. Images were captured at 40X magnification. Primary coronary microvascular endothelial cells (CMEC) from WT and Nox2 middle-aged (11–12 months) mice were challenged with high glucose (25 mM) plus insulin (1.2 nM) for 24 hours, followed by 30 minutes of DCF (10  $\mu$ M) incubation. The nuclei were labelled with DAPI in blue colour. CMECs were then investigated with an Olympus BX61 fluorescent microscope equipped with a FITC filter (excitation/emission: 470-495/510-550 nm) to measure the intracellular ROS production.

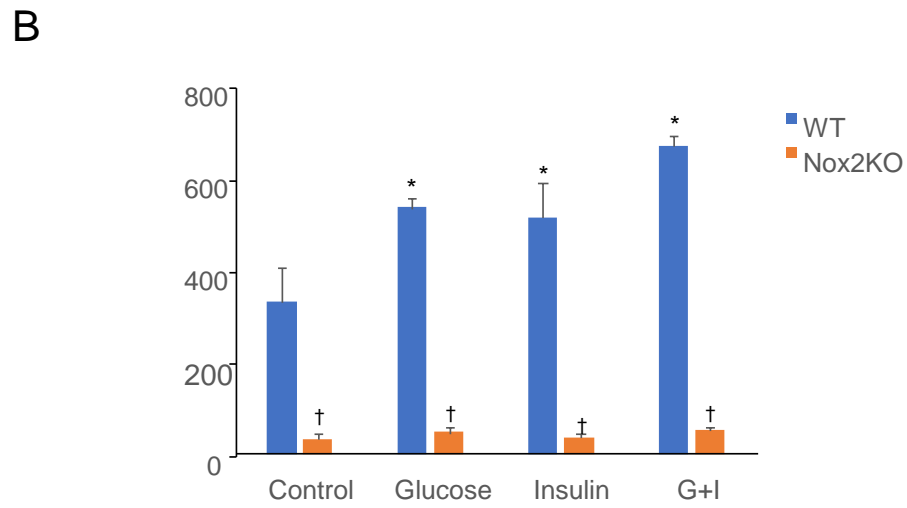
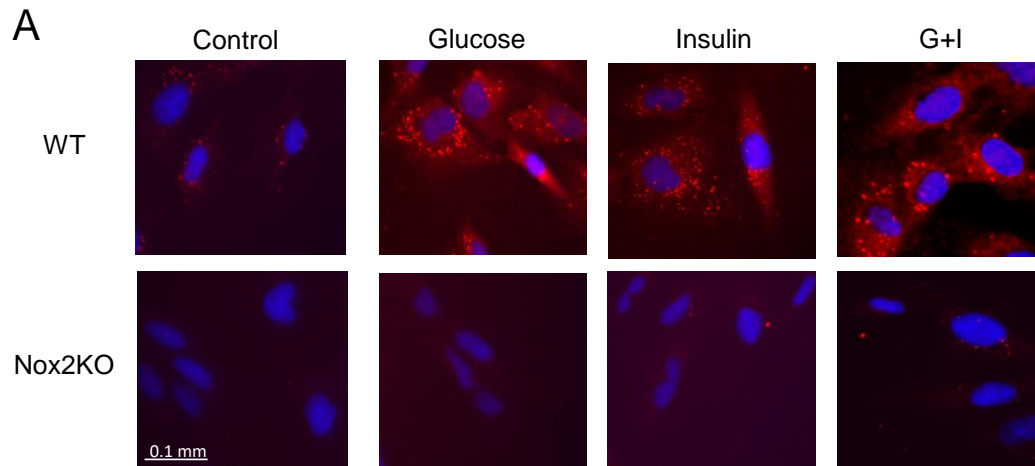
B) Quantitative analysis of fluorescent intensities of cell images. Data was shown as mean  $\pm$  SD, n =3 separated CMEC isolation/group. Six mice were used for each CMEC isolation. Comparison were made by two-way ANOVA with bonferroni *post-hoc* test. \* p<0.05 for indicated values versus control values in the same genetic groups. †p<0.05 for indicated values versus WT G+I values.

C) ROS production was detected in WT/Nox2KO CMEC homogenates by NADPH-dependent lucigenin (5 $\mu$ M) chemiluminescence assay. Cells were challenged with either high glucose (25 mM) alone, insulin (1.2 nM) alone or high glucose (25 mM) plus insulin (1.2 nM) for 24 hours. Data was expressed as mean  $\pm$  SD, n=3. Comparisons were made by two-way ANOVA with bonferroni post-hoc test. \*p<0.05 versus WT controls, †p<0.05 for indicated values versus WT values under the same condition.

#### **5.2.4 The effect of high glucose and insulin on endothelial Nox2 activation detected by immunofluorescence**

The expression of Nox2 in endothelial cells in the presence of high glucose, high insulin or the combination of high glucose plus insulin (G+I) was detected by immunofluorescence using CMECs isolated from WT and Nox2 middle-aged (11-12 months) mice. The red fluorescent intensity stained for Nox2 significantly increased in WT CMECs when challenged with high glucose alone, high insulin alone or high glucose plus insulin in comparison to WT controls (figure 5.4A). However, there was no expression as expected in Nox2KO CMEC and there was no difference in the expression of Nox2 between four experimental groups of Nox2KO CMECs. These finding was confirmed by the quantification of the fluorescent intensity of Nox2 staining (figure 5.4B).

Figure 5.4 The effect of high glucose and insulin on endothelial Nox2 activation in WT versus Nox2KO CMECs detected by immunofluorescence



Legend to figure 5.4

- A) Representative fluorescent images captured at 40X magnification. Primary coronary microvascular endothelial cells (CMEC) from WT and Nox2 middle-aged (11–12 months) mice were challenged with PBS (the solvent of stimuli), high glucose (25 mM) alone and high glucose (25 mM) plus insulin (1.2 nM) alone for 24 hours, followed by 2% PFA fixation. CMECs were then stained for Nox2 expression (Cy3, red) and nuclei were stained with DAPI (blue). Immunofluorescence was investigated with an Euromex fluorescent microscope to measure Cy3 (excitation: 530-560 nm; emission: 575-650 nm) fluorescence.
- B) Quantitative analysis of fluorescent intensities of cell images. Data was shown as mean  $\pm$  SD, n =3 separated CMEC isolation/group. Six mice were used for each CMEC isolation. Comparison were made by two-way ANOVA with bonferroni *post-hoc* test. \* p<0.05 for indicated values versus WT control values. †p<0.05 for indicated values versus WT values under the same condition.

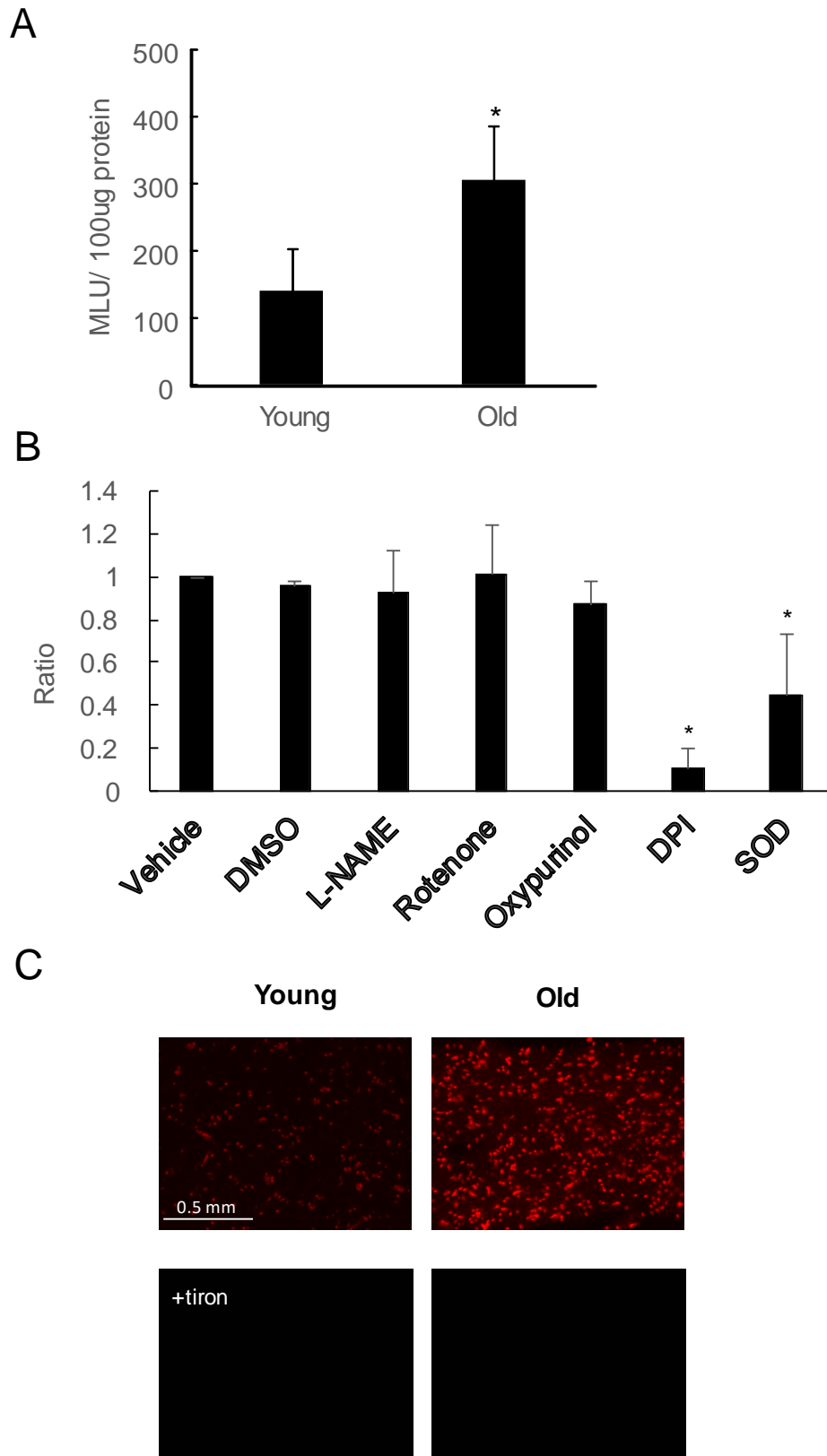
### **5.2.5 The effect of ageing on human brain superoxide production detected by lucigenin chemiluminescence and DHE fluorescence**

The superoxide production in brain homogenates of young (20-40 years old) and old (over 60 years old) humans was assessed by lucigenin chemiluminescence (figure 5.5A). There was 2-fold increase in superoxide production in old brain homogenates compared with young controls.

An inhibitor assay was carried out to determine the source of superoxide in old human brains (figure 5.5B). Brain homogenates were incubated with either buffer, 100  $\mu\text{M}$  of the nitric oxide synthase (NOS) inhibitor N(G)-Nitro-L-arginine Methyl Ester (L-NAME), 100  $\mu\text{M}$  of the xanthine oxidase inhibitor oxypurinol (oxy), 20  $\mu\text{M}$  of the NADPH oxidase inhibitor diphenyleneiodonium (DPI), 50  $\mu\text{M}$  of the mitochondrial complex-1 enzymes rotenone (Rot) or 200U/ml of superoxide dismutase (SOD). There was a significant decrease in ROS production in the presence of SOD or DPI but not in the presence of L-NAME, rotenone or oxypurinol.

The ROS production in human brains of young (20-40 years old) and old (over 60 years old) was also assessed by DHE fluorescence (figure 5.5C). In human brains, the red DHE fluorescence was increased with ageing. Tiron, a non-enzymic superoxide scavenger was added to confirm that only the superoxide was detected rather than other species of ROS. The red DHE fluorescence was nearly undetectable in all groups.

Figure 5.5 The effect of ageing on human brain superoxide production detected by lucigenin chemiluminescence and DHE fluorescence



### Legend to figure 5.5

A) ROS production was detected in brain homogenates by NADPH-dependent lucigenin (5 $\mu$ M) chemiluminescence at young (20-40 years old) and old (over 60 years old) humans. Data was expressed as mean  $\pm$  SD with a number of 8 human tissues per group. Comparisons were made by one-way ANOVA with bonferroni *post-hoc* test. \* $p$ <0.05 versus young controls.

B) Inhibitor assay in old human brain homogenates to confirm the source of superoxide. Homogenates were incubated with DMSO, 100  $\mu$ M L-NAME, 200 U/mL superoxide dismutase (SOD), 20  $\mu$ M diphenyleneiodonium (DPI), 50  $\mu$ M rotenone (Rot) or 100  $\mu$ M oxypurinol (Oxy) for 15 minutes before measurement of superoxide production by NADPH-dependent lucigenin (5 $\mu$ M) chemiluminescence. Data was expressed as mean  $\pm$  SD with a number of 8 brains per group. Comparisons were made by one-way ANOVA with bonferroni *post-hoc* test. \* $p$ <0.05 versus vehicle.

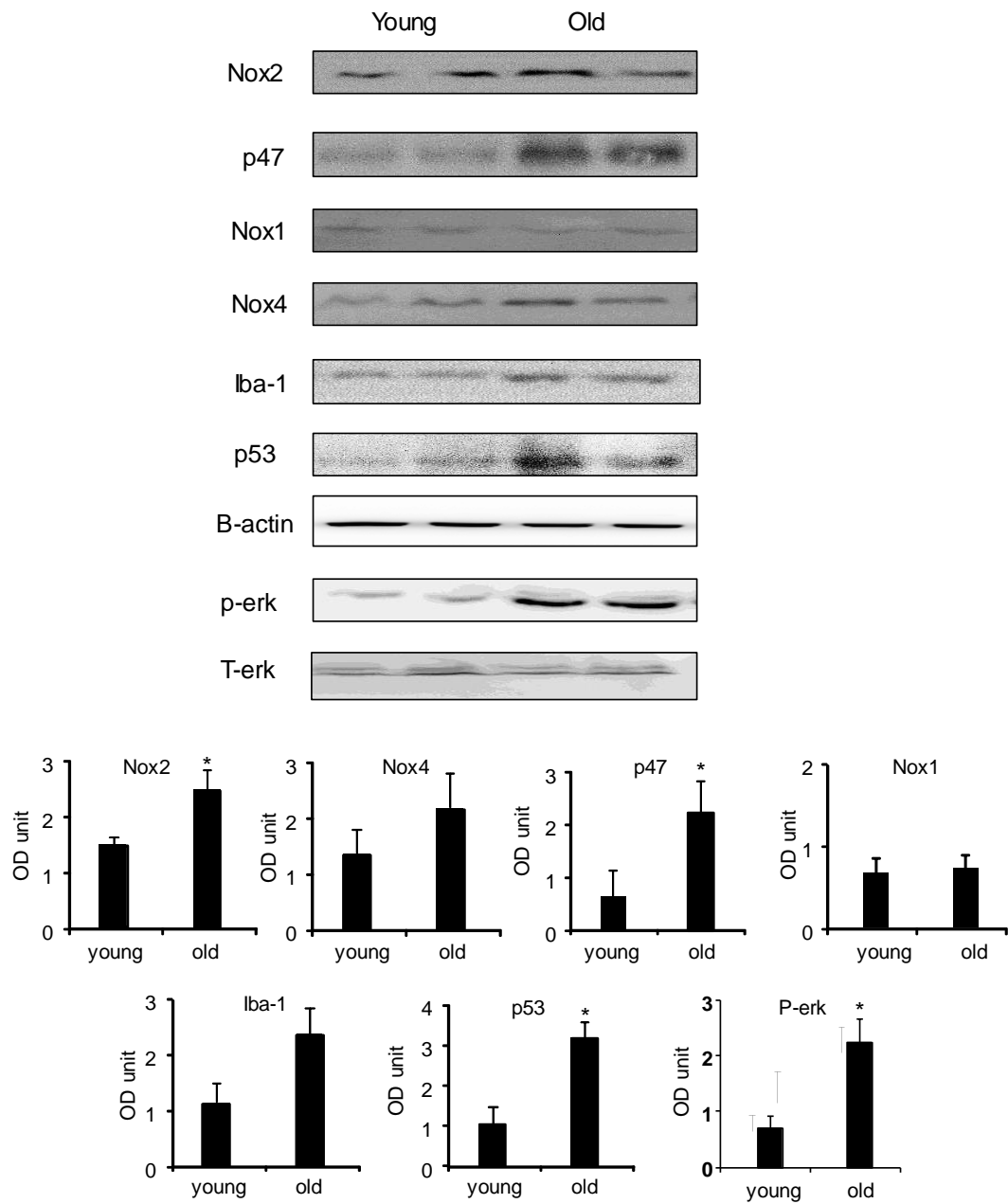
C) 10 $\mu$ m thickness of frozen brain sections from young (20-40 years old) and ageing (over 60 years old) humans were incubated with 2 $\mu$ M of dihydroethidium (DHE) for 5min. A fluorescent microscope with a Cy3 filter (excitation: 530-560 nm; emission: 575-650 nm) was used to measure the intracellular ROS production. Representative fluorescent images of *in situ* brain ROS production detected by DHE fluorescence. Images were captured at 10X magnification. 10mM of tiron was applied prior to DHE staining and incubated for 10min.

### **5.2.6 The effect of ageing on NADPH oxidase subunit expression and cell apoptosis in human brain detected by Western blot**

To further define a role for Nox2 in the oxidative regulation of ageing human brain, the expression of Nox subunit was examined by Western blot using brain homogenates from young and old human (figure 5.6). Compared to young brains, there were significant increases in the levels of Nox2, p47<sup>phox</sup> expressions. However, the levels of Nox1 expression did not increase with ageing. There was also an ageing-related increase in the levels of Nox4 between young and old brains however it was not statistically significant.

ERK1/2 is one of the redox-sensitive signaling molecules which can respond to ageing progress via NADPH oxidase. To investigate MAPK activation with ageing, young and old brain homogenates were used to examine the phosphorylation of ERK1/2 Western blotting. The levels of total ERK detected in the same samples were used as loading controls. Compared to young brains, the levels of ERK1/2 phosphorylation were increased significantly, which was accompanied by significant increase in the levels of p53 (cell apoptosis-related gene product) expression in old brains. In addition, the levels of Iba-1 (microglia activation) expression was also examined between young and old human brains and a significant increase was seen with ageing.

Figure 5.6 The effect of ageing on NADPH oxidase subunit expression and cell apoptosis in human brain detected by Western blot



### Legend to figure 5.6

The brain homogenates from young (20-40 years old) and old (over 60 years old) humans were used for detecting the levels of expression of NADPH subunits and microglia by Western blot. Levels of protein expression of Nox1, Nox2, Nox4, p47<sup>phox</sup>, Iba-1, p53 and p-erk were investigated. B-actin detected in the same sample was used as a loading control and the p-erk bands were quantified and normalized to the total-erk detected in the same samples. The optical densities (OD) of were quantified digitally and normalized to either B-actin or t-erk levels. Data was shown as mean  $\pm$  SD from 6 brains per group. Comparisons were made by one-way ANOVA with bonferroni *post-hoc* test. \*p<0.05 versus young human brains.

### 5.3 Discussion

The global Nox2-activation and increased ROS production with ageing was shown in a recent study (Fan et al., 2017) and in chapter 3. However, whether the Nox2 from endothelium plays a role in the development of endothelial dysfunction with ageing brain remains unknown. Therefore, we have used the endothelium specific Nox2 overexpression mice (Nox2 transgenic mice) generated from Channon's group (Bendall et al., 2007). To further determine the role of endothelium-dependent Nox2 in the ageing brain, brains from Nox2 transgenic (Nox2Tg) mice were grouped into young (3-4 months) and early ageing (12-14 months), along with age-match WT brains as the control groups. Firstly, ROS production was assessed using either brain homogenates or brain sections from each group. Nox2Tg brains produced significant higher ROS compared with age-matched WT mice. This provides evidence for a role of endothelial Nox2 contributing to ROS generation. Furthermore, Nox2Tg brains from young mice had a similar ROS production as the WT early ageing mice and Nox2Tg early ageing brains had a dramatically higher ROS production. This finding suggests that Nox2 derived from endothelium may play an important role with ageing and accelerating ageing progress.

Vascular disease are often linked with endothelial dysfunction and increased production of ROS derived from vascular NADPH oxidases in endothelial cells (Konior et al., 2014). To further investigate the role of Nox2 in ageing-related endothelial dysfunction, the endothelia cells in brains from Nox2Tg mice at young (3-4 months) and early ageing (12-14 months), along with age-matched WT brains were examined by immunofluorescence. Compared with WT young brains, there was a significant decrease in the CD31 expression in WT old brains which was as expected. This

reduction became further exacerbated at old age in Nox2Tg mice. This evidence again supports that Nox2 plays an important role in age-related endothelial dysfunction with ageing.

High glucose and insulin are potent activators of the endothelial Nox2 enzyme (Finkel and Holbrook, 2000, Sukumar et al., 2013). To further examine hyperglycaemia and hyperinsulinaemia-induced Nox2 activation in endothelial ageing, CMECs isolated from middle aged (11–12 months) WT and Nox2KO mice were applied. ROS production was firstly assessed by DCF fluorescence. There was significant difference in the level of ROS production between WT CMECs stimulated with high glucose plus insulin and WT CMECs control, which was absent in Nox2KO CMECs stimulated with high glucose and insulin. Furthermore, whether Nox2 is activated in endothelial cells when challenged with high glucose plus insulin is examined by immunofluorescence using CMECs isolated from middle aged (11–12 months) WT and Nox2KO mice. The levels of Nox2 expression were significantly higher when CMECs were exposed to high glucose plus insulin which was abolished in Nox2KO CMECs. Our in vitro data are in support of that Nox2 plays a crucial role in glucose metabolic disorder-associated oxidative damage of endothelial cells and vascular ageing and knockout of Nox2 can prevent high glucose/insulin-induced ROS production. Isolating CMECs from Nox2Tg mice would potentially be the next important step to further support the critical role of Nox2 in endothelial ageing. Additionally, CMECs from aged WT/Nox2Tg/Nox2KO mice would be interesting to further study with to establish the significant role of Nox2 in vascular ageing.

To support that increased ROS and oxidative stress occur with ageing in humans as well as in mice, the superoxide production in young and old age human brain tissue was

investigated by lucigenin chemiluminescence and DHE fluorescence. Superoxide production was significantly increased in ageing brain samples compared to young controls and the superoxide scavenger tiron significantly decreased superoxide production at all age groups which confirmed the specificity for superoxide. An inhibitor assay was then carried out in the old brain samples and there was no difference in the presence of L-NAME, rotenone or oxypurinol. However, there was a significant decrease in the superoxide production in the presence of SOD or DPI, supporting that Nox2 is the major source of superoxide in the old human brains.

Western blot was carried out to confirm the increasing Nox2 expression with ageing in human brain, together with Nox1, p47<sup>phox</sup> and Nox4. The significant increase was found in the levels of expressions of Nox2 and p47 in ageing human brain compared to young controls. However, there was no significant difference in the levels of expressions of Nox1 and Nox4 between young and old brain samples. This has further confirmed Nox2-derived oxidative stress in the ageing brain. To examine the activation of redox signaling pathways with ageing in human brains, ERK1/2 phosphorylation in brain samples were investigated using phosphorylation-specific monoclonal antibodies. Consequently, the levels of expression of phosphorylated ERK1/2 significantly increased with ageing. Furthermore, the increasing Nox2 was also accompanied with increasing levels of expression of p53 and Iba-1. These findings suggest that Nox2 is involved in the activation of redox signaling pathways, cell apoptosis and microglia activation with ageing in human brain.

## Chapter 6

### General discussion and future work

#### 6.1 General Discussion

The Nox2 enzyme has long been recognised as a major source of superoxide production in the neutrophils and in the vascular system. There are evidence showing that Nox2-derived oxidative stress plays a role in the development of cardiovascular diseases (Li and Shah, 2004, Li et al., 2007, Sukumar et al., 2013, Fan et al., 2017). In particular, Nox2 has also been seen to be widely expressed throughout the central nervous system and plays a crucial role in the development of neurodegenerative diseases, including vascular dementia and Alzheimer's diseases (Hernandes and Britto, 2012, Park et al., 2008, Qin et al., 2013). However, the effects of Nox2 with ageing are not fully understood. Therefore, this PhD study focuses on investigating the role of Nox2-derived superoxide production in ageing-related brain oxidative stress, cerebral endothelial damage and brain dysfunction.

The age process is often associated with accumulated free radicals, in particular the reactive oxygen species. At least seven different isoforms of NADPH oxidase (Nox1-Nox5, Duox1 and Duox2) are widely expressed in different tissues (Bedard and Krause, 2007, Kawahara et al., 2007, Nauseef, 2008). In this study, we showed a global Nox2 activation by an age-related increase in the levels of Nox2-derived ROS production in several vital organs of WT mice including the heart, liver, lung, spleen, kidney and brain. Knockout of Nox2 or inhibiting Nox2 significantly reduced the levels of ageing-associated ROS production in these organs at old age. With an interest of brain, we showed an age-related increase in the superoxide production. Furthermore, we have

used four different methods to consolidate this finding. By doing this, we also found the deletion of Nox2 significantly decreases in the age induced superoxide production while there was no difference in the levels of hydrogen peroxide generation between the WT and Nox2KO in ageing brains. Overall these findings suggest a crucial role of Nox2 in the ageing-related in the superoxide production in these organs, especially the brain.

In the previous studies, elimination of Nox2 prevented ageing mice from developing obesity despite the fact that there was no difference in food intake between the WT and Nox2KO mice at any age. In addition, we found that there was no increase of organ weight with ageing in WT and Nox2KO mice. This led to us to investigate the activity of the mice with ageing. The rhythm of the mice was found to be similar in both WT and Nox2KO at young age and followed the rhythm reported in the literature (Kopp, 2001, Nishi et al., 2010). The total activity in WT ageing mice was seen to be decreased compared with young mice, which is supported by the literature showing a decrease in activity between young and ageing mice (Jeon et al., 2006). ROS-induced oxidative stress has been reported in the literature to be associated with decreased activity in rats and humans (Flora et al., 2007, Powers and Jackson, 2008). Nox2 was also indicated to be associated with behavioral dysfunction in ageing mice (Park et al., 2008). In our study, a decline in total activity with ageing in WT mice ageing was accompanied by an increase in superoxide production in the brain. Ageing Nox2KO mice displayed preserved total activity accompanied by a significant decrease in superoxide production in ageing brain. These findings strongly suggest a role of Nox2-derived oxidative stress in the ageing-related decline of activity.

The catalytic subunit of NADPH oxidase has 7 isoforms including Nox1-5 and Duox1-2 (Bengtsson et al., 2003). Nox2 has been found to be involved in vascular inflammation and atherosclerotic lesion formation (Konior et al., 2014). It was reported in the literature that Nox2 activation occurs during ageing in both mice and rats (Kelly et al., 2009, Park et al., 2008). Our study extended our understanding of NADPH oxidase by showing an ageing-associated increase in Nox2 expression in WT ageing brains, together with increasing levels of expression of p22<sup>phox</sup>, p40<sup>phox</sup>, p47<sup>phox</sup>, p67<sup>phox</sup> and Rac. This was accompanied by ageing-related cerebral vascular damage, a significant increase in ERK1/2 activation and reduction in p38MAPK activation. However, the deletion of Nox2 remains the levels of expression of p22<sup>phox</sup>, p40<sup>phox</sup>, p47<sup>phox</sup>, p67<sup>phox</sup> and Rac and preserves the levels of expression of ERK1/2 and p38MAPK. In addition, knockout of Nox2 also protects against ageing-induced vascular damage in the brain. Although the redox-signaling pathways underlying cerebral vascular ageing remain unclear, it is possible that Nox2 signaling through ERK1/2 is involved in ageing-associated deterioration of brain function.

Microglial cells act as the immune cells in the central nervous system which have long been a subject of investigation in the ageing-related neurodegenerative diseases (Mosher and Wyss-Coray, 2014). Microglia usually have their dramatic responses to the pathophysiology of the disease. In the early stage of Alzheimer's diseases, oxidative stress caused by ROS in microglia is well recognized as a contributor to neuronal loss (Wilkinson and Landreth, 2006). Activation of microglial NADPH oxidase is believed to be the primary source of ROS (Mosher and Wyss-Coray, 2014). Our study has demonstrated the microglia activation and proliferation in the ageing brain in both mice and humans, which was accompanied with significantly increased Nox2 expression. Furthermore, the ageing-related neuronal loss in the brains was shown in mice and our

study confirms the link between Nox2 activation and oxidative stress leading to neuron death. However, these pathological changes were not found in the Nox2KO ageing brain. These findings in my PhD research have therefore provided strong evidence that Nox2 activation plays an important role in the cerebral endothelial damage, microglial dysfunction and neuron death in ageing-related locomotor dysfunction and neurodegenerative diseases.

## 6.2 Future work

This research provides investigations into the role of Nox2-driven oxidative stress in the vascular system in the ageing brain however there are still further investigations that needed to be carried out:

1. Assessing the locomotor function using young and ageing Nox2Tg mice in comparisons to age-match WT and Nox2KO mice. This can further prove that Nox2 may have a critical role in the development of ageing. Knocking out Nox2 may potentially delay the ageing process while overexpressing Nox2 may accelerate ageing.
2. To look at the endothelial, microglial and neuronal cells by immunofluorescence in the human brain sections to confirm the data from mice.
3. Isolating cerebral endothelial cells from WT and Nox2KO young and ageing mice and stimulating them with high glucose plus insulin to confirm the data from CMECs
4. Performing in vitro gene expression with siRNA transfection of endothelial cells to discover the potential key signaling molecules. It would be interesting to see whether knocking out Nox2 from endothelial cells can have a potential role of regulating the expression of signaling pathways proteins (e.g. MAPK proteins) or other potential signaling molecules. It would be also important to compare the role of Nox1, Nox2, Nox4, p47, p22 or other genes regarding regulation of different signaling pathways.

## References

- Akiyama, H., Arai, T., Kondo, H., Tanno, E., Haga, C. and Ikeda, K. (2000) 'Cell mediators of inflammation in the Alzheimer disease brain', *Alzheimer Dis Assoc Disord*, 14 Suppl 1, pp. S47-53.
- Ambasta, R. K., Kumar, P., Griendling, K. K., Schmidt, H. H., Busse, R. and Brandes, R. P. (2004) 'Direct interaction of the novel Nox proteins with p22phox is required for the formation of a functionally active NADPH oxidase', *J Biol Chem*, 279(44), pp. 45935-41.
- Azevedo, F. A., Carvalho, L. R., Grinberg, L. T., Farfel, J. M., Ferretti, R. E., Leite, R. E., Jacob Filho, W., Lent, R. and Herculano-Houzel, S. (2009) 'Equal numbers of neuronal and nonneuronal cells make the human brain an isometrically scaled-up primate brain', *J Comp Neurol*, 513(5), pp. 532-41.
- Balaban, R. S., Nemoto, S. and Finkel, T. (2005) 'Mitochondria, oxidants, and aging', *Cell*, 120(4), pp. 483-95.
- Banfi, B., Malgrange, B., Knisz, J., Steger, K., Dubois-Dauphin, M. and Krause, K. H. (2004) 'NOX3, a superoxide-generating NADPH oxidase of the inner ear', *J Biol Chem*, 279(44), pp. 46065-72.
- Banfi, B., Maturana, A., Jaconi, S., Arnaudeau, S., Laforge, T., Sinha, B., Ligeti, E., Demaurex, N. and Krause, K. H. (2000) 'A mammalian H<sup>+</sup> channel generated through alternative splicing of the NADPH oxidase homolog NOH-1', *Science*, 287(5450), pp. 138-42.
- Barger, S. W., Goodwin, M. E., Porter, M. M. and Beggs, M. L. (2007) 'Glutamate release from activated microglia requires the oxidative burst and lipid peroxidation', *J Neurochem*, 101(5), pp. 1205-13.

- Bauersachs, J. and Schafer, A. (2004) 'Endothelial dysfunction in heart failure: mechanisms and therapeutic approaches', *Curr Vasc Pharmacol*, 2(2), pp. 115-24.
- Becker, B. F. (1993) 'Towards the physiological function of uric acid', *Free Radic Biol Med*, 14(6), pp. 615-31.
- Bedard, K. and Krause, K. H. (2007) 'The NOX family of ROS-generating NADPH oxidases: physiology and pathophysiology', *Physiol Rev*, 87(1), pp. 245-313.
- Bell, K. F. and Claudio Cuello, A. (2006) 'Altered synaptic function in Alzheimer's disease', *Eur J Pharmacol*, 545(1), pp. 11-21.
- Bendall, J. K., Rinze, R., Adlam, D., Tatham, A. L., de Bono, J., Wilson, N., Volpi, E. and Channon, K. M. (2007) 'Endothelial Nox2 overexpression potentiates vascular oxidative stress and hemodynamic response to angiotensin II: studies in endothelial-targeted Nox2 transgenic mice', *Circ Res*, 100(7), pp. 1016-25.
- Bengtsson, S. H., Gulluyan, L. M., Dusting, G. J. and Drummond, G. R. (2003) 'Novel isoforms of NADPH oxidase in vascular physiology and pathophysiology', *Clin Exp Pharmacol Physiol*, 30(11), pp. 849-54.
- Bennett, M. R. (2001) 'Reactive oxygen species and death: oxidative DNA damage in atherosclerosis', *Circ Res*, 88(7), pp. 648-50.
- Bevers, L. M., Braam, B., Post, J. A., van Zonneveld, A. J., Rabelink, T. J., Koomans, H. A., Verhaar, M. C. and Joles, J. A. (2006) 'Tetrahydrobiopterin, but not L-arginine, decreases NO synthase uncoupling in cells expressing high levels of endothelial NO synthase', *Hypertension*, 47(1), pp. 87-94.
- Block, M. L. (2008) 'NADPH oxidase as a therapeutic target in Alzheimer's disease', *BMC Neurosci*, 9 Suppl 2, pp. S8.

- Block, M. L. and Hong, J. S. (2007) 'Chronic microglial activation and progressive dopaminergic neurotoxicity', *Biochem Soc Trans*, 35(Pt 5), pp. 1127-32.
- Boche, D., Cunningham, C., Docagne, F., Scott, H. and Perry, V. H. (2006) 'TGFbeta1 regulates the inflammatory response during chronic neurodegeneration', *Neurobiol Dis*, 22(3), pp. 638-50.
- Booth, P. L. and Thomas, W. E. (1991) 'Evidence for motility and pinocytosis in ramified microglia in tissue culture', *Brain Res*, 548(1-2), pp. 163-71.
- Brandes, R. P. and Kreuzer, J. (2005) 'Vascular NADPH oxidases: molecular mechanisms of activation', *Cardiovasc Res*, 65(1), pp. 16-27.
- Brown, G. C. (2007) 'Mechanisms of inflammatory neurodegeneration: iNOS and NADPH oxidase', *Biochem Soc Trans*, 35(Pt 5), pp. 1119-21.
- Brown, G. C. and Bal-Price, A. (2003) 'Inflammatory neurodegeneration mediated by nitric oxide, glutamate, and mitochondria', *Mol Neurobiol*, 27(3), pp. 325-55.
- Brown, G. C. and Neher, J. J. (2010) 'Inflammatory neurodegeneration and mechanisms of microglial killing of neurons', *Mol Neurobiol*, 41(2-3), pp. 242-7.
- Bruce-Keller, A. J., White, C.L., Gupta, S., Knight, A.G., Pistell, P.J., Ingram, D.K., Morrison, C.D. and Keller, J.N. (2010) 'NOX activity in brain aging: exacerbation by high fat diet', *Free Radic Biol Med*, 49(1), pp. 22-30.
- Bruce, A. J., Boling, W., Kindy, M. S., Peschon, J., Kraemer, P. J., Carpenter, M. K., Holtsberg, F. W. and Mattson, M. P. (1996) 'Altered neuronal and microglial responses to excitotoxic and ischemic brain injury in mice lacking TNF receptors', *Nat Med*, 2(7), pp. 788-94.
- Buettner, G. R. and Jurkiewicz, B. A. (1996) 'Catalytic metals, ascorbate and free radicals: combinations to avoid', *Radiat Res*, 145(5), pp. 532-41.

- Cahill-Smith, S. and Li, J. M. (2014) 'Oxidative stress, redox signalling and endothelial dysfunction in ageing-related neurodegenerative diseases: a role of NADPH oxidase 2', *Br J Clin Pharmacol*, 78(3), pp. 441-53.
- Cai, H. and Harrison, D. G. (2000) 'Endothelial dysfunction in cardiovascular diseases: the role of oxidant stress', *Circ Res*, 87(10), pp. 840-4.
- Carrano, A., Hoozemans, J. J., van der Vies, S. M., Rozemuller, A. J., van Horssen, J. and de Vries, H. E. (2011) 'Amyloid Beta induces oxidative stress-mediated blood-brain barrier changes in capillary amyloid angiopathy', *Antioxid Redox Signal*, 15(5), pp. 1167-78.
- Carrano, A., Hoozemans, J. J., van der Vies, S. M., van Horssen, J., de Vries, H. E. and Rozemuller, A. J. (2012) 'Neuroinflammation and blood-brain barrier changes in capillary amyloid angiopathy', *Neurodegener Dis*, 10(1-4), pp. 329-31.
- Cheret, C., Gervais, A., Lelli, A., Colin, C., Amar, L., Ravassard, P., Mallet, J., Cumano, A., Krause, K. H. and Mallat, M. (2008) 'Neurotoxic activation of microglia is promoted by a nox1-dependent NADPH oxidase', *J Neurosci*, 28(46), pp. 12039-51.
- Chrissobolis, S. and Faraci, F. M. (2008) 'The role of oxidative stress and NADPH oxidase in cerebrovascular disease', *Trends Mol Med*, 14(11), pp. 495-502.
- Clement, H. W., Vazquez, J. F., Sommer, O., Heiser, P., Morawietz, H., Hopt, U., Schulz, E. and von Dobschutz, E. (2010) 'Lipopolysaccharide-induced radical formation in the striatum is abolished in Nox2 gp91phox-deficient mice', *J Neural Transm (Vienna)*, 117(1), pp. 13-22.
- Colton, C. A. and Gilbert, D. L. (1987) 'Production of superoxide anions by a CNS macrophage, the microglia', *FEBS Lett*, 223(2), pp. 284-8.

- Combs, C. K., Karlo, J. C., Kao, S. C. and Landreth, G. E. (2001) 'beta-Amyloid stimulation of microglia and monocytes results in TNFalpha-dependent expression of inducible nitric oxide synthase and neuronal apoptosis', *J Neurosci*, 21(4), pp. 1179-88.
- Cribb, A. E., Peyrou, M., Muruganandan, S. and Schneider, L. (2005) 'The endoplasmic reticulum in xenobiotic toxicity', *J Drug Metab Rev*, 37(3), pp. 405-42.
- Davalos, D., Grutzendler, J., Yang, G., Kim, J. V., Zuo, Y., Jung, S., Littman, D. R., Dustin, M. L. and Gan, W. B. (2005) 'ATP mediates rapid microglial response to local brain injury in vivo', *Nat Neurosci*, 8(6), pp. 752-8.
- De Deken, X., Wang, D., Many, M. C., Costagliola, S., Libert, F., Vassart, G., Dumont, J. E. and Miot, F. (2000) 'Cloning of two human thyroid cDNAs encoding new members of the NADPH oxidase family', *J Biol Chem*, 275(30), pp. 23227-33.
- Desai, N., Sabanegh, E., Jr., Kim, T. and Agarwal, A. (2010) 'Free radical theory of aging: implications in male infertility', *Urology*, 75(1), pp. 14-9.
- Didion, S. P. and Faraci, F. M. (2002) 'Effects of NADH and NADPH on superoxide levels and cerebral vascular tone', *Am J Physiol Heart Circ Physiol*, 282(2), pp. H688-95.
- Di Meo, S., Reed, T. T., Venditti, P. and Victor, V. M. (2016) 'Role of ROS and RNS sources in physiological and pathological conditions', *Oxid Med Cell Longev*.
- Dohi, K., Ohtaki, H., Nakamachi, T., Yofu, S., Satoh, K., Miyamoto, K., Song, D., Tsunawaki, S., Shioda, S. and Aruga, T. (2010) 'Gp91phox (NOX2) in classically activated microglia exacerbates traumatic brain injury', *J Neuroinflammation*, 7, pp. 41.

- Donato, A. J., Eskurza, I., Silver, A. E., Levy, A. S., Pierce, G. L., Gates, P. E. and Seals, D. R. (2007) 'Direct evidence of endothelial oxidative stress with aging in humans: relation to impaired endothelium-dependent dilation and upregulation of nuclear factor-kappaB', *Circ Res*, 100(11), pp. 1659-66.
- Droge, W. (2002) 'Free radicals in the physiological control of cell function', *Physiol Rev*, 82(1), pp. 47-95.
- Drummond, G. R., Cai, H., Davis, M. E., Ramasamy, S. and Harrison, D. G. (2000) 'Transcriptional and posttranscriptional regulation of endothelial nitric oxide synthase expression by hydrogen peroxide', *Circ Res*, 86(3), pp. 347-54.
- Drummond, G. R., Selemidis, S., Griendling, K. K. and Sobey, C. G. (2011) 'Combating oxidative stress in vascular disease: NADPH oxidases as therapeutic targets', *Nat Rev Drug Discov*, 10(6), pp. 453-71.
- Du, J., Fan, L. M., Mai, A. and Li, J. M. (2013) 'Crucial roles of Nox2-derived oxidative stress in deteriorating the function of insulin receptors and endothelium in dietary obesity of middle-aged mice', *Br J Pharmacol*, 170(5), pp. 1064-77.
- Dugan, L. L., Ali, S. S., Shekhtman, G., Roberts, A. J., Lucero, J., Quick, K. L. and Behrens, M. M. (2009) 'IL-6 mediated degeneration of forebrain GABAergic interneurons and cognitive impairment in aged mice through activation of neuronal NADPH oxidase', *PLoS One*, 4(5), pp. e5518.
- Enroth, C., Eger, B. T., Okamoto, K., Nishino, T., Nishino, T. and Pai, E. F. (2000) 'Crystal structures of bovine milk xanthine dehydrogenase and xanthine oxidase: structure-based mechanism of conversion', *Proc Natl Acad Sci U S A*, 97(20), pp. 10723-8.

- ErDOS, B., Kirichenko, N., Whidden, M., Basgut, B., Woods, M., Cudykier, I., Tawil, R., Scarpace, P. J. and Tumer, N. (2011) 'Effect of age on high-fat diet-induced hypertension', *Am J Physiol Heart Circ Physiol*, 301(1), pp. H164-72.
- Fan, L. M., Cahill-Smith, S., Geng, L., Du, J., Brooks, G. and Li, J. M. (2017) 'Aging-associated metabolic disorder induces Nox2 activation and oxidative damage of endothelial function', *Free Radic Biol Med*, 108, pp. 940-951.
- Fan, L. M., Douglas, G., Bendall, J. K., McNeill, E., Crabtree, M. J., Hale, A. B., Mai, A., Li, J. M., McAteer, M. A., Schneider, J. E., Choudhury, R. P. and Channon, K. M. (2014) 'Endothelial cell-specific reactive oxygen species production increases susceptibility to aortic dissection', *Circulation*, 129(25), pp. 2661-72.
- Fan, L. M. and Li, J. M. (2014) 'Evaluation of methods of detecting cell reactive oxygen species production for drug screening and cell cycle studies', *J Pharmacol Toxicol Methods*, 70(1), pp. 40-7.
- Farber, K. and Kettenmann, H. (2005) 'Physiology of microglial cells', *Brain Res Brain Res Rev*, 48(2), pp. 133-43.
- Fetler, L. and Amigorena, S. (2005) 'Neuroscience. Brain under surveillance: the microglia patrol', *Science*, 309(5733), pp. 392-3.
- Finkel, T. and Holbrook, N. J. (2000) 'Oxidants, oxidative stress and the biology of ageing', *Nature*, 408(6809), pp. 239-47.
- Flora, S. J., Saxena, G. and Mehta, A. (2007) 'Reversal of lead-induced neuronal apoptosis by chelation treatment in rats: role of reactive oxygen species and intracellular Ca(2+)', *J Pharmacol Exp Ther*, 322(1), pp. 108-16.
- Floyd, R. A. and Hensley, K. (2002) 'Oxidative stress in brain aging. Implications for therapeutics of neurodegenerative diseases', *Neurobiol Aging*, 23(5), pp. 795-807.

- Forman, H. J. and Torres, M. (2002) 'Reactive oxygen species and cell signaling: respiratory burst in macrophage signaling', *Am J Respir Crit Care Med*, 166(12 Pt 2), pp. S4-8.
- Francia, P., delli Gatti, C., Bachschmid, M., Martin-Padura, I., Savoia, C., Migliaccio, E., Pelicci, P. G., Schiavoni, M., Luscher, T. F., Volpe, M. and Cosentino, F. (2004) 'Deletion of p66shc gene protects against age-related endothelial dysfunction', *Circulation*, 110(18), pp. 2889-95.
- Freeman, B. A. and Crapo, J. D. (1982) 'Biology of disease: free radicals and tissue injury', *Lab Invest*, 47(5), pp. 412-26.
- Fukai, T. (2007) 'Endothelial GTPCH in eNOS uncoupling and atherosclerosis', *Arterioscler Thromb Vasc Biol*, 27(7), pp. 1493-5.
- Fulton, D. J. (2009) 'Nox5 and the regulation of cellular function', *Antioxid Redox Signal*, 11(10), pp. 2443-52.
- Flurkey, K., Curren, J. M. and Harrison, D. E. (2007) 'The mouse in ageing research. In *The Mouse in Biomedical Research* (ed. J. G. Fox), pp. 637-672.
- Galbusera, C., Orth, P., Fedida, D. and Spector, T. (2006) 'Superoxide radical production by allopurinol and xanthine oxidase', *Biochem Pharmacol*, 71(12), pp. 1747-52.
- Galimov, E. R. (2010) 'The role of p66shc in oxidative stress and apoptosis'. *Acta Nat*, 2(4), pp. 44-51.
- Gao, H. M., Hong, J. S., Zhang, W. and Liu, B. (2002) 'Distinct role for microglia in rotenone-induced degeneration of dopaminergic neurons', *J Neurosci*, 22(3), pp. 782-90.

- Gao, H. M., Liu, B., Zhang, W. and Hong, J. S. (2003) 'Critical role of microglial NADPH oxidase-derived free radicals in the in vitro MPTP model of Parkinson's disease', *FASEB J*, 17(13), pp. 1954-6.
- Garden, G. A. and Moller, T. (2006) 'Microglia biology in health and disease', *J Neuroimmune Pharmacol*, 1(2), pp. 127-37.
- Glabe, C. (2001) 'Intracellular mechanisms of amyloid accumulation and pathogenesis in Alzheimer's disease', *J Mol Neurosci*, 17(2), pp. 137-45.
- Gorelick, P. B., Scuteri, A., Black, S. E., Decarli, C., Greenberg, S. M., Iadecola, C., Launer, L. J., Laurent, S., Lopez, O. L., Nyenhuis, D., Petersen, R. C., Schneider, J. A., Tzourio, C., Arnett, D. K., Bennett, D. A., Chui, H. C., Higashida, R. T., Lindquist, R., Nilsson, P. M., Roman, G. C., Sellke, F. W., Seshadri, S., American Heart Association Stroke Council, C. o. E., Prevention, C. o. C. N. C. o. C. R., Intervention, Council on Cardiovascular, S. and Anesthesia (2011) 'Vascular contributions to cognitive impairment and dementia: a statement for healthcare professionals from the american heart association/american stroke association', *Stroke*, 42(9), pp. 2672-713.
- Groenendyk, J. and Michalak, M. (2005) 'Endoplasmic reticulum quality control and apoptosis', *Acta Biochim Pol*, 52(2), pp. 381-95.
- Guilarte, T. R., Loth, M. K. and Guariglia, S. R. (2016) 'TSPO Finds NOX2 in Microglia for Redox Homeostasis', *Trends Pharmacol Sci*.
- Guyton, K. Z., Gorospe, M., Kensler, T. W. and Holbrook, N. J. (1996) 'Mitogen-activated protein kinase (MAPK) activation by butylated hydroxytoluene hydroperoxide: implications for cellular survival and tumor promotion', *Cancer Res*, 56(15), pp. 3480-5.

- Guzik, T. J. and Channon, K. M. (2005) 'Measurement of vascular reactive oxygen species production by chemiluminescence', *Methods Mol Med*, 108, pp. 73-89.
- Guzik, T. J., West, N. E., Pillai, R., Taggart, D. P. and Channon, K. M. (2002) 'Nitric oxide modulates superoxide release and peroxynitrite formation in human blood vessels', *Hypertension*, 39(6), pp. 1088-94.
- Haass, C. and Selkoe, D. J. (2007) 'Soluble protein oligomers in neurodegeneration: lessons from the Alzheimer's amyloid beta-peptide', *Nat Rev Mol Cell Biol*, 8(2), pp. 101-12.
- Halliwell, B. (2006) 'Oxidative stress and neurodegeneration: where are we now?', *J Neurochem*, 97(6), pp. 1634-58.
- Harman, D. (1956) 'Aging: a theory based on free radical and radiation chemistry', *J Gerontol*, 11(3), pp. 298-300.
- Harrigan, T. J., Abdullaev, I. F., Jourdeuil, D. and Mongin, A. A. (2008) 'Activation of microglia with zymosan promotes excitatory amino acid release via volume-regulated anion channels: the role of NADPH oxidases', *J Neurochem*, 106(6), pp. 2449-62.
- Harrison, D., Griendling, K. K., Landmesser, U., Hornig, B. and Drexler, H. (2003) 'Role of oxidative stress in atherosclerosis', *Am J Cardiol*, 91(3A), pp. 7A-11A.
- Hartley, S.L., Handen, B.L., Devenny, D., Mihaila, L., Hardison, R., Lao, P.J., Klunk, W.E., Bulova, P., Johnson, S.C. and Christian, B.T. (2017) 'Cognitive decline and brain amyloid- $\beta$  accumulation across 3 years in adults with Down syndrome', *Neurobiology of aging*, 58, pp. 68-76.
- Hensley, K., Floyd, R. A., Zheng, N. Y., Nael, R., Robinson, K. A., Nguyen, X., Pye, Q. N., Stewart, C. A., Geddes, J., Markesbery, W. R., Patel, E., Johnson, G. V.

- and Bing, G. (1999) 'p38 kinase is activated in the Alzheimer's disease brain', *J Neurochem*, 72(5), pp. 2053-8.
- Hernandes, M. S. and Britto, L. R. (2012) 'NADPH oxidase and neurodegeneration', *Curr Neuropharmacol*, 10(4), pp. 321-7.
- Herrera, A. P., Snipes, S. A., King, D. W., Torres-Vigil, I., Goldberg, D. S. and Weinberg, A. D. (2010) 'Disparate inclusion of older adults in clinical trials: priorities and opportunities for policy and practice change', *Am J Public Health*, 100 Suppl 1, pp. S105-12.
- Heyworth, P. G., Cross, A. R. and Curnutte, J. T. (2003) 'Chronic granulomatous disease', *Curr Opin Immunol*, 15(5), pp. 578-84.
- Hoek, R. M., Ruuls, S. R., Murphy, C. A., Wright, G. J., Goddard, R., Zurawski, S. M., Blom, B., Homola, M. E., Streit, W. J., Brown, M. H., Barclay, A. N. and Sedgwick, J. D. (2000) 'Down-regulation of the macrophage lineage through interaction with OX2 (CD200)', *Science*, 290(5497), pp. 1768-71.
- Houston, D. K., Nicklas, B. J. and Zizza, C. A. (2009) 'Weighty concerns: the growing prevalence of obesity among older adults', *J Am Diet Assoc*, 109(11), pp. 1886-95.
- Hur, J., Lee, P., Kim, M. J., Kim, Y. and Cho, Y. W. (2010) 'Ischemia-activated microglia induces neuronal injury via activation of gp91phox NADPH oxidase', *Biochem Biophys Res Commun*, 391(3), pp. 1526-30.
- Iadecola, C. (2013) 'The pathobiology of vascular dementia', *Neuron*, 80(4), pp. 844-66.
- Infanger, D. W., Sharma, R. V. and Davisson, R. L. (2006) 'NADPH oxidases of the brain: distribution, regulation, and function', *Antioxid Redox Signal*, 8(9-10), pp. 1583-96.

- Jackson, S. H., Gallin, J. I. and Holland, S. M. (1995) 'The p47phox mouse knock-out model of chronic granulomatous disease'. *J Exp Med*, 182(3), pp. 751-8.
- Jekabsone, A., Mander, P. K., Tickler, A., Sharpe, M. and Brown, G. C. (2006) 'Fibrillar beta-amyloid peptide Abeta1-40 activates microglial proliferation via stimulating TNF-alpha release and H2O2 derived from NADPH oxidase: a cell culture study', *J Neuroinflammation*, 3, pp. 24.
- Jeon, J. Y., Bradley, R. L., Kokkotou, E. G., Marino, F. E., Wang, X., Pissios, P. and Maratos-Flier, E. (2006) 'MCH<sup>-/-</sup> mice are resistant to aging-associated increases in body weight and insulin resistance', *Diabetes*, 55(2), pp. 428-34.
- Jin, W. (2010) 'Age-related increase of beta1-adrenergic receptor gene expression in rat liver: a potential mechanism contributing to increased beta-adrenergic receptor density and responsiveness during aging', *J Recept Signal Transduct Res*, 30(1), pp. 24-30.
- Jin, W., Bu X., Liu Y., Shen, L., Zhuang, Z., Jiao, S., Zhu, C., Wang, Q., Zhou, H., Zhang, T. and Wang, Y. (2017) 'Plasma amyloid-beta levels in patients with different types of cancer', *Neurotox Res*, 31, pp. 283-8.
- Johnson, S. C., Rabinovitch, P. S. and Kaeberlein, M. (2013) 'mTOR is a key modulator of ageing and age-related disease', *Nature*, 493(7432), pp. 338-45.
- Kawahara, T., Quinn, M. T. and Lambeth, J. D. (2007) 'Molecular evolution of the reactive oxygen-generating NADPH oxidase (Nox/Duox) family of enzymes', *BMC Evol Biol*, 7, pp. 109.
- Kelly, K. A., Li, X., Tan, Z., VanGilder, R. L., Rosen, C. L. and Huber, J. D. (2009) 'NOX2 inhibition with apocynin worsens stroke outcome in aged rats', *Brain Res*, 1292, pp. 165-72.

- Koch, G. L. (1990) 'The endoplasmic reticulum and calcium storage', *Bioessays*, 12 (11), pp. 527-31.
- Konior, A., Schramm, A., Czesnikiewicz-Guzik, M. and Guzik, T. J. (2014) 'NADPH oxidases in vascular pathology', *Antioxid Redox Signal*, 20(17), pp. 2794-814.
- Konishi, H., Tanaka, M., Takemura, Y., Matsuzaki, H., Ono, Y., Kikkawa, U. and Nishizuka, Y. (1997) 'Activation of protein kinase C by tyrosine phosphorylation in response to H<sub>2</sub>O<sub>2</sub>', *Proc Natl Acad Sci U S A*, 94(21), pp. 11233-7.
- Kopp, C. (2001) 'Locomotor activity rhythm in inbred strains of mice: implications for behavioural studies', *Behav Brain Res*, 125(1-2), pp. 93-6.
- Koppenol, W. H. (1993) 'The centennial of the Fenton reaction', *Free Radic Biol Med*, 15(6), pp. 645-51.
- Krause, M. P., Hallage, T., Gama, M. P., Goss, F. L., Robertson, R. and da Silva, S. G. (2007) 'Association of adiposity, cardiorespiratory fitness and exercise practice with the prevalence of type 2 diabetes in Brazilian elderly women', *Int J Med Sci*, 4(5), pp. 288-92.
- Kuhns, D. B., Alvord, W. G., Heller, T., Feld, J. J., Pike, K. M., Marciano, B. E., Uzel, G., DeRavin, S. S., Priel, D. A., Soule, B. P., Zarembek, K. A., Malech, H. L., Holland, S. M. and Gallin, J. I. (2010) 'Residual NADPH oxidase and survival in chronic granulomatous disease', *N Engl J Med*, 363(27), pp. 2600-10.
- Lamb, B. T., Sisodia, S. S., Lawler, A. M., Slunt, H. H., Kitt, C. A., Kearns, W. G., Pearson, P. L., Price, D. L. and Gearhart, J. D. (1993) 'Introduction and expression of the 400 kilobase amyloid precursor protein gene in transgenic mice', *Nat Genet*, 5(1), pp. 22-30.

- Lamb, B. T., Bardel, K. A., Kulnane, L. S., Anderson, J. J., Holtz, G., Wagner, S. L., Sisodia, S. S. and Hoeger, E. J. (1999) 'Amyloid production and deposition in mutant amyloid precursor protein and presenilin-1 yeast artificial chromosome transgenic mice', *Nat Neurosci*, 2(8), pp. 695-7.
- Lambeth, J. D. (2004) 'NOX enzymes and the biology of reactive oxygen', *Nat Rev Immunol*, 4(3), pp. 181-9.
- Landmesser, U., Dikalov, S., Price, S. R., McCann, L., Fukai, T., Holland, S. M., Mitch, W. E. and Harrison, D. G. (2003) 'Oxidation of tetrahydrobiopterin leads to uncoupling of endothelial cell nitric oxide synthase in hypertension', *J Clin Invest*, 111(8), pp. 1201-9.
- Lassegue, B. and Griendling, K. K. (2010) 'NADPH oxidases: functions and pathologies in the vasculature', *Arterioscler Thromb Vasc Biol*, 30(4), pp. 653-61.
- Lee, H. B., Yu, M. R., Yang, Y., Jiang, Z. and Ha, H. (2003) 'Reactive oxygen species-regulated signaling pathways in diabetic nephropathy', *J Am Soc Nephrol*, 14(8 Suppl 3), pp. S241-5.
- Li, J. M., Fan, L. M., Christie, M. R. and Shah, A. M. (2005) 'Acute tumor necrosis factor alpha signaling via NADPH oxidase in microvascular endothelial cells: role of p47phox phosphorylation and binding to TRAF4', *Mol Cell Biol*, 25(6), pp. 2320-30.
- Li, J. M., Fan, L. M., George, V. T. and Brooks, G. (2007) 'Nox2 regulates endothelial cell cycle arrest and apoptosis via p21cip1 and p53', *Free Radic Biol Med*, 43(6), pp. 976-86.

- Li, J. M., Mullen, A. M. and Shah, A. M. (2001) 'Phenotypic properties and characteristics of superoxide production by mouse coronary microvascular endothelial cells', *J Mol Cell Cardiol*, 33(6), pp. 1119-31.
- Li, J. M. and Shah, A. M. (2003) 'ROS generation by nonphagocytic NADPH oxidase: potential relevance in diabetic nephropathy', *J Am Soc Nephrol*, 14(8 Suppl 3), pp. S221-6.
- Li, J. M. and Shah, A. M. (2004) 'Endothelial cell superoxide generation: regulation and relevance for cardiovascular pathophysiology', *Am J Physiol Regul Integr Comp Physiol*, 287(5), pp. R1014-30.
- Li, X. Y., Luo, B. L. and Chen, H. M. (2009) '[The function of nuclear factor-erythroid 2-related factor 2 and its association with I-kappa B kinases alpha/beta in a rat model of chronic obstructive pulmonary disease.]', *Zhonghua Jie He He Hu Xi Za Zhi*, 32(12), pp. 935-9.
- Li, Y., Zhu, H., Kuppusamy, P., Roubaud, V., Zweier, J. L. and Trush, M. A. (1998) 'Validation of lucigenin (bis-N-methylacridinium) as a chemilumigenic probe for detecting superoxide anion radical production by enzymatic and cellular systems', *J Biol Chem*, 273(4), pp. 2015-23.
- Liochev, S. I. (2013) 'Reactive oxygen species and the free radical theory of aging', *Free Radic Biol Med*, 60, pp. 1-4.
- Liochev, S. I. (2014) 'Free radicals: how do we stand them? Anaerobic and aerobic free radical (chain) reactions involved in the use of fluorogenic probes and in biological systems', *Med Princ Pract*, 23(3), pp. 195-203.
- Liu, H., Wang, J., Wang, J., Wang, P. and Xue, Y. (2015) 'Paeoniflorin attenuates A $\beta$ <sub>1-42</sub>-induced inflammation and chemotaxis of microglia in vitro and inhibits NF- $\kappa$ B- and VEGF/Flt-1 signaling pathways', *Brain Research*, 1618, pp. 149-58.

- Liu, Y., Qin, L., Wilson, B. C., An, L., Hong, J. S. and Liu, B. (2002) 'Inhibition by naloxone stereoisomers of beta-amyloid peptide (1-42)-induced superoxide production in microglia and degeneration of cortical and mesencephalic neurons', *J Pharmacol Exp Ther*, 302(3), pp. 1212-9.
- Loumaye, E., Ferrer-Sueta, G., Alvarez, B., Rees, J. F., Clippe, A., Knoop, B., Radi, R. and Trujillo, M. (2011) 'Kinetic studies of peroxiredoxin 6 from *Arenicola marina*: rapid oxidation by hydrogen peroxide and peroxynitrite but lack of reduction by hydrogen sulfide', *Arch Biochem Biophys*, 514(1-2), pp. 1-7.
- Lovell, M. A., Xie, C. and Markesbery, W. R. (2001) 'Acrolein is increased in Alzheimer's disease brain and is toxic to primary hippocampal cultures', *Neurobiol Aging*, 22(2), pp. 187-94.
- MacCarthy, P. A., Grieve, D. J., Li, J. M., Dunster, C., Kelly, F. J. and Shah, A. M. (2001) 'Impaired endothelial regulation of ventricular relaxation in cardiac hypertrophy: role of reactive oxygen species and NADPH oxidase', *Circulation*, 104(24), pp. 2967-74.
- Madamanchi, N. R., Vendrov, A. and Runge, M. S. (2005) 'Oxidative stress and vascular disease', *Arterioscler Thromb Vasc Biol*, 25(1), pp. 29-38.
- Mander, P. and Brown, G. C. (2005) 'Activation of microglial NADPH oxidase is synergistic with glial iNOS expression in inducing neuronal death: a dual-key mechanism of inflammatory neurodegeneration', *J Neuroinflammation*, 2, pp. 20.
- Mander, P. K., Jekabsone, A. and Brown, G. C. (2006) 'Microglia proliferation is regulated by hydrogen peroxide from NADPH oxidase', *J Immunol*, 176(2), pp. 1046-52.

- Mangoni, A. A. and Jackson, S. H. (2004) 'Age-related changes in pharmacokinetics and pharmacodynamics: basic principles and practical applications', *Br J Clin Pharmacol*, 57(1), pp. 6-14.
- Mariani, E., Polidori, M. C., Cherubini, A. and Mecocci, P. (2005) 'Oxidative stress in brain aging, neurodegenerative and vascular diseases: an overview', *J Chromatogr B Analyt Technol Biomed Life Sci*, 827(1), pp. 65-75.
- Marin, J. and Rodriguez-Martinez, M. A. (1999) 'Age-related changes in vascular responses', *Exp Gerontol*, 34(4), pp. 503-12.
- Markesbery, W. R. (1997) 'Oxidative stress hypothesis in Alzheimer's disease', *Free Radic Biol Med*, 23(1), pp. 134-47.
- Marnett, L. J. (1999) 'Lipid peroxidation-DNA damage by malondialdehyde', *Mutat Res*, 424(1-2), pp. 83-95.
- Martin, G. M. (2011) 'The biology of aging: 1985-2010 and beyond', *FASEB J*, 25(11), pp. 3756-62.
- Mattson, M. P., Duan, W., Chan, S. L., Cheng, A., Haughey, N., Gary, D. S., Guo, Z., Lee, J. and Furukawa, K. (2002) 'Neuroprotective and neurorestorative signal transduction mechanisms in brain aging: modification by genes, diet and behavior', *Neurobiol Aging*, 23(5), pp. 695-705.
- McCord, J. M. and Fridovich, I. (1969) 'The utility of superoxide dismutase in studying free radical reactions. I. Radicals generated by the interaction of sulfite, dimethyl sulfoxide, and oxygen', *J Biol Chem*, 244(22), pp. 6056-63.
- McGeer, P. L., Schulzer, M. and McGeer, E. G. (1996) 'Arthritis and anti-inflammatory agents as possible protective factors for Alzheimer's disease: a review of 17 epidemiologic studies', *Neurology*, 47(2), pp. 425-32.

- Meda, L., Cassatella, M. A., Szendrei, G. I., Otvos, L., Jr., Baron, P., Villalba, M., Ferrari, D. and Rossi, F. (1995) 'Activation of microglial cells by beta-amyloid protein and interferon-gamma', *Nature*, 374(6523), pp. 647-50.
- Meischl, C. and Roos, D. (1998) 'The molecular basis of chronic granulomatous disease', *Springer Semin Immunopathol*, 19(4), pp. 417-34.
- Miura, H., Bosnjak, J. J., Ning, G., Saito, T., Miura, M. and Gutterman, D. D. (2003) 'Role for hydrogen peroxide in flow-induced dilation of human coronary arterioles', *Circ Res*, 92(2), pp. e31-40.
- Modrick, M. L., Didion, S. P., Sigmund, C. D. and Faraci, F. M. (2009) 'Role of oxidative stress and AT1 receptors in cerebral vascular dysfunction with aging', *Am J Physiol Heart Circ Physiol*, 296(6), pp. H1914-9.
- Moller, T., Hanisch, U. K. and Ransom, B. R. (2000) 'Thrombin-induced activation of cultured rodent microglia', *J Neurochem*, 75(4), pp. 1539-47.
- Molshanski-Mor, S., Mizrahi, A., Ugolev, Y., Dahan, I., Berdichevsky, Y. and Pick, E. (2007) 'Cell-free assays: the reductionist approach to the study of NADPH oxidase assembly, or "all you wanted to know about cell-free assays but did not dare to ask"', *Methods Mol Biol*, 412, pp. 385-428.
- Montezano, A. C., Burger, D., Ceravolo, G. S., Yusuf, H., Montero, M. and Touyz, R. M. (2011) 'Novel Nox homologues in the vasculature: focusing on Nox4 and Nox5', *Clin Sci (Lond)*, 120(4), pp. 131-41.
- Mosher, K. I. and Wyss-Coray, T. (2014) 'Microglial dysfunction in brain aging and Alzheimer's disease', *Biochem Pharmacol*, 88(4), pp. 594-604.
- Murdoch, C. E., Alom-Ruiz, S. P., Wang, M., Zhang, M., Walker, S., Yu, B., Brewer, A. and Shah, A. M. (2011) 'Role of endothelial Nox2 NADPH oxidase in

- angiotensin II-induced hypertension and vasomotor dysfunction', *Basic Res Cardiol*, 106(4), pp. 527-38.
- Nauseef, W. M. (2008) 'Biological roles for the NOX family NADPH oxidases', *J Biol Chem*, 283(25), pp. 16961-5.
- Neniskyte, U., Fricker, M. and Brown, G. C. (2016) 'Amyloid  $\beta$  induces microglia to phagocytose neurons via activation of protein kinase Cs and NADPH oxidase', *Int J Biochem Cell Biol*, 81(Pt B), pp. 346-55.
- Neniskyte, U., Vilalta, A. and Brown, G. C. (2014) 'Tumour necrosis factor  $\alpha$ -induced neuronal loss is mediated by microglial phagocytosis', *FEBS Lett*, 588(17), pp. 2952-6.
- Neumann, H. (2001) 'Control of glial immune function by neurons', *Glia*, 36(2), pp. 191-9.
- Nimmerjahn, A., Kirchhoff, F. and Helmchen, F. (2005) 'Resting microglial cells are highly dynamic surveillants of brain parenchyma in vivo', *Science*, 308(5726), pp. 1314-8.
- Nishi, A., Ishii, A., Takahashi, A., Shiroishi, T. and Koide, T. (2010) 'QTL analysis of measures of mouse home-cage activity using B6/MSM consomic strains', *Mamm Genome*, 21(9-10), pp. 477-85.
- Novella, S., Dantas, A. P., Segarra, G., Vidal--Gomez, X., Mompeon, A., Garabito, M., Hermenegildo, C. and Medina, P. (2013) 'Aging-related endothelial dysfunction in the aorta from female senescence-accelerated mice is associated with decreased nitric oxide synthase expression', *Exp Gerontol*, 48(11), pp. 1329-37.
- Oakley, F. D., Abbott, D., Li, Q. and Engelhardt, J. F. (2009) 'Signaling components of redox active endosomes: the redoxosomes', *Antioxid Redox Signal*, 11(6), pp. 1313-33.

- Owusu-Ansah, E., Yavari, A., Mandal, S. and Banerjee, U. (2008) 'Distinct mitochondrial retrograde signals control the G1-S cell cycle checkpoint', *Nat Genet*, 40(3), pp. 356-61.
- Oxenham, H. and Sharpe, N. (2003) 'Cardiovascular aging and heart failure', *Eur J Heart Fail*, 5(4), pp. 427-34.
- Pan, X., Zhu, Y., Lin, N., Zhang, J., Ye, Q., Huang, H. and Chen, X., (2011) 'Microglial phagocytosis induced by fibrillar  $\beta$ -amyloid is attenuated by oligomeric  $\beta$ -amyloid implications for Alzheimer's disease', *Mol Neurodegener*, 6, pp. 45.
- Panday, A., Sahoo, M. K., Osorio, D. and Batra, S. (2015) 'NADPH oxidases: an overview from structure to innate immunity-associated pathologies', *Cell Mol Immunol*, 12(1), pp. 5-23.
- Paravicini, T. M., Drummond, G. R. and Sobey, C. G. (2004) 'Reactive oxygen species in the cerebral circulation: physiological roles and therapeutic implications for hypertension and stroke', *Drugs*, 64(19), pp. 2143-57.
- Pardridge, W. M. (2007) 'Blood-brain barrier delivery', *Drug Discov Today*, 12(1-2), pp. 54-61.
- Park, L., Anrather, J., Girouard, H., Zhou, P. and Iadecola, C. (2007) 'Nox2-derived reactive oxygen species mediate neurovascular dysregulation in the aging mouse brain', *J Cereb Blood Flow Metab*, 27(12), pp. 1908-18.
- Park, L., Zhou, P., Pitstick, R., Capone, C., Anrather, J., Norris, E. H., Younkin, L., Younkin, S., Carlson, G., McEwen, B. S. and Iadecola, C. (2008) 'Nox2-derived radicals contribute to neurovascular and behavioral dysfunction in mice overexpressing the amyloid precursor protein', *Proc Natl Acad Sci U S A*, 105(4), pp. 1347-52.

- Park, Y. M., Park, M. Y., Suh, Y. L. and Park, J. B. (2004) 'NAD(P)H oxidase inhibitor prevents blood pressure elevation and cardiovascular hypertrophy in aldosterone-infused rats', *Biochem Biophys Res Commun*, 313(3), pp. 812-7.
- Patino, P. J., Perez, J. E., Lopez, J. A., Condino-Neto, A., Grumach, A. S., Botero, J. H., Curnutte, J. T. and Garcia de Olarte, D. (1999) 'Molecular analysis of chronic granulomatous disease caused by defects in gp91-phox', *Hum Mutat*, 13(1), pp. 29-37.
- Peters, R. (2006) 'Ageing and the brain', *Postgrad Med J*, 82(964), pp. 84-88.
- Pollock, J. D., Williams, D. A., Gifford, M. A., Li, L. L., Du, X., Fisherman, J., Orkin, S. H., Doerschuk, C. M. and Dinauer, M. C. (1995) 'Mouse model of X-linked chronic granulomatous disease, an inherited defect in phagocyte superoxide production', *Nat Genet*, 9(2), pp. 202-9.
- Porasuphatana, S., Tsai, P. and Rosen, G. M. (2003) 'The generation of free radicals by nitric oxide synthase', *Comp Biochem Physiol C Toxicol Pharmacol*, 134(3), pp. 281-9.
- Potenza, M. A., Gagliardi, S., Nacci, C., Carratu, M. R. and Montagnani, M. (2009) 'Endothelial dysfunction in diabetes: from mechanisms to therapeutic targets', *Curr Med Chem*, 16(1), pp. 94-112.
- Powers, S. K. and Jackson, M. J. (2008) 'Exercise-induced oxidative stress: cellular mechanisms and impact on muscle force production', *Physiol Rev*, 88(4), pp. 1243-76.
- Qin, L., Liu, Y., Cooper, C., Liu, B., Wilson, B. and Hong, J. S. (2002) 'Microglia enhance beta-amyloid peptide-induced toxicity in cortical and mesencephalic neurons by producing reactive oxygen species', *J Neurochem*, 83(4), pp. 973-83.

- Qin, L., Liu, Y., Hong, J. S. and Crews, F. T. (2013) 'NADPH oxidase and aging drive microglial activation, oxidative stress, and dopaminergic neurodegeneration following systemic LPS administration', *Glia*, 61(6), pp. 855-68.
- Qiu, X., Brown, K., Hirschey, M. D., Verdin, E. and Chen, D. (2010) 'Calorie restriction reduces oxidative stress by SIRT3-mediated SOD2 activation', *Cell Metab*, 12(6), pp. 662-7.
- Rae, J., Newburger, P. E., Dinauer, M. C., Noack, D., Hopkins, P. J., Kuruto, R. and Curnutte, J. T. (1998) 'X-Linked chronic granulomatous disease: mutations in the CYBB gene encoding the gp91-phox component of respiratory-burst oxidase', *Am J Hum Genet*, 62(6), pp. 1320-31.
- Raivich, G. (2005) 'Like cops on the beat: the active role of resting microglia', *Trends Neurosci*, 28(11), pp. 571-3.
- Richter, T. and von Zglinicki, T. (2007) 'A continuous correlation between oxidative stress and telomere shortening in fibroblasts', *Exp Gerontol*, 42(11), pp. 1039-42.
- Rigo, A., Stevanato, R., Finazzi-Agro, A. and Rotilio, G. (1977) 'An attempt to evaluate the rate of the Haber-Weiss reaction by using OH radical scavengers', *FEBS Lett*, 80(1), pp. 130-2.
- Rimaniol, A. C., Haik, S., Martin, M., Le Grand, R., Boussin, F. D., Dereuddre-Bosquet, N., Gras, G. and Dormont, D. (2000) 'Na<sup>+</sup>-dependent high-affinity glutamate transport in macrophages', *J Immunol*, 164(10), pp. 5430-8.
- Rodriguez-Manas, L., El-Assar, M., Vallejo, S., Lopez-Doriga, P., Solis, J., Petidier, R., Montes, M., Nevado, J., Castro, M., Gomez-Guerrero, C., Peiro, C. and Sanchez-Ferrer, C. F. (2009) 'Endothelial dysfunction in aged humans is related with oxidative stress and vascular inflammation', *Aging Cell*, 8(3), pp. 226-38.

- Rollo, C. D. (2010) 'Aging and the Mammalian regulatory triumvirate', *Aging Dis*, 1(2), pp. 105-38.
- Roos, C. M., Hagler, M., Zhang, B., Oehler, E. A., Arghami, A. and Miller, J. D. (2013) 'Transcriptional and phenotypic changes in aorta and aortic valve with aging and MnSOD deficiency in mice', *Am J Physiol Heart Circ Physiol*, 305(10), pp. H1428-39.
- Rubin, L. L. and Staddon, J. M. (1999) 'The cell biology of the blood-brain barrier', *Annu Rev Neurosci*, 22, pp. 11-28.
- Salvatore, M. F., Pruett, B. S., Spann, S. L. and Dempsey, C. (2009) 'Aging reveals a role for nigral tyrosine hydroxylase ser31 phosphorylation in locomotor activity generation', *PLoS One*, 4(12), pp. e8466.
- Sasaki, T., Unno, K., Tahara, S., Shimada, A., Chiba, Y., Hoshino, M. and Kaneko, T. (2008) 'Age-related increase of superoxide generation in the brains of mammals and birds', *Aging Cell*, 7(4), pp. 459-69.
- Sawada, M., Imamura, K. and Nagatsu, T. (2006) 'Role of cytokines in inflammatory process in Parkinson's disease', *J Neural Transm Suppl*, (70), pp. 373-81.
- Schreck, R., Rieber, P. and Baeuerle, P. A. (1991) 'Reactive oxygen intermediates as apparently widely used messengers in the activation of the NF-kappa B transcription factor and HIV-1', *EMBO J*, 10(8), pp. 2247-58.
- Schroder, K., Zhang, M., Benkhoff, S., Mieth, A., Pliquett, R., Kosowski, J., Kruse, C., Luedike, P., Michaelis, U. R., Weissmann, N., Dimmeler, S., Shah, A. M. and Brandes, R. P. (2012) 'Nox4 is a protective reactive oxygen species generating vascular NADPH oxidase', *Circ Res*, 110(9), pp. 1217-25.

- Shen, H. M., Lin, Y., Choksi, S., Tran, J., Jin, T., Chang, L., Karin, M., Zhang, J. and Liu, Z. G. (2004) 'Essential roles of receptor-interacting protein and TRAF2 in oxidative stress-induced cell death', *Mol Cell Biol*, 24(13), pp. 5914-22.
- Skatchkov, M. P., Sperling, D., Hink, U., Mulsch, A., Harrison, D. G., Sindermann, I., Meinertz, T. and Munzel, T. (1999) 'Validation of lucigenin as a chemiluminescent probe to monitor vascular superoxide as well as basal vascular nitric oxide production', *Biochem Biophys Res Commun*, 254(2), pp. 319-24.
- Sokolove, P. G. and Bushell, W. N. (1978) 'The chi square periodogram: its utility for analysis of circadian rhythms', *J Theor Biol*, 72(1), pp. 131-60.
- Sorce, S. and Krause, K. H. (2009) 'NOX enzymes in the central nervous system: from signaling to disease', *Antioxid Redox Signal*, 11(10), pp. 2481-504.
- Stadtman, E. R. (2004) 'Role of oxidant species in aging', *Curr Med Chem*, 11(9), pp. 1105-12.
- Stampfli, S. F., Akhmedov, A., Gebhard, C., Lohmann, C., Holy, E. W., Rozenberg, I., Spescha, R., Shi, Y., Luscher, T. F., Tanner, F. C. and Camici, G. G. (2010) 'Aging induces endothelial dysfunction while sparing arterial thrombosis', *Arterioscler Thromb Vasc Biol*, 30(10), pp. 1960-7.
- Stence, N., Waite, M. and Dailey, M. E. (2001) 'Dynamics of microglial activation: a confocal time-lapse analysis in hippocampal slices', *Glia*, 33(3), pp. 256-66.
- Streit, W. J. (2002) 'Microglia as neuroprotective, immunocompetent cells of the CNS', *Glia*, 40(2), pp. 133-9.
- Sukumar, P., Viswambharan, H., Imrie, H., Cubbon, R. M., Yuldasheva, N., Gage, M., Galloway, S., Skromna, A., Kandavelu, P., Santos, C. X., Gatenby, V. K., Smith, J., Beech, D. J., Wheatcroft, S. B., Channon, K. M., Shah, A. M. and Kearney,

- M. T. (2013) 'Nox2 NADPH oxidase has a critical role in insulin resistance-related endothelial cell dysfunction', *Diabetes*, 62(6), pp. 2130-4.
- Sun, J., Druhan, L. J. and Zweier, J. L. (2010) 'Reactive oxygen and nitrogen species regulate inducible nitric oxide synthase function shifting the balance of nitric oxide and superoxide production', *Arch Biochem Biophys*, 494(2), pp. 130-7.
- Sung, S. M., Jung, D. S., Kwon, C. H., Park, J. Y., Kang, S. K. and Kim, Y. K. (2007) 'Hypoxia/reoxygenation stimulates proliferation through PKC-dependent activation of ERK and Akt in mouse neural progenitor cells', *Neurochem Res*, 32(11), pp. 1932-9.
- Takac, I., Schroder, K. and Brandes, R. P. (2012) 'The Nox family of NADPH oxidases: friend or foe of the vascular system?', *Curr Hypertens Rep*, 14(1), pp. 70-8.
- Takahashi, Y., Kuro, O. M. and Ishikawa, F. (2000) 'Aging mechanisms', *Proc Natl Acad Sci U S A*, 97(23), pp. 12407-8.
- Takeya, R. and Sumimoto, H. (2003) 'Molecular mechanism for activation of superoxide-producing NADPH oxidases', *Mol Cells*, 16(3), pp. 271-7.
- Teng, L., Fan, L. M., Meijles, D. and Li, J. M. (2012) 'Divergent effects of p47(phox) phosphorylation at S303-4 or S379 on tumor necrosis factor-alpha signaling via TRAF4 and MAPK in endothelial cells', *Arterioscler Thromb Vasc Biol*, 32(6), pp. 1488-96.
- Thomas, M. P., Chartrand, K., Reynolds, A., Vitvitsky, V., Banerjee, R. and Gendelman, H. E. (2007) 'Ion channel blockade attenuates aggregated alpha synuclein induction of microglial reactive oxygen species: relevance for the pathogenesis of Parkinson's disease', *J Neurochem*, 100(2), pp. 503-19.
- Toledo, J. B., Arnold, S. E., Raible, K., Brettschneider, J., Xie, S. X., Grossman, M., Monsell, S. E., Kukull, W. A. and Trojanowski, J. Q. (2013) 'Contribution of

- cerebrovascular disease in autopsy confirmed neurodegenerative disease cases in the National Alzheimer's Coordinating Centre', *Brain*, 136(Pt 9), pp. 2697-706.
- Tomilov, A. A., Bicocca, V., Schoenfeld, R. A., Giorgio, M., Migliaccio, E., Ramsey, J. J., Hagopian, K., Pelicci, P. G. and Cortopassi, G. A. (2010) 'Decreased superoxide production in macrophages of long-lived p66Shc knock-out mice', *J Biol Chem*, 285(2), pp. 1153-65.
- Tsamis, A., Krawiec, J. T. and Vorp, D. A. (2013) 'Elastin and collagen fibre microstructure of the human aorta in ageing and disease: a review', *J R Soc Interface*, 10(83), pp. 20121004.
- Turchan-Cholewo, J., Dimayuga, V. M., Gupta, S., Gorospe, R. M. C., Keller, J. N. and Bruce-Keller, A. J. (2009) 'NADPH oxidase drives cytokine and neurotoxin release from microglia and macrophages in response to HIV-Tat. *Antioxidants & Redox Signaling*, 11(2), pp. 193–204.
- Ueno, M. (2007) 'Molecular anatomy of the brain endothelial barrier: an overview of the distributional features', *Curr Med Chem*, 14(11), pp. 1199-206.
- Valeri, B. O., Gaspardo, C. M., Martinez, F. E. and Linhares, M. B. (2012) 'Does the neonatal clinical risk for illness severity influence pain reactivity and recovery in preterm infants?', *Eur J Pain*, 16(5), pp. 727-36.
- Valko, M., Rhodes, C. J., Moncol, J., Izakovic, M. and Mazur, M. (2006) 'Free radicals, metals and antioxidants in oxidative stress-induced cancer', *Chem Biol Interact*, 160(1), pp. 1-40.
- Vallet, P., Charnay, Y., Steger, K., Ogier-Denis, E., Kovari, E., Herrmann, F., Michel, J. P. and Szanto, I. (2005) 'Neuronal expression of the NADPH oxidase NOX4,

- and its regulation in mouse experimental brain ischemia', *Neuroscience*, 132(2), pp. 233-8.
- van Someren, V., Burmester, M., Alusi, G. and Lane, R. (2000) 'Are sleep studies worth doing?', *Arch Dis Child*, 83(1), pp. 76-81.
- Vendrov, A.E., Vendrov, K.C., Smith, A., Yuan, J., Sumida, A., Robidoux, J., Runge, M.S. and Madamanchi, N.R. (2015) 'NOX4 NADPH oxidase-dependent mitochondrial oxidative stress in aging-associated cardiovascular disease', *Antioxid Redox Signal*, 23(18), pp. 1389-1409.
- Victor, V. M., Rocha, M., Sola, E., Banuls, C., Garcia-Malpartida, K. and Hernandez-Mijares, A. (2009) 'Oxidative stress, endothelial dysfunction and atherosclerosis', *Curr Pharm Des*, 15(26), pp. 2988-3002.
- Vignais, P. V. (2002) 'The superoxide-generating NADPH oxidase: structural aspects and activation mechanism', *Cell Mol Life Sci*, 59(9), pp. 1428-59.
- Walsh, M. E., Shi, Y. and Van Remmen, H. (2014) 'The effects of dietary restriction on oxidative stress in rodents', *Free Radic Biol Med*, 66, pp. 88-99.
- Walter, L. and Neumann, H. (2009) 'Role of microglia in neuronal degeneration and regeneration', *Semin Immunopathol*, 31(4), pp. 513-25.
- Walton, N. M., Sutter, B. M., Laywell, E. D., Levkoff, L. H., Kearns, S. M., Marshall, G. P., 2nd, Scheffler, B. and Steindler, D. A. (2006) 'Microglia instruct subventricular zone neurogenesis', *Glia*, 54(8), pp. 815-25.
- Wang, T., Liu, B., Qin, L., Wilson, B. and Hong, J. S. (2004) 'Protective effect of the SOD/catalase mimetic MnTMPyP on inflammation-mediated dopaminergic neurodegeneration in mesencephalic neuronal-glia cultures', *J Neuroimmunol*, 147(1-2), pp. 68-72.

- Wassmann, S., Wassmann, K. and Nickenig, G. (2004) 'Modulation of oxidant and antioxidant enzyme expression and function in vascular cells', *Hypertension*, 44(4), pp. 381-6.
- Wei, J. Y. (1992) 'Age and the cardiovascular system', *N Engl J Med*, 327(24), pp. 1735-9.
- Wilking, M., Ndiaye, M., Mukhtar, H. and Ahmad, N. (2013) 'Circadian rhythm connections to oxidative stress: implications for human health', *Antioxid Redox Signal*, 19(2), pp. 192-208.
- Wilkinson, B. L., Cramer, P. E., Varvel, N. H., Reed-Geaghan, E., Jiang, Q., Szabo, A., Herrup, K., Lamb, B. T. and Landreth, G. E. (2012) 'Ibuprofen attenuates oxidative damage through NOX2 inhibition in Alzheimer's disease', *Neurobiol Aging*, 33(1), pp. 197 e21-32.
- Wilkinson, B. L. and Landreth, G. E. (2006) 'The microglial NADPH oxidase complex as a source of oxidative stress in Alzheimer's disease', *J Neuroinflammation*, 3, pp. 30.
- Wu, Y. H. and Swaab, D. F. (2007) 'Disturbance and strategies for reactivation of the circadian rhythm system in aging and Alzheimer's disease', *Sleep Med*, 8(6), pp. 623-36.
- Yankner, B. A., Lu, T. and Loerch, P. (2008) 'The aging brain', *Annu Rev Pathol*, 3, pp. 41-66.
- Zeeshan, H. M., Lee, G. H., Kim, H. R. and Chae, H. J. (2016) 'Endoplasmic reticulum stress and associated ROS', *Int J Mol Sci*, 17(3), pp. 237.
- Zekry, D., Epperson, T. K. and Krause, K. H. (2003) 'A role for NOX NADPH oxidases in Alzheimer's disease and other types of dementia?', *IUBMB Life*, 55(6), pp. 307-13.

Zhang, F., Qian, L., Flood, P. M., Shi, J. S., Hong, J. S. and Gao, H. M. (2010)

'Inhibition of I $\kappa$ B kinase-beta protects dopamine neurons against lipopolysaccharide-induced neurotoxicity', *J Pharmacol Exp Ther*, 333(3), pp. 822-33.

Zheng, X., Yang, Z., Yue, Z., Alvarez, J. D. and Sehgal, A. (2007) 'FOXO and insulin

signaling regulate sensitivity of the circadian clock to oxidative stress', *Proc Natl Acad Sci U S A*, 104(40), pp. 15899-904.